# SIMULATION AND OPTIMIZATION OF ELECTRIC POWER GENERATION BY SOLAR PONDS

by

A. Moshref, B.Sc. (Iran), M.Sc. (George Washington U.)

A thesis submitted to the Faculty of Graduate Studies and Research in partial fulfillment of the requirements for the degree of Doctor of Philosophy.

Department of Electrical Engineering,

McGill University;

Montreal, Canada.

November, 1983.

**©** 

#### ABSTRACT

welop a methodology for the simulation and optimization of electric power generation by solar ponds.

A mathematical model for the analysis of the economic performance of a solar pond electric power system using a heat engine is developed. A salient feature of this model is a simple method for the analysis of a Rankine cycle. Other features include a mathematical model of the solar pond, of the energy exchange properties of the heat exchangers, as well as of the power required by the circulating pumps. The net electric power is expressed in terms of the thermodynamic properties of the organic working fluid, the temperatures of various thermodynamic states, the flow rates, the temperature and geometry of the solar pond, and the local dlimatic conditions. The system sizing and operating conditions which minimize the cost per kilowatt hour of electric energy is then determined through an optimization routine.

The optimal storage depth and heat extraction scheduling are obtained by a semi-analytical method as well as a discrete optimal control technique. The possibility of an ice storage to act as a cooling source for a Solar Pond Power Plant has also been investigated, which showed considerable improvement in the system's efficiency and reduction of electric energy cost.

The possibility of making the Non-Convective Zone of a solar pond float over a layer of fresh water has been investigated. The economical feasibility study of the concept for electric power generation was achieved using the model developed earlier.

The thesis finally examines the means of enhancing the thermal storage under a solar pond by circulating the Lower Convective Zone brine through a network of buried horizontal pipes in the warmer part of the year. This heat stored can be used for the operation of a heat engine during the winter time if the Lower Convective Zone brine is then used as a heat sink rather than a heat source.

The present thesis has shown that the commonly held belief that a Solar Power Plant can only function at acceptable efficiencies under semi-tropical conditions is a fallacy. Proper modifications to the construction and operating conditions of a Solar Pond Power Plant in northern climates resulted in electric energy costs of .8.5 ¢/KWh which is comparable with that estimated by the Israelis for a Solar Pond Power Plant in semi-tropical conditions.

#### RESUME

Le but principal de cette thèse a été d'élaborer une méthodologie pour la simulation et pour l'optimisation de la génération de puissance électrique par des bassins solaires.

Une modèle mathématique est formulé pour l'analyse du système bassin solaire-générateur électrique, utilisant une machine thermique. Une méthode simple est proposée pour l'analyse du cycle de Rankine. D'autres points d'importance sont la modélisation du bassin solaire, des propriétés d'échanges d'énergie des échangeurs de chaleur, et de la puissance requise par les pompes de circulation. La puissance nette tirée du bassin solaire-générateur est exprimée en fonction des propriétés thermodynamiques, du réfrigérant organique, des températures des différents états thermodynamiques, des débits, de la température et de la géométrie du bassin solaire, et des conditions climatiques locales. Le dimensionement et les conditions d'exploitation correspondant au rendement économique optimal sont déterminés à l'aide d'un programme d'optimisation.

La profondeur optimale d'entreposage et la gestion de l'extraction de chaleur sont obtenues à partir d'une méthode semi-analytique ainsi que par une commande optimale en temps discret. Le stockage de glace servant de source de refroidissement pour le bassin solaire-générateur électrique a été étudié. Il en résulterait une amélioration appréciable dans l'efficacité du système et une reduction importante du coût.

La possibilité de faire flotter la couche non-convective d'un étang solaire sur une couche d'eau douce a été envisagée. L'étude de faisabilité économique d'un tel projet pour la génération de puissance électrique peut être poursuivie avantageusement avec le modèle décrit ci-haut.

On examine également des moyens pour améliorer le stockage thermique sous le bassin solaire. Il s'agirait d'enfouir un réséau de tuyaux horizontaux sous le bassin, et d'y faire circuler de la saumure extraite du fond du bassin pendant la période chaude de l'année. La chaleur emmagasinée pourrait servir à l'exploitation de la machine thermi-

que pendant l'hiver. La saumure servirait alors comme dissipateur de chaleur plutôt que de source thermique.

Cette thèse démontre le non-fondé de l'opinion voulant que le bassin solaire-générateur électrique ne soit efficace que dans les conditions semi-tropicales. Les modifications appropriées dans la construction et dans le mode d'exploitation du bassin solaire-générateur électrique pour les climats nordiques résulteraient en des coûts de l'ordre de 8.5¢/KWh. Cela est comparable au coût estimé par des chercheurs Israéliens pour un bassin solaire-générateur électrique en region semi-tropicale.

#### **ACKNOWLEDGEMENTS**

I wish to acknowledge with a deep sense of gratitude and indebtedness, the assistance and cooperation of all those who have contributed both directly and indirectly to the completion of this investigation.

My special thanks to Professor Daniel Crevier, for his invaluable guidance, patience, constant encouragement, and his friendship through all facets of this research.

I am also thankful to Dr. C.C. Paige, from the School of Computer Science, for the generous contribution of his time and valuable consultations and also for providing the GRG package.

The counsel and advice of Drs. P.R. Bélanger, Chairman of the Department of Electrical Engineering and C.L. Murphy from the Department of Mechanical Engineering, are greatly appreciated.

The cooperation of Mr. R.L. French, Deputy Manager of Salton Sea Solar Pond Project at Jet Propulsion Laboratory, for providing some design details of the Salton Sea Solar Pond Power Plant is highly appreciated.

Special thanks to Ms. P. Hyland for her patience and skillful typing of the manuscript.

Thanks are extended to all friends and colleagues at McGill for their support and good company.

The scholarships from McGill's Faculty of Graduate Studies and Research and financial support both from Agriculture Canada and the Natural Sciences and Engineering Research Council of Canada are gratefully acknowledged.

Finally, I would like to express my sincere thanks to my wife, Mansoureh, and our son, Kamran, for their unwaivering support and constant encouragement.

# TABLE OF CONTENTS

		Page
ABSTRACT		i
RESUME		ii
ACKNOWLEDGEMENTS		iv
TABLE OF CONTENTS		vi
NOMENCLATURE		· ×
ABBREVIATIONS		xxii
CHAPTER I	INTRODUCTION	1
1.2.3 1.2.4 1.2.5 1.2.6 1.3 1.3.1 1.3.2 1.4	Salt-Gradient Solar Pond Saturated Salt-Gradient Solar Ponds Shallow Solar Ponds Gel and Viscosity Stabilized Ponds Partitioned Solar Ponds Subject of the Present Thesis Historical Background of Salt-Gradient Solar Pond Research	2 2 3 6 7' 8 8 9 11 15 21 23 26
CHAPTER II	PREDICTION OF SOLAR POND THERMAL BEHAVIOR	29
2.1 2.2 2.2.1 2.2.2	Governing Equations of Pond Tem- perature Behavior Analytical Steady State Solution with Sinusoidal Excitation Time Independent Solution Time Dependent Solution	29 33 38 40
2.3 2.4	Examples Static Efficiency	43 48

Ġ

			Page
		** **	
	2.5	Numerical Solution using Finite	
	3,5	Difference Technique	51
	2.5.1	<del>-</del>	7.
		tical Solutions	62
	2.5.2		~~
		Declination Angle	64
CHAPTER	III	OPTIMIZATION OF A SOLAR POND POWER PLANT	
CHAPTER	111	PART I: STATIC OPTIMIZATION	67
		FART 1: STATE OF TIMEZATION	
	3.1	Introduction .	67
	3.2	A Solar Pond Power Plant (SPPP)	67
	3.3	Power Cycle Analysis	70
-	3.4	Heat Exchangers	79
	3.5	Auxiliary Pumps	82
	3.6	Optimization	85
	3.6.1	Flow Diagram of the Optimization	89
	3.6.2	Numerical Results and Discussions	92
CHAPTER	IV	OPTIMIZATION OF SOLAR POND FOWER PLANT	
	_,	PART II : OPTIMAL HEAT EXTRACTION	,
•		AND STORAGE DEPTH '	98
			,,,
	4.1	Introduction .	98
	4.2	Assumptions	98
	4.3	Semi-Analytical Solution	100
	4.3.1	Approximate Analytical Solution	
		of the Pond Governing Equations	101
	4.3.2		103
	4.3.3	<del>-</del>	106
	4.4	Examples	108
	4.5	Mathematical Programming Method	117
	4.5.1	Optimal Control Formulation	117
	4.6	Examples	120-
,			
CHAPTER	. <b>V</b>	COST REDUCTION TECHNIQUES	125
	5.1.	Introduction	105
	5.1. 5.2	The Floating Solar Pond	125
	5.2.1		125 136
·	5.2.2	Stabilization of the NCZ over	130
	J . L . L	Fresh Water (Uniform Concentration)	129
	5.2.3	Stabilization of the NCZ over	143
		Fresh Water (Linear Salt Gradient)	132
	5.3	Optimization of a Floating SPPP	137
	5.4	Ice Storage as a Heat Sink for SPPP	139
		•	

(J.

٥.

		o	Pag
		· ·	
•	5.4.1	Introductory Remarks	139
	5.4.2	Structure and Mechanism of Ice Storage	14.
	5.4.3	Sizing of the Ice Storage	14.
	5.4.4	Static Optimization of SPPP	
	5.4.5	with Ice Storage	149
	5.4.5	Optimal Heat Extraction and LCZ Thick-	
		ness of SPPP with Ice Storage	14
CHAPTER	VI	REVERSE OPERATION: UNDERGROUND STORAGE	150
	6.1	Introduction	150
	6.2	Pipe Storage System	150
	6.3	Mathematical Model	15
	6.3.1	The Pond Model	153
	6.3.2		. 153
	6.3.3	<del>-</del>	154
	6.3.4	•	ຸ 15€
	6.4	Model Validation	157
	6.5	Reverse Operation	<sub>a</sub> 158
_	6.6	Optimal Heat Extraction and Injection	,
•		in SPPP with Underground Storage	' 159
•	6.6.1	Formulation of Discrete Optimal Control	1.0
	~ "	for SPPP with Ground Storage	160
	6.7	Example $\varphi$	164
HAPTER	VII	CONCLUSIONS AND RECOMMENDATIONS	- t
	,	FOR FUTURE RESEARCH	169
	7.1	The Significance of this Research	- 169
	7.2	Conclusions	
	7.3	Recommendation for Future Research	176
EFERENCES	5	•	179
PPENDIX	A	ABSORPTION OF SOLAR RADIATION	
a I Laidan	•	IN A SOLAR POND	, 197
PPENDIX	В	OPTIMALITY CONDITIONS	202
	B.1	Conditions for a Minimum with Non-	•
		linear Equality Constraints .	202
	B.2	Optimality Conditions for a Minimum	٠,
		with Monlinear Inequality Constraints	206

0

viii

	·		Page
	2	_	
APPENDIX	С	THERMAL ANALYSIS OF THE AUXILIARY POND	209
•	C.1	Night Time Operation	209
	C.2	Day Time Operation	212
	C.3	Temperature Response of the Auxiliary Pond	213

## NOMENCLATURE

Α

AB, Ac, Ap

 $^{\rm A}{\rm aux}$ 

Ą

A,

a<sup>L</sup>, a<sup>U</sup>

b

Cc, CH

C<sub>KWh</sub>

CGen' Chex' Cpipes' Cpond' Cpump' Ctur

Cg

 $C_{+}C_{+}$ 

surface area of the solar pond.

surface areas of the boiler,

condenser, and pre-heater.

surface area of the auxiliary pond.

cross-sectional area of a buoy.

surface area of the ice storage.

vectors of the lower and upper
limits on the inequality constraints.

a dummy variable.

specific heat of the cold and hot fluids.

cost per kilowatt-hour of electric energy.

costs of generator, heat exchangers, piping, pond, pumps, and turbine.

specific heat of the brine in LCZ.

total installation costs.

\_.≥

Ct1' Ct2

installation costs independent and dependent on the thickness of the  $\ensuremath{\mathsf{LCZ}}$  .

 $C_{\mathbf{w}}$ 

specific heat of fresh water.

 $c_{\mathbf{p}}^{0}$ 

low-pressure specific heat.

D

declination of the sun.

Do

declination of sun at equinox.

đ

diameter of the pipes carrying brine and cooling water.

d<sub>1</sub>, d<sub>2</sub>

optimum temperature drop across boiler and condenser.

dy

maximum height of the membrane deformation.

Dy A dy

differential operator.

E. E<sup>-1</sup>

shift and inverse shift operator.

Etat

total annual costs of the SPPP .

 $E_{+i}, i = 1, 8$ 

dummy variables.

e<sub>0</sub>, e<sub>1</sub>

coefficients of the linear approximation in equation (4.9).

f

**(**)

friction factor.

 $f_{i}$ , i = 1, 6

dummy variables.

f(T)

thermodynamic properties on the saturated lines as a function of temperature.

f(x)

the objective function of the optimization problem.

g

acceleration due to gravity.

g (x)

equality functional.

 $H_{1}, \dot{t} = 1, 6$ 

enthalpies of the points in figures 3.2 and 3.3.

H or H (t)

solar radiation incident at earth's surface.

H, H

average and amplitude of H s for sinusoidal approximation.

h

height of water in the equilibrium duct. -

h,

head loss due to friction.

ho

head loss due to obstacles in the flow.

h

static head.

h,

total head loss.

h

height of the immersed part of a buoy.

h<sub>fc' h</sub>fr

forced and free convection coefficients,

h<sub>sl</sub>

heat of fusion.

h(x)

inequality functional.

H(x. +1

radiation reaching depth  $\mathbf{x}$  at time  $\mathbf{t}$  .

 $H_{\lambda}^{i}$ ,  $H_{\lambda}^{t}$ 

incident and transmitted radiation having wavelength  $\lambda$  .

I

interest rate.

i

angle of incidence.

Ţ

4

CKWh

Kf

thermal conductivity of foam.

ĸ,

thermal conductivity of the insulation blanket.

K

pump power factor.

K, K

thermal conductivity of brine and ground.

L

pipe length in Chapter III ;
latitude of the pond site in
Appendix A .

2.

thickness of the foam.

ັສ

length of the underground pipe.

<sup>l</sup>e

thickness of the LCZ .

٤,,

thickness of the UCZ..

٤,

l<sub>2</sub>

M<sub>iO</sub>, M<sub>wO</sub>

M<sub>1</sub>(t), M<sub>W</sub>(t)

m<sub>1</sub>, m<sub>2</sub>, m<sub>3</sub>

N

<sup>n</sup>1′ <sup>n</sup>2

nc, nr

0 + r

P<sub>1</sub>, P<sub>2</sub>

heat extraction depth.

distance of the heat sink from the bottom of the pond.

initial amount of ice and water in the ice storage pit.

amount of ice and water in the ice storage at time t .

flow rate of brine, working, fluid, and cooling water.

index of refraction.

numbers of sublayers in the NCZ and ground.

number of rows and columns of pipes in the underground pipe network.

annual costs of operation and repair.

turbine inlet and outlet pressures.

Pd' Pu

 $Q_{\mathbf{A}}$ 

QB, CC, CP

 $Q_{\mathbf{R}}$ 

÷

qb, q

Ro

Re

r

~

-i

 $S_{i}$ , i = 1, 6

downward and upward pressures exerted on the membrane.

heat added to the power cycle.

heat exchanged in the boiler, condenser, and pre-heater.

heat rejected by the power cycle.

heat flux yector.

bottom and top heat losses from the ice storage pit.

half the interpipe distance.

Reynolds number.

vector of the residual in least squares approximation.

angle of refraction.

radius of pipe in the underground pipe network.

entropies of the points in Figures 3.2 and 3.3.

Ta or Ta(t)

ι τ̄a, τ̄a

Ŧ'a

T<sub>C</sub>, T<sub>H</sub>

Ts or Ts(t)

īs' is

0

ī, ī

T<sub>W</sub>

T5' T6

T<sub>1</sub> (x, t), T<sub>2</sub> (x, t)

ambient temperature.

average and amplitude of Ta for sinusoidal approximation.

temperature of the cooling water at condenser outlet.

outlet and inlet temperatures of the turbine.

temperature of the LCZ .

average and amplitude of  $T_S$  for sinusoidal approximation.

temperature of brine.at preheater and boiler outlet.

temperature of the heat sink.

temperatures of the points 5 and 6 in Figures 3.2 and 3.3.

temperatures of the NCZ and ground as a function of depth and time.

T<sub>3</sub>(t)

Tsky' Taux

 $T^M$ ,  $T^m$ 

to, tf

t<sub>i</sub>

U or U(t)

ΰ, τ̈́

 $\sigma_{\rm B}$ ,  $\sigma_{\rm C}$ ,  $\sigma_{\rm P}$ 

Ŭ

 $\mathbf{U}_1$  or  $\mathbf{U}_1(\mathbf{t})$ 

temperature of the buffer zone.

temperatures of the sky and auxiliary pond.

maximum and minimum values of  ${\bf T}_{\rm S}$  .

initial and final time.

thickness of the insulation blanket.

heat extracted from the LCZ .

average and amplitude of U for sinusoidal approximation.

overall heat transfer coefficients of the boiler, condenser, and preheater.

edge loss coefficient.

heat injected or extracted from the underground storage.

fluid velocity.

volume of the ice storage.

wind velocity.

 $v_{lf}$ 

specific volume of the saturated liquid.

w<sub>p1</sub>, w<sub>p2</sub>, w<sub>p3</sub>

pumping power of the brine, working fluid, and cooling water pumps.

Wnt

net electric power.

work of the turbine.

X

vector of the optimization variable.

 $\underline{x}^{m}$ ,  $\underline{x}^{M}$ 

lower and upper limits on  $\underline{x}$ .

quality factor.

thermal diffusivity of brine and ground.

a dummy variable.

 $\delta_a$ ,  $\delta_s$ ,  $\delta_u$ 

phase lag of ambient and LCZ temperatures and heat extraction with respect to solar radiation.

ΔΤ

temperature difference between LCZ and ambient temperatures.

η<sub>cy</sub>, η<sub>c</sub>

Rankine and Carnot cycle's efficiency.

ηn

weighting coefficient.

η\_

static efficiency of the pond.

η<sub>G'</sub>η<sub>t</sub>

efficiency of the generator and turbine.

 $\mu_{\mathtt{f}}$ 

kinematic viscosity.

 $\mu_n$ 

absorption coefficient.

μ<sub>n</sub>

an effective absorption coefficient.

ρ<sub>1</sub>, ρ<sub>2</sub>

density of brine and ground.

ρ<sub>i</sub>

C

ρs

 $\sigma_1$ ,  $\sigma_2$ 

σ sb

density of ice.

density of the brine in LCZ .

skin depth of brine and ground.

Stefan-Boltzmann constant.

coefficient of transmission.

time constant.

angular velocity.

## ABBREVIATIONS

CD Central Difference.

CRF Capital Recovery Factor.

FBD First Backward Difference.

FFD First Forward Difference.

F-11 Freon 11 (C  $Cl_3F$ ).

F-113 Freon 113 ( $C Cl_2 F - C Cl F_2$ )..

FSPPR Floating Solar Pond Power Plant.

GRG Generalized Reduced Gradient.

LCZ Lower Convective Zone.

LMTD Logarithmic Mean Temperature Difference.

NCZ Non-convective Zone.

OTEC Ocean Thermal Energy Conversion.

SBD # Second Backward Difference.

SFD Second Forward Difference.

SPPP Solar Pond Power Plant.

UCZ Upper Convective Zone.

#### CHAPTER I

( }

#### INTRODUCTION

Fossil fuels historically have been the major source of energy for the generation of electricity. During this century, petroleum and natural gas have been used extensively because of their low cost and abundant supply. In recent years, however, their increasing cost and decreasing availability have led major users of energy to seek alternate sources. Coal, although more plentiful and less expensive than other fossil fuels, costs more to transport and creates significant environmental problems in its minimg and burning. Uranium, once considered the natural successor to petroleum, has its own set of problems which will certainly delay its widespread use and may preclude it altogether in some locations. As a result of these limitations on expanded use of the conventional energy sources, greater attention is being paid to renewable energy sources, and specially to solar energy.

Solar energy systems are by nature capital intensive, but are potentially attractive under certain conditions:

- (1) 'The expectation that in the future the cost of conventional fuels will rise faster than the cost of construction.
- (2) The desire to guarantee an uninterruptible source of energy not dependent upon the whims of foreign suppliers.

(3) A desire to keep at home foreign-exchange currency that would otherwise be spent abroad for imported fuels.

The solar pond is one of the most attractive solar energy options because of its inherent storage capacity; unlike other means of solar heating, it is continuously available regardless of time of day. Moreover, of all the solar energy options, the solar pond is the only one which is applicable for baseload electric power generation.

#### 1.1 The Solar Pond: Generic Definition

A fraction of the sun's radiation can penetrate through several meters of clear water; natural bodies of water collect a considerable amount of energy from the sun, but lose it to the atmosphere through convection of the heated water to the surface.

The term "solar pond" is commonly used to describe a number of different solar collectors, all of which involve the use of water as an absorber of solar radiation, and means of preventing the absorbed heat from escaping through the surface.

## 1.2 Review of Existing Solar Pond Concepts

#### 1.2.1 Salt-Gradient Solar Pond

The most advanced and promising of these concepts is that of the salt-gradient pond. It consists in a body of water in which a density gradient, positive downward, is maintained artificially. The light penetrating into the water is absorbed. The deeper water is heated by absorption of radiation; since it contains more salt and is therefore more dense than the water lying immediately above it, it does not rise to the surface and lose its heat to the atmosphere, as would happen in a normal body of water. Thus a temperature gradient, also positive downwards, is established as heat losses can occur only by conduction to the surface. Therefore the temperature of the entire pond increases, the warmest layer being at the bottom.

The salinity gradient induces a continuous salt migration to the surface. Although this transport of salt to the surface may occur very slowly, it is necessary to inject concentrated brine or salt periodically at the bottom of the pond and to desalinate the surface layer or wash it with fresh water so as to maintain the gradient.

A practical solar salt-gradient pond always has at least three distinct layers, as illustrated in Figure 1.1. There will be at the surface a convective layer, where the salt concentration is uniform with depth. Beneath this layer is the salt gradient zone (non-convecting zone), in which the buoyancy effect of thermal expansion is offset: this layer acts as a thermal insulator and also provides thermal storage. At the bottom of the pond is a second convective layer with a uniform salt concentration equal to that of the bottom of the gradient zone.

To understand the origin of the two convective layers, let us first assume that the pond is non-convective over all its depth.

Then after a day of intensive heating from the sun, the temperature gradient at the bottom of the pond would be so large as to exceed the stability limit for salt gradient stabilization (Tabor and Weinberger, 1981). This situation will induce convection at the bottom, which will result in a layer of uniform temperature and salt concentration at the bottom. The thickness of the bottom convective layer can be controlled, and for seasonal storage it is desirable to make it deep enough to give rise to a large heat storage capacity: the bottom convective layer is often referred to as the storage layer for this reason. The storage layer also facilitates heat extraction.

The existence of the surface convective layer can be explained by a similar argument, as a result of night-time radiation

cooling, and heat losses due to evaporation. In addition, wind action may mix the surface layer, and can in fact drive the surface convective zone to an unacceptable depth. A property of the surface convective layer, which is useful in modelling the thermal behavior of the pond, is the observed fact that the temperature of this layer is always approximately equal to the average ambient air temperature.

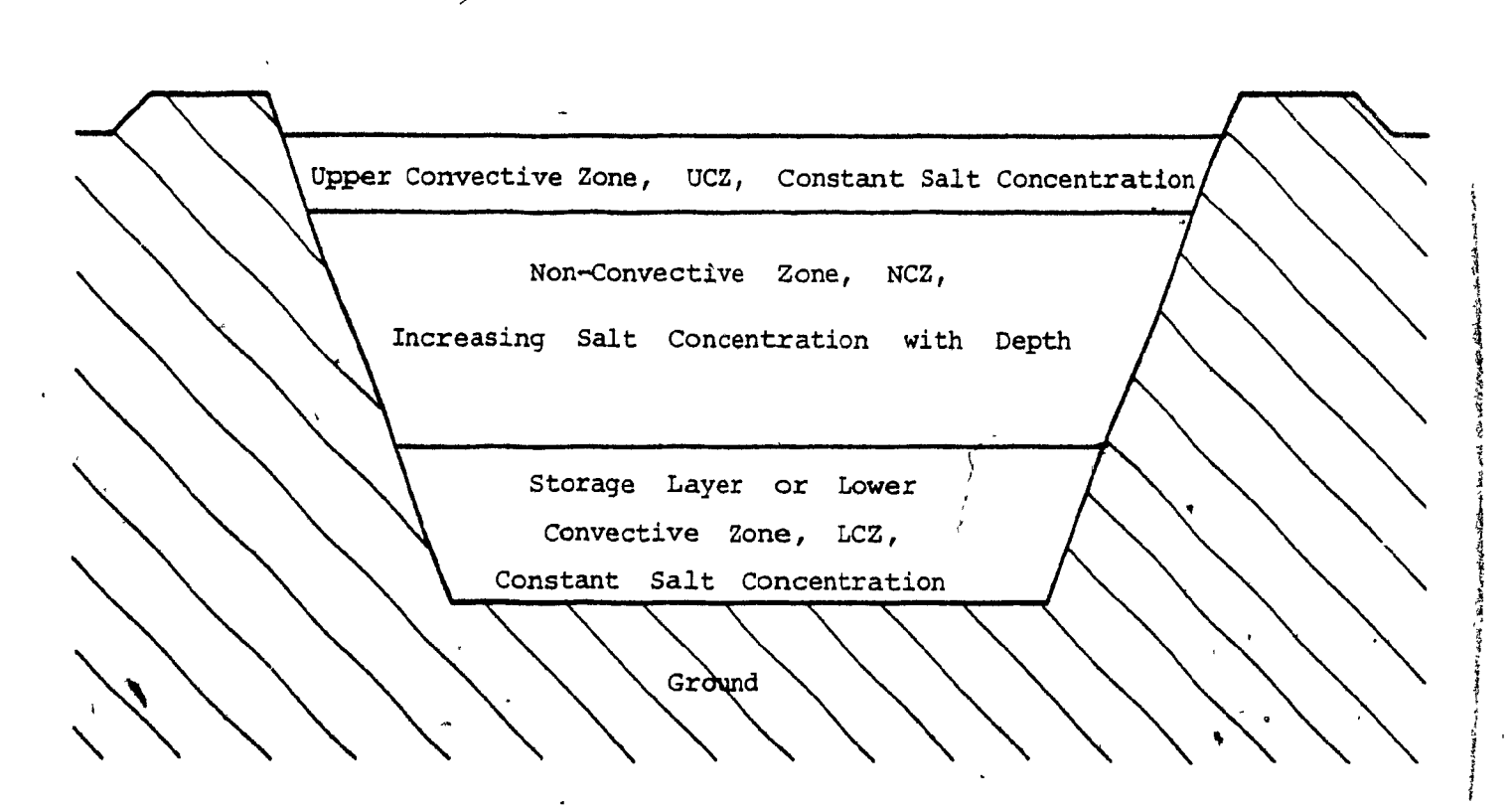


Figure 1.1 Cross Section of a Salt-gradient Solar Pond.

The salt-gradient solar pond, in spite of its simple description, is a complex physical system which interacts strongly with the local meteorology and geology. A large number of factors must be considered in its analysis: in particular, wind effects which mix the pond from the top; ground heat losses and contamination of ground water by salt leakage; stability of the double diffusive system (heat and mass diffusion); absorption of radiation in the presence of a salinity gradient; and problems such as evaporation and precipitation, which are generally geographically dependent and must be solved for local conditions.

One of the major advantages of a salt-gradient solar pond over all other types of solar collectors for the purposes of generating electricity, is that the solar pond includes both hot water storage at the bottom of the pond (or lower convective zone, or LCZ) and cold water storage at its surface (or upper convective zone, or UCZ).

The existence of these storage layers, which is inherent in the pond construction, allows production of electricity 24 hours a day (Assaf et al, 1981).

## 1.2.2 Saturated Salt-Gradient Solar Ponds

These are generally referred to simply as saturated solar ponds in the literature. Their principle consists of using a salt

with a solubility which significantly increases with temperature such as KNO<sub>3</sub>, borax, Ca Cl<sub>2</sub>. In most cases, this property will result in a net increase in density of the saturated solution with temperature (Ochs, 1979). If a pond containing such a salt is kept at saturation throughout its depth the salt concentration gradient would be self-generated and self-maintaining (Mehta, 1980). There would still occur a diffusion of salt from the bottom to the surface of the pond, but this mechanism would be compensated by the crystallization of salt in the upper, colder layers, and the sinking of the crystals back to the bottom. The major disadvantages of saturated ponds is that they require much larger amounts of salt than the unsaturated ponds, and that they cannot be realized with sodium chloride.

#### 1.2.3 Shallow Solar Ponds

The shallow solar pond was proposed and developed at Lawrence Livermore Laboratories (Dickinson, et al, 1976). These ponds are very thin (about 10 cm) water layers encased in long plastic bags. The underside of the bags are blackened and their tops are transparent. They are supported by a horizontal concrete foundation and overlaid by fiberglass glazing. Since the water must be pumped to separate storage tanks at times of low solar radiation, the economic attractiveness of these ponds is marred by the high cost of plumbing and separate storage tanks.

A shallow solar pond electric generating system for higher latitudes using circular cylindircal reflectors was proposed by Kooi (1978). The analysis was mostly concerned with its optical design. It was shown that a significant increase in annual power production can be accomplished by an effective tilting mechanism for the reflector. The electric power was calculated roughly without modelling of system components and no economical analysis was made.

### 1.2.4 Gel and Viscosity Stabilized Ponds

( },

It has been proposed to use gels and viscosity increasing substances, either alone or in combination with salt, to make the pond non-convective. In Lyon, France (Anonymous, 1980) and in New Mexico (Wilkins, 1982) theoretical as well as experimental investigations on Gel ponds are in progress.

## 1.2.5 Partitioned Solar Ponds

In order to reduce internal convection in the pond, it could be divided into a number of different layers by means of horizontal and vertical partitions. Honeycomb structures have been proposed to divide the pond into smaller cells, thereby suppressing convection (Hull,

1979). At the Jet Propulsion Laboratory a saltless honeycomb solar pond has been proposed and the results of outdoor testing are reported in Lin (1983).

## 1.2.6 Subject of the Present Thesis

The present thesis is devoted to salt-gradient solar ponds and adaptations of it such as the floating salt-gradient, and enhanced ground storage salt-gradient solar ponds. The next section reviews only the natural solar ponds and those research works which dealt with electric power application of solar ponds. The reader is referred to the review paper by Tabor (1981), the paper by Nielsen (1980), and the state-of-the-art review by Crevier (1980), for further research activities concerning other applications of solar ponds.

# 1.3 Historical Background of Salt-Gradient Solar Pond Research

There are numerous examples of natural and artificial lakes which possess density gradients due to vertical salt concentration gradients. In the limnological literature these lakes are called "meromictic lakes" and the salt concentration gradient, the "halocline" (Tabor and Weinberger, 1981). If the halocline is sufficiently steep

and if the surface of the pond is protected from wind-mixing by surrounding geographical features, then the incident solar radiation
can cause a considerable temperature rise above ambient in the body
of the lake. The resulting temperature gradient, the "thermocline",
parallels the halocline. The halocline assures the greater density
of the lower depths even when heated by solar radiation.

The first natural solar lake described in the literature is probably the most impressive. Kalecsinsky (1902), described the Medve Lake, which is situated in Transylvania (at 42° 44'N). A temperature of 70°C was recorded in it at a depth of 1.32 m at the end of summer. The minimum temperature was 26°C during the early spring. The bottom of the lake had a near saturation of 26% of Na Cl. More recently Anderson (1958), has described a natural solar lake near Oroville in the state of Washington. The lake, called appropriately "Hot Lake", lies in a wind-protected area at Kruger mountain (48° 58'N). Temperatures greater than 50°C during midsummer were recorded at a depth of 2 m. During the winter the surface of the lake is covered with ice. Natural solar lakes have also been found in Israel (Por, 1970), Venezuelan Antilles (Hunder, 1974), and under a permanent ice cover in Lake Vanda (77° 35'S) in the Antarctic (Wilson, 1962).

## 1.3.1 Research in Israel

In 1948 Dr. R. Bloch, Research Director of the Dead Sea works, suggested the study of solar lakes with a view toward practical utilization. Under controlled conditions, it was to be expected that higher temperatures and useful collection efficiencies could be achieved in artificial ponds. It was only a decade later, however, that interest in solar ponds began to receive the funding necessary to implement the research. The primary goal was the generation of electric power by using the pond as a heat source for a heat engine driving a generator (Tabor, 1963). Other potential applications include space heating; industrial process heat; space cooling; desalination; and agricultural crop drying and other farm uses.

In 1978, a small 6 KW turbine was coupled to a 1500 sq.m. pond and demonstrated the feasibility of the system. In December 1979, a much larger system was put into operation; this is the 150 KW Ein-Boqeq solar pond power plant (Bronicki, 1982). In December, at a brine temperature of 77°C, 145 KW were produced with an overall turbogenerator efficiency of 5.7%. In the summer, when the pond temperature reached 93°C a peak gross power of 245 KW was achieved. Currently, operation of the 150 KW facility at Ein-Boqeq is being monitored under varying system conditions, and valuable data are being gathered and interpreted. The power plant has been connected to the Israeli power grid since 1981.

11/1

A program of broad significance is presently being implemented in Israel where multi-megawatt solar power stations combining low temperature turbogenerators with solar ponds are being built.

A pond 40,000 m<sup>2</sup> in area having a depth of about 4 meters will be running a 2.5 MW unit by the summer of 1983 (Harleman, 1983) . A second pond (250,000 m<sup>2</sup>) filled with Dead Sea brine is almost completed, and will be coupled to a 5 MW turbogenerator.

Although Israelis are presently the leaders in solar pond technology, specially for electric power application, they have published very little about the design, methodology, optimization, and experimental results.

Because of the storage capacity of the solar pond, the solar pond power plant can be used as a peaking plant. For example, the 150 KW plant in Ein Boqeq which used a pond of only 7,000 m<sup>2</sup> area, (adequate for a continuous output of 20 KW) could temporarily deliver about seven times its continuous rated output (Tabor, 1981). This peaking capacity can considerably raise the economic value of such a station when integrated into a grid system (Bronicki, 1980). Therefore solar pond power plants, like hydro-electric plants, can provide, on demand, peaks of power far in excess of their mean capacity.

A joint study of Ormat Turbine and the Israel Electric Corporation has recommended that solar pond power plants be used first in the national power grid system as peaking plants, operating 750 to 1250 hours per year, and replacing gas turbines. As solar pond technology becomes more established and cheaper, plants supplying intermediate loads can be introduced, perhaps by 1985. Ultimately, the large solar lakes could be built by 1995, and their plants could supply base loads (Bronicki, 1981).

Tabor (1981) reported that the cost of solar pond power systems per unit power generating capacity flatten out for units larger than 20 - 40 MW. This is of great interest to developing countries, since they can install generating capacity in relatively small steps as demand grows. Today's fossil-fueled or nuclear power stations, by contrast, must have a capacity of several hundred megawatts to be competitive.

Assaf (1976), proposed a theoretical scheme which turns a salt lake into a solar pond. He was mostly concerned with the wind action on the pond surface and its mixing effect on the NCZ. In the paper the energy recovery rate was taken as that of an equivalent Carnot engine and the power output, per unit area of the pond, was maximized with respect to LCZ temperature and depth of NCZ. The analysis did not include the Rankine power cycle characteristics, heat exchangers or auxiliary pumps. The optimization even failed when he obtained the optimum LCZ temperature of 160°C which is much higher than the boiling point of brine. The optimization was repeated with

respect to NCZ depth while fixing the LCZ temperature arbitrarily at 80°C or 100°C.

Ophir and Nadav (1982) , proposed a solar pond for production of electric power as well as desalinated water. They estimated energy costs of 5.5-9.62 ¢/kwh for single purpose solar ponds (electric power only) in the Dead Sea and Mediterranean areas respectively. For dual purpose plants, depending on the selling price for desalinated water, the energy cost ranged from 7.3-1%.3 for a water selling price of  $0.5 \text{ $\%/m}^3$ ; 5.0-12.3 for  $0.6 \text{ $\%/m}^3$ ; and 2.7-6.3 for  $0.7 \text{ $\%/m}^3$ . Their analysis is based on a solar pond specific cost of  $13/m^2$ , and a pond collection efficiency of 20 per cent.

A solar pond power plant operated with a direct contact boiler was thermally analyzed by Sonn and Letan (1982). The analysis by Sonn and Letan did not however consider the interaction of the many system elements. The main benefits of the proposed direct contact exchanger appear to be of three kinds: non-fouling of heat transfer surfaces, high heat transfer rates, and a reduction in cost. The disadvantage of the direct contact heat exchanger for a solar pond

In a direct contact, boiler, heat is transferred directly across the phase boundary between the pond brine and a vaporizing organic fluid.

power plant is related to material losses due to dissolution of the working fluid in the LCZ brine. Since an experimental demonstration of a direct contact heat exchanger for a solar pond remains to be performed, and because the closed cycle power generation schemes have already shown their feasibility, the direct contact heat exchanger was not considered in the present work.

#### 1.3.2 Research in the United States

In 1975, a brief study was conducted by Bechtel Corporation to assess the general technical and economic feasibility of using salt-gradient solar ponds as a means of generating electric power. This study used F-11 as the working fluid, and a pond of 1 km<sup>2</sup> was considered. It concluded that the cost of a solar pond power plant was five times larger than that of a conventional plant of equal capacity.

A solar pond driven desalination and electric power production system was proposed by Johnson et al (1981). A thermodynamic analysis of the energy and mass balances of the system has been performed and a performance model of the system has been developed.

For typical operating conditions of a solar pond<sup>1</sup>, a required surface area

<sup>&</sup>lt;sup>1</sup>For the average solar radiation in Utah (250  $\frac{W}{2}$ ), a pond temperature of 80°C and cooling water temperature of 20°C, the average pond efficiency of 15 per cent was assumed.

of 10 km<sup>2</sup> was obtained. The electrical output was assumed to be equal to the electrical demand of the multi-effect distillation plant. Their analysis did not include a detailed modelling of the solar pond power system. Cost evaluation and system optimization were not attempted.

Jayadev and Henderson (1980), developed a simulation program to analyze the thermal performance of solar ponds. A simple economic optimization which maximized delivered energy per capital cost with respect to LCZ and NCZ thicknesses was also performed with the help of repeated simulations. In all of the reported research activities so far, the relative sizes of the various components of the solar pond power plant, (solar pond, heat exchangers, power cycle, pumping system) have not been determined through economic optimization considering all of the component costs and their mathematical models and manner of integration.

The Salton Sea Solar Pond Power Plant concept became the focus of a publicly funded project in November, 1979 (French and Lin, 1981).

This project, which is sponsored by Southern California Edison and the State of California, has been highly publicized. The first phase of the project, the concept and feasibility study, was completed in 1981.

The results indicate that in-lake installation of a commercial power plant is technically feasible, environmentally acceptable, and economi-

cally attractive. The start-up of a 5 MW prototype unit is planned for 1984, to be followed in 1990 with the first of 600 MW (twelve 50 MW modules). The 5 MW plant will cost \$6,800 per kilowatt installed, while the commercial plant costs are below \$2,000 per kilowatt installed. In the commercial plant, the cost of the solar pond system is about 50% of the total cost, whereas in the 5 MW the pond system is about 75% of the total cost.

In June, 1982, a few pages of the Salton Sea Solar Pond feasibility study were made available to the author (French, 1982).

It seems that the design of the solar pond power plant system includes and optimization procedure through which optimal operating conditions and sizing of different systems' components is achieved. A request for obtaining the complete report on the feasibility study was turned down (French, 1982) and therefore it is not possible to comment on the methodology and optimization used in this study.

Calculations based on measured transmittance of Salton Sea brines show that the potential for electric power generation by a solar pond is strongly influenced by the fraction of radiation transmitted to the LCZ. Simple carbon treatment roughly quadrupled the expected electric power output of the Salton Sea pond. However, a brine sample from another site did not respond to carbon treatment. A preliminary cost estimate indicates that the capital costs for water treatment, of

which carbon treatment would be only a part, will be less than 10% of the capital cost of the Salton Sea 5 MW pond (Marsh et al, 1981).

A comprehensive assessment was made of the regional applicability and potential of salt-gradient solar ponds in the United States (Lin, 1982) . The report concluded that, excepting Alaska, ponds are applicable in all regions for at least two of the considered market sectors (residential, commercial and institutional buildings sector; industrial process heat sector; agricultural process heat sector; electric power sector; and desalination sector). on the basis of conservative exploitation of the available resources, the American national electric power pond potential is 3.46 quads / year . The study also concluded that a 5 MW solar pond power plant is competitive with a new oil-fired facility of the same capacity in the South west, Hawaii, and Puerto Rico regions (if pond cost can be held below  $50 \text{ s/m}^2$  , then ponds are also competitive in the Salt Lake, Red River, Gulf Coast, and Tennessee Valley regions); similarly, a 600 MW plant would be competitive with a coal-fired plant in the Southwest, Red River, and Hawaii.

()

THE PROPERTY OF

<sup>1</sup> quads =  $180 \times 10^6$  bbl (29 \*  $10^6$  m<sup>3</sup>) of petroleum =  $10^{11}$  Kwh, electrical

Argonne National Laboratory has recently completed two studies for a 5 MW power plant combining two developmental technologies, Solar Ponds (SP) and Ocean Thermal Energy Conversion (OTEC), into a hybrid system that offers potential advantages over either pure SP or pure OTEC system for production of electric power. The proposed SPOTEC concept uses a solar pond as a heat source instead of warm surface sea water, and deep ocean water for the heat rejection instead of pond surface water in the operation of a Rankine-Cycle system. The report does not include the system model-ling nor a cost estimate of the concept (Hillis et al, 1983).

()

For energy conversion applications involving a closed fluid cycle of the Rankine type, the maximum and the minimum cycle temperatures are dictated by the source and sink temperatures of that particular application. However, the selection of a working fluid or of a mixture of fluids, and the selection of the maximum and minimum cycle pressures, which in turn establishes the thermodynamic region of operation, involve a stupendous effort if they must be done in a manner optimizing performance. Thermodynamic properties charts and tables, based on accurate experimental data, are not available for some fluids, which require exclusion of these fluids from consideration. Even for the fluids where good data is available, to investigate all thermodynamic regions with each of the fluids is a very cumbersome task.

Pradhan and Larson (1980), developed a procedure for the analysis of power cycles based on the Generalized Properties of fluids. The method is suited to high speed digital computers.

It is shown that, for <u>initial</u> search purposes for new fluids, this method gives reasonable accuracy. The advantages of the method are its minimal data requirement for cycle analysis and ease of implementation on digital computers. The inaccuracy of the method (errors in efficiency assessment can be as high as 10%) is its main shortcoming. The method can only be recommended for initial evaluation of several alternative fluids:

The present thesis offers a simple method for the analysis of a Rankine cycle which is suitable for use with an optimization The method is based on approximating the thermodynamic properties such as enthalpy, entropy, etc. of the working fluid on the saturated vapor and liquid lines as a function of boiler and condenser These properties are expressed as polynomial functions temperatures. of the temperatures. The properties of the points not lying on the saturation lines are calculated using the first law of thermodynamics. The method is applicable to any fluid for which sufficient data is available in the form of charts or tables. The method is given preference to the Generalized Properties method for cycle analysis primarily for its excellent accuracy, although it requires more data input.

Bohn et al (1980), proposed the use of thermoelectric conversion in a new ocean thermal energy conversion concept. They described the concept and its advantages and provided a preliminary analysis of the performance and cost of a 400 MW thermoelectric OTEC plant.

In another work, Benson and Jayadev (1981), proposed the electric power generation by thermoelectric energy conversion for low grade heat systems such as OTEC, solar ponds, and geothermal. The efficiency of thermoelectric conversion (thermal to electrical) is at best 20 per cent of the theoretical Carnot efficiency. In spite of its greater reliability and freedom from maintenance requirements, this technology does not appear to be an economical alternative to the heat engine, the efficiency of which can reach more than 60 per cent of the Carnot cycle (Tabor, (1981); (see also Chapter III of the present thesis).

#### 1.4 Motivation for the Research

The present thesis is primarily concerned with the simulation and optimization of electric power generation by solar ponds.

The motivation for choosing the non-convecting solar pond for the purpose of electric power generation are as follows:

- solar energy in the multi-kilowatt multi-megawatt range,
  thereby filling the gap between classical solar collectors and very
  sophisticated satellite concepts now being studied for the gigawatt
  range. Electric power generation in the 500 KW to 5 MW or
  larger ranges by solar ponds is possible at estimated costs that are
  presently competitive with those of alternative technologies in areas
  not having an electricity grid and where the basic materials for pond
  construction (salt and water) are inexpensive.
- · Energy storage in the form of sensible heat is a built-in property of a solar pond power system; due to this unique feature, an annual load factor as high as 0.9 is possible, which is at least two times higher than that of any other solar system. The other important factor in favor of the solar pond technology is that the commercial status of this system is certainly better than that of any other collector system. While the other solar energy conversion systems are waiting for technical and economical break-through, the solar pond power system can be built in a cost effective way using the present technology and materials. In experiments with small solar ponds, temperatures greater than 106°C were obtained (Weeks et al, (1981) and thermal collection efficiencies greater than 15 per cent for heat extraction at 70°C to 90°C are achieved (Tabor, (1981)). 1,1

O

The decision to concentrate on simulation and optimization was motivated by the fact that this constitutes a special but important

aspect of solar pond research. All other reported research is so far concerned either with fundamental aspects of solar pond physics such as stability and radiation absorption, or solar pond applications other than electric power generation; when electric power generation is considered, it is not treated in a systematic basis. For example, solar pond sizing and optimization has in the past been achieved by repeated simulations, which does not permit the handling of a large number of variables which happens when optimizing a solar pond power plant system.

Although the basic problems associated with solar ponds were delineated by Tabor in 1963, the problem of solar pond power system optimization has not been properly investigated in the intervening two decades (Lin, (1982)).

## 1.5 Claim of Originality

To the best of the author's knowledge the following are the original contributions of this thesis to the solar pond technology:

Analytical solution of the governing equations of the solar pond thermal behavior for the three layer pond namely, NCZ , LCZ , and a lower insulation layer of finite depth underneath the pond.

- 2. Static Optimization of a solar pond power plant :
  - development of a method for very accurate power
     cycle analyses,
  - formulation of net electric power produced by the solar pond power plant taking into account actual pond, heat exchangers and thermal cycle characteristics,
  - determination of the optimal system component sizes
     and operating conditions for the above formulation.
- 3. Dynamic Optimization of solar pond power plant:
  - development of a semi-analytical method to arrive at optimal heat extraction and storage depth for sinusoidal excitation,
  - formulation of energy cost in the form of optimal control problem and its solution through discretization of control and using mathematical programming to obtain optimal control;
  - comparison of the optimal heat extraction for two different climates,
  - comparison of the two different working fluids (F-113 > and F-11) for solar pond power plants.

- Introduction of a new solar pond concept: the floating pond:
  - derivation of stability criterion of the floating structure for uniform salt concentration,
  - derivation of stability criterion of the floating structure for linear salt gradient,
  - Static Optimization of a floating solar pond power plant.
- 5. Introduction of ice storage concept for solar pond power plants:
  - thermal analysis of the ice storage and determination of its required size to meet the cooling requirement of a solar pond power plant,
  - determination of optimal heat extraction from solar pond power plant having an ice storage and achievement of major energy cost reduction by introducing the ice storage concept.
- 6. The solar pond power plant with underground storage concept:
  - development of the mathematical model and its solution using finite difference,

- optimization of the solar pond power plant with reversed operation,
- determination of optimal heat extraction from solar pond and optimal heat injection or extraction from underground.

#### 1.6 Outline of the Thesis

0

The remainder of this thesis is organized as follows:

Chapter II, prediction of solar pond thermal behavior, begins with the development of the governing equations of the pond's temperature from the fundamental laws of heat transfer. Then the analytical solution of the governing equations for sinusoidal excitations is derived. Parametric study of the analytical solution as well as static efficiency are presented. A numerical solution technique using finite differences is then attempted and the effect of ice coverage and variation of the sun's declination angle are discussed.

In Chapter III, the optimization of a solar pond power plant is achieved through mathematical modelling of the system's components and the use of an optimization routine to find optimal design and operating conditions. In this chapter a simple computerized method for power cycle analysis is developed. Then models of the

heat exchangers and auxiliary pumps are presented and discussed.

The chapter ends with examples of the optimization techniques developed and discusses the effects of different working fluids as well as climatic conditions on the yield and the energy cost of a solar pond power system.

tion and storage depth. It starts with a discussion of the assumptions used in the chapter, which are based on the results of Chapter III. A semi-analytical technique for the determination of an optimal time table of heat extraction and storage depth is then developed. Formulation of the problem as an optimal control problem is presented as an alternative to the semi-analytical method, and its solution through discretization of the control variable (heat extraction) is discussed. A numerical solution provides a comparison of the two methods.

introduces a new solar pond concept, the floating pond. The stability criterion of the floating structure is derived. The optimization of a floating solar pond power plant is then carried out and conclusions on the economic advantages of this type of pond over ordinary solar ponds are drawn. Next the ice storage concept is proposed as a cooling medium for the power plant. The sizing of an ice storage facility which meets the heat rejection requirements of

a solar pond power plant with a given capacity is achieved by simple thermal analysis. The complete system optimization is performed and its superior economics and performances over an ordinary solar gond power system are shown.

Chapter VI, entitled reverse operation: underground storage, starts with an introduction which is followed by the development of the governing equations. The model solution by a finite difference technique and the validation of the model's assumptions are then presented. The optimal heat extraction from the storage layer of the pond as well as optimal heat injection or extraction from underground are attempted in a manner similar to that presented in Chapter IV. An example of such a solar pond power plant is presented and concluding remarks are given.

0

Finally, in Chapter VII, the conclusions of the present thesis along with recommendations for further research are presented.

#### CHAPTER II

#### PREDICTION OF SOLAR POND THERMAL BEHAVIOR

## 2.1 Governing Equations of Pond Temperature Behavior

()

**(**}

As described earlier a solar pond will have three distinct layers, namely upper convective zone (UCZ), non-convecting zone (NCZ) or gradient layer or insulation layer, and lower convective zone (LCZ) or storage layer. In this section mathematical models of the above zones as well as the layer of ground underneath a solar pond will be developed and different solution techniques along with results and comparison of the different models will be discussed.

First, consider the NCZ which is bounded by the UCZ and LCZ (Figure 2.1). It is assumed that a stable salt gradient is present in the NCZ (due to dissolved salt) so that heat transfer can take place in this zone only by conduction. According to Fourier's law of conduction the heat flux vector  $\overrightarrow{q}$  is given by:

$$\dot{\vec{q}} = -\kappa_1 \nabla \tau_1$$

where  $K_1$  is the thermal conductivity and  $\nabla$   $T_1$  is the temperature gradient. Therefore the amount of heat flowing out of a closed surface can be given as follows:

$$\oint \cdot \overrightarrow{q} \cdot \overrightarrow{ds} = \oint (-\kappa_1 \nabla \tau_1) \cdot \overrightarrow{ds}$$
s

Applying the Divergence theorem to the above equation yields :

$$Q_{\text{cond}} = \oint_{S} \overrightarrow{q} \cdot \overrightarrow{ds} = \iiint_{V} \nabla \cdot (-K_{1} \nabla T_{1}) dV$$

where  $\hat{V}$  is the volume enclosed by the surface S. Therefore the heat flux flowing into the volume V due to conduction is:

$$Q_{cond} = \iiint \nabla \cdot (K_1 \nabla T_1) dV$$

The heat incident on the surface S due to solar radiation flux is given by:

$$Q_{\text{rad}} = - \oint_{S} \overset{\rightarrow}{q}_{\text{rad}} \cdot \overset{\rightarrow}{ds} = - \iiint_{V} \nabla \cdot \overset{\rightarrow}{q}_{\text{rad}} \cdot dV$$

The amount of heat in the volume, V can be expressed as

follows:

$$Q_V = \iiint_V \rho_1 c_1 T_1 dV$$

where  $\rho_1$  and  $C_1$  are density and specific heat of the brine. The time rate of change of heat in the volume V is given by:

$$\frac{\partial Q_{\mathbf{v}}}{\partial \mathbf{t}} = \frac{\partial}{\partial \mathbf{t}} \iiint_{\mathbf{v}} \rho_{1} C_{1} T_{1} d\mathbf{v}$$

Equating the heat flowing into the volume due to conduction and radiation to the rate of change of heat will result in the following:

$$Q_{cond} + Q_{rad} = \frac{\partial Q_{V}}{\partial t}$$

or,

$$\iiint_{\mathbf{V}} \left[ \nabla \cdot (\mathbf{K}_{1} \nabla \mathbf{T}_{1}) - \nabla \cdot \mathbf{q}_{\mathbf{rad}} - \frac{\partial}{\partial \mathbf{t}} (\rho_{1} \mathbf{C}_{1} \mathbf{T}_{1}) \right] d\mathbf{V} = 0$$

Assuming that the integrand is continuous, the above yields :

$$\frac{\partial}{\partial t} \left( \rho_1 C_1 T_1 \right) = \nabla \cdot \left( K_1 \nabla T_1 \right) + H_1 \tag{2.1}$$

where  $H_1$  is the source function (solar radiation) defined by :

$$H_1 = -\nabla \cdot \vec{q}_{rad}$$

for constant properties the above equation becomes :

$$\rho_1 c_1 \frac{\partial T_1}{\partial t} = K_1 \nabla^2 T_1 + H_1 \tag{2.2}$$

equation; for the time independent case it reduces to the Poisson equation and if the source term is ignored the Laplacian equation is obtained.

The governing equation for the ground below the LCZ will be the same as equation (2.1) with the difference that the source term will not be present:

$$K_2 \nabla^2 T_2 = \rho_2 C_2 \frac{\partial T_2}{\partial t}$$
 (2.3)

where subscript 2 refers to the ground layer physical properties.

The storage layer as mentioned earlier is a convective region and here it will be assumed that radiation reaching the top of this zone is absorbed completely in the LCZ, i.e., the radiation reflected by the pond bottom is not accounted for in our analysis 1. Taking the LCZ as a control volume the heat balance equation can be written as follows:

Viskanta (1978) considered the radiation reflection of the solar pond bottom. If the bottom of the pond has poor absorption coefficient then one has to take into account the bottom reflection losses.

$$A^{\rho}_{s} \stackrel{C}{=} \stackrel{\ell}{=} \frac{\partial T_{s}}{\partial t} = H - U - \oint_{s} (K_{1} \cdot \nabla T_{1} + K_{2} \cdot \nabla T_{2}) \cdot \overrightarrow{ds}$$

where A is the surface area of the pond. The first term (H) on the right hand side is heat absorbed due to radiation in LCZ and the second term is the useful heat (U) extracted from the LCZ and the last term represents the heat lost by conduction to the NCZ and ground.

In the following sections, analytical as well as numerical solutions to equations (2.2) - (2.4), in a single dimension, will be presented.

# 2.2 Analytical Steady State Solution with Sinusoidal Excitation

The model described in what follows is an extension of the one developed by Weinberger (1964) for a single layer pond (NCZ only), and later modified by Rabl and Nielsen (1975) for two layer ponds (NCZ and LCZ).

The analysis is strictly valid only for a pond of infinite area; ponds of finite area can however be modeled by incorporating edge (side) losses as a heat extraction term in the LCZ heat balance

equation (Crevier, 1981). It is assumed that solar radiation as well as the ambient air temperature are periodic with only one harmonic term. They consist in the superposition of an average component and a sinusoidally varying component; all have a period of one year, and are usually out of phase with each other (Nielsen, 1978). Since the solar pond provides long term storage, having large thermal inertia, it is insensitive to the hourly and daily variations of the radiation and ambient temperature (Crevier, 1980, Sodha et al, 1981). Solar radiation will arbitrarily be assigned a phase angle of zero. Solar radiation and ambient temperature will therefore be given by the following functions:

$$H_{s}(t) = \overline{H}_{s} + \widetilde{H}_{s} \cos \omega t \qquad (2.5)$$

$$T_a(t) = \bar{T}_a + \bar{T}_a \cos(\omega t - \delta_a)$$
 (2.6)

where the average value terms  $\vec{H}_s$ ,  $\vec{T}_a$ , and the amplitude terms  $\vec{H}_s$ ,  $\vec{T}_a$ , are assumed known. The phase angle  $\delta_a$  is the known phase difference of ambient temperature with respect to radiation. The summer solstice (June 21) corresponds to t=0, and the angular frequency  $\omega=\frac{2\pi}{1~{\rm year}}$  corresponds to a period of one year. The heat extraction rate from the LCZ of the pond will also be assumed to have the following sinusoidal form:

$$U(t) = \bar{U} + \hat{V} \cos (\omega t - \delta_{U})$$
 (2.7)

----- k

Depending upon the end application of the extracted heat the above formulation may or may not be a good approximation. The LCZ temperature will be a linear function of the excitations and should also take the form of a sinusoid with the same frequency (Carslaw and Jaeger, 1959):

$$T_s(t) = \tilde{T}_s + \tilde{T}_s \cos(\omega t - \delta_s)$$
 (2.8)

where  $\boldsymbol{\bar{T}}_{_{\boldsymbol{S}}}$  ,  $\boldsymbol{\dot{T}}_{_{\boldsymbol{S}}}$  , and  $\boldsymbol{\delta}_{_{\boldsymbol{S}}}$  are unknown yet to be determined.

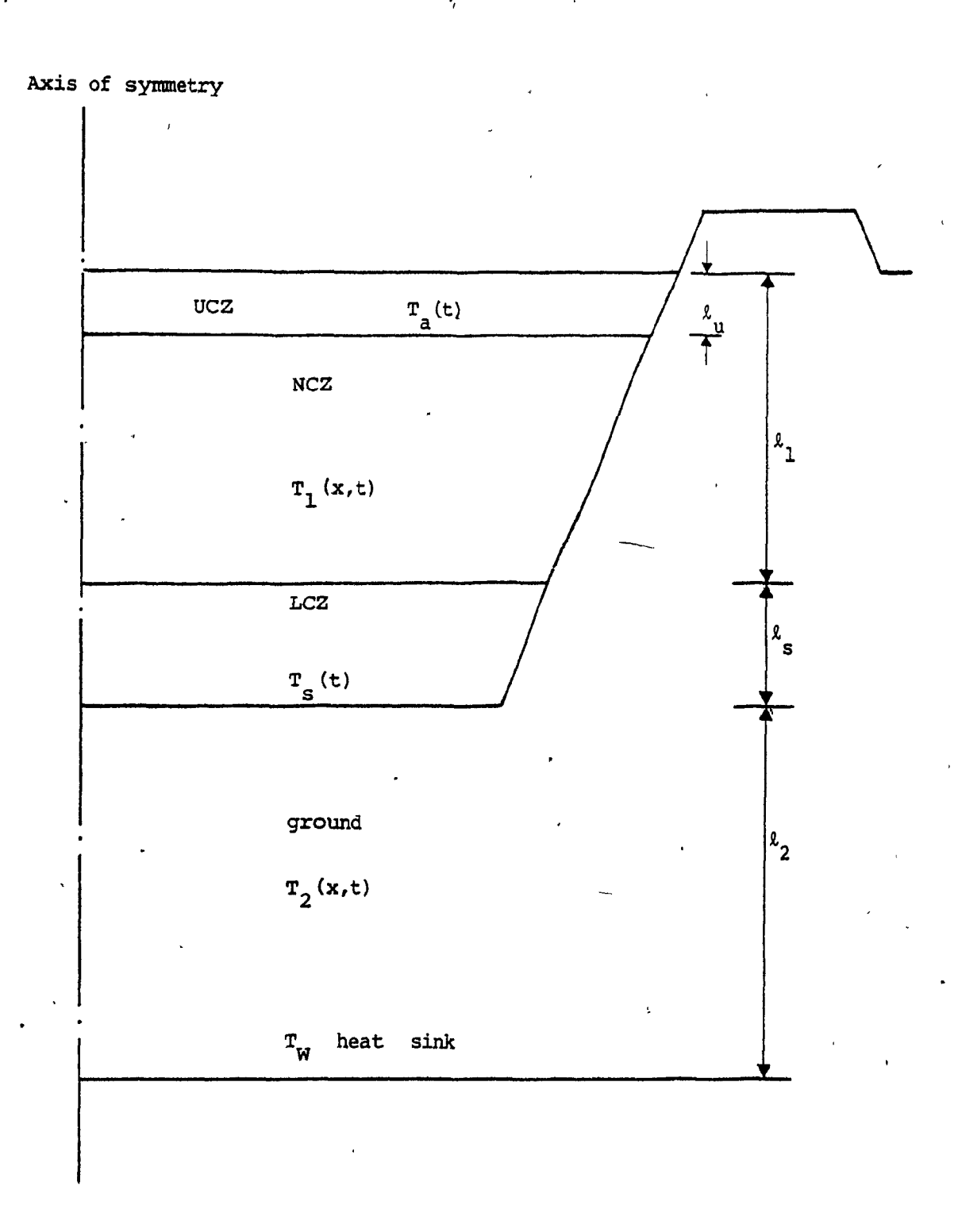
We will use, as described in Appendix A , the following combination of four exponentials as an approximation for the radiation reaching a depth  $\, x \,$  (measured positive downwards):

$$H(x, t) = \tau H_{s}(t) \sum_{n=1}^{\infty} \eta_{n} e$$
 (2.9)

where  $\tau$  is a coefficient of transmission, H(t) and  $\mu_n^*$  are given by equations (2.5) and (A.2) respectively.

The governing equations, (2.2) - (2-4), of the three layers namely NCZ, LCZ, and the ground underneath the pond, can be written in one dimension as follows (see Figure 2.1 for clarity of nomenclature). For the NCZ:

$$\frac{\partial T_1(x, t)}{\partial t} = \alpha_1 \frac{\partial^2 T_1(x, t)}{\partial x^2} - \frac{\alpha_1}{K_1} \frac{\partial H(x, t)}{\partial x}$$
 (2.10)



( }

(Î

Figure 2.1 Cross Section of a Solar Pond with corresponding Labels.

where  $\alpha_1$  is the thermal diffusivity of the brine given by :

$$\alpha_1 = \frac{K_1}{\rho_1 C_1}$$

with the boundary condition of :

$$T_1(\ell_u, t) = T_a(t)$$
 ,  $T_1(\ell_1, t) = T_s(t)$  (2.11)

where  $\ell_{\rm u}$  is the thickness of UCZ and  $\ell_{\rm l}$  is the distance of the bottom of NCZ from the surface, which is usually referred to as the extraction depth in the literature (Crevier, (1980)). For LCZ:

$$\rho_{s} C_{s} \ell_{s} \frac{d T_{s}(t)}{dt} = H(\ell_{1}, t) - U(t) - K_{1} \frac{\partial T_{1}(x, t)}{\partial x}$$

$$+ K_{2} \frac{\partial T_{2}(x, t)}{\partial x}$$

$$x = \ell_{1}$$

$$(2.12)$$

and finally the heat diffusion in the ground -:

$$\frac{\partial T_2(x, t)}{\partial t} = \alpha_2 \frac{\partial^2 T_2(x, t)}{\partial x^2}$$
 (2.13)

where  $\alpha_2$  is the thermal diffusivity of the soil. The boundary conditions can be expressed as:

$$T_2^{(l_1 + l_S, t)} = T_s^{(t)}, \quad T_2^{(l_1 + l_S + l_2, t)} = T_W$$
 (2.14)

where  $T_{\overline{W}}$  is the temperature of a heat sink assumed to be located at a finite distance from the ground level.

The solution of the governing equations will be carried out in parts, namely for time independent and time varying components.

# 2.2.1 Time Independent Solution

A time independent solution of the governing equations can easily be found by setting all time varying terms in equations (2.5) - (2.14) to zero. The equations then reduce to the following:

$$K_1 = \frac{d^2 T_1}{dx^2} = \frac{d}{dx} (\tau \tilde{H} \sum_{n=1}^{4} \eta_n e^{-\mu_n^* x})$$
 (2.15)

$$\tau \tilde{H}_{S} \sum_{n=1}^{2} \eta_{n} e^{-\mu_{n}^{*} \ell_{1}} - \tilde{U} - K_{1} \frac{d T_{1}}{dx}|_{x = \ell_{1}} + K_{2} \frac{d T_{2}}{dx}|_{x = \ell_{1} + \ell_{S}} = 0$$

(2,16)

$$\frac{d^2 T}{dx^2} = 0 {(2.17)}$$

The last equation upon simple integration yields (using boundary condition equation (2.14)):

$$K_2 \frac{d T_2}{dx}\Big|_{x = l_1 + l_3} = K_2 \frac{T_s - T_w}{l_2}$$
 (2.18)

Integration of equation (2.15) using the boundary condition (2.11) gives the following expression for the temperature gradient:

$$K_{1} \frac{d T_{1}}{dx}\Big|_{x = \ell_{1}} = \tau \tilde{H}_{s} \sum_{n=1}^{4} \eta_{n} e^{-\mu_{n}^{*}\ell_{1}} + \frac{\tau \tilde{H}_{s}}{\ell_{1}^{*}-\ell_{u}} \frac{\ell_{1}^{*}}{\ell_{1}^{*}-\ell_{u}} \frac{\ell_{2}^{*}-\tilde{H}_{1}^{*}}{\ell_{1}^{*}-\ell_{u}^{*}} + K_{1} \frac{\tilde{T}_{s} - \tilde{T}_{s}}{\ell_{1}^{*}-\ell_{u}}$$

$$(2.19)$$

Substitution of equations (2.18) and (2.19) into (2.16) gives the following result for  $\bar{T}_{c}$ :

$$\bar{T}_{s} = \frac{\bar{T}_{a} - \frac{\ell_{1} - \ell_{u}}{K_{1}} \bar{u} + \frac{\tau \bar{H}_{s}}{K_{1}} \frac{4}{n_{1}} \frac{\eta_{n}}{\mu_{n}^{*}} (e^{-\mu_{n}^{*} \ell_{u}} - e^{-\mu_{n}^{*} \ell_{1}}) + \frac{\kappa_{2}}{K_{1}} \frac{\ell_{1} - \ell_{u}}{\ell_{2}} T_{w}}{1 + \frac{\kappa_{2}}{K_{1}} \frac{\ell_{1} - \ell_{u}}{\ell_{2}}}$$
(2.20)

This solution reduces to the one given by Rabl and Nielsen (1975), when the depth of the heat sink tends to infinity and for no surface convective layer.

### 2.2.2 Time Dependent Solution

The calculation of the time dependent components  $\tilde{T}_S$  and  $\delta_S$  is rather tedious. The steady state temperature in the ground below the pond is given by Carslaw and Jaeger, (1959) :

$$\tilde{T}_{2}(x, t) = \tilde{T}_{S} e^{i(\omega t - \delta_{S})} \left\{ \frac{\sinh \left[ (l+i) \left( (l_{2} + l_{1} + l_{S} - x) / \sigma_{2} \right) \right]}{2 \sinh \left[ (l+i) \left( l_{2} / \sigma_{2} \right) \right]} \right\}$$

where  $\sigma_2 = \sqrt{2} \alpha_2 / \omega$  is the depth at which temperature oscillations of frequency  $\omega$  are damped to 1/e of their surface value; by analogy with electrodynamics,  $\sigma_2$  is called the skin depth. To find the temperature gradient at the top of LCZ we first calculate the steady state temperature in the NCZ due to its boundary conditions, equation (2.11), and due to absorption of radiation, by solving (2.10) for time varying terms which yields the following solution (Carslaw and Jaeger, 1959):

$$\begin{array}{l} \Upsilon_{1} = \Upsilon_{a} & \stackrel{\text{i } (\omega t - \delta_{a})}{=} & \frac{\sinh \left[ (1+i) \left( \ell_{1} - \ell_{u} - x \right) \ / \ \sigma_{1} \right]}{2 \sinh \left[ (1+i) \left( \ell_{1} - \ell_{u} \right) \ / \ \sigma_{2} \right]} \\ + \Upsilon_{s} & \stackrel{\text{i } (\omega t - \delta_{s})}{=} & \frac{\sinh \left[ (1+i) \left( x \ / \ \sigma_{1} \right) \right]}{2 \sinh \left[ (1+i) \left( \ell_{1} - \ell_{u} \right) \ / \ \sigma_{1} \right]} \\ + \frac{\tau \mathring{H}_{s}}{2 \ K_{1}} & \frac{4}{n=1} & \frac{\eta_{n}}{\mu_{n}} & e^{-\mu_{n}^{*} \ell_{u}} \left( \frac{e^{i\omega t}}{1 - \left[ 2i \ / \ (\mu_{n}^{*2} \sigma_{1}^{2}) \right]} \right) \end{array} .$$

The substitution of equations (2.21) and (2.22) into (2.12) will yield a solution for  $\overset{\sim}{T}_S$  and  $\delta_S$ ; the results are as follow:

$$\frac{\tilde{T}_{s}}{(\frac{K_{1}}{\sigma_{1}} E_{2+} + \frac{K_{2}}{\sigma_{2}} E_{3+}) (\cos \delta_{s} + E_{4} \sin \delta_{s})}$$

and °

$$\delta_{S} = \arctan \left(\frac{E_{5} + E_{4} E_{1}}{E_{1} - E_{4} E_{5}}\right)$$

where :

$$E_{2+} = \frac{\sinh \left[ 2(\ell_1 - \ell_u) / \sigma_1 \right] + \sin \left[ 2(\ell_1 - \ell_u / \sigma_1) \right]}{\cosh \left[ 2(\ell_1 - \ell_u) / \sigma_1 \right] - \cos \left[ 2(\ell_1 - \ell_u) / \sigma_1 \right]}$$

$$E_{3+} = \frac{\sinh (2l_2/\sigma_2) + \sin (2l_2/\sigma_2)}{\cosh (2l_2/\sigma_2) - \cos (2l_2/\sigma_2)}$$

$$E_{4} = \frac{\rho_{S} c_{S} l_{S} \omega + (K_{1} / \sigma_{1}) E_{2-} + (K_{2} / \sigma_{2}) E_{3-}}{(K_{1} / \sigma_{1}) E_{2+} + (K_{2} / \sigma_{2}) E_{3+}}$$

$$E_{1} = \tau \sqrt{\frac{n}{n}} \sum_{n=1}^{\infty} \eta_{n} e^{-\mu_{n}^{*}(\ell_{1} - \ell_{u})} - \sqrt{u} \cos \delta_{u} + (2 K_{1} / \sigma_{1}) \cdot \tilde{T}_{a}$$

$$= (E_{6+} \cos \delta_a - E_{6-} \sin \delta_a) + E_7$$

$$E_5 = -\tilde{U} \sin \delta_u + (2 K_1 / \sigma_1) \cdot \tilde{T}_a \cdot (E_{6+} \sin \delta_a + E_{6-} \cos \delta_a) + E_8$$

where :

$$E_{6+} = \frac{\sin[(\ell_1 - \ell_u)/\sigma_1] \cdot \cosh[(\ell_1 - \ell_u)/\sigma_1) + \sinh[(\ell_1 - \ell_u)/\sigma_1] \cdot \cos[(\ell_1 - \ell_u)/\sigma_1]}{\cosh[2(\ell_1 - \ell_u)/\sigma_1] - \cos[2(\ell_1 - \ell_u)/\sigma_1]}$$

$$E_{7} = \tau H_{S} \sum_{n=1}^{4} \frac{\eta_{n}}{1 + 0.25 (\mu_{n}^{*} \sigma_{1})^{4}} \left\{ -\frac{(\mu_{n}^{*} \sigma_{1})^{4}}{4} e^{-\mu_{n}^{*} (\ell_{1}^{*} - \ell_{u})} + (\mu_{n}^{*} \sigma_{1}^{*}) \right\}$$

$$\cdot \left[ \frac{(\mu_{n}^{\star}\sigma_{1})^{2}}{2} E_{6+} + E_{6-} + 0.5 \cdot e^{-\mu_{n}^{\star}(\ell_{1}-\ell_{u})} (E_{2-} - \frac{(\mu_{n}^{\star}\sigma_{1})^{2}}{2} E_{2+})\right] \right\}$$

$$E_{8} = \hat{\tau} \stackrel{\gamma}{H}_{S} \stackrel{4}{\sum_{n=1}^{2}} \frac{\eta_{n}}{1 + 0.25 (\mu_{n}^{*} \sigma_{1})^{4}} \left\{ \frac{(\mu_{n}^{*} \sigma_{1})^{2}}{2} e^{-\mu_{n}^{*} (\ell_{1}^{*} - \ell_{u})} + (\mu_{n}^{*} \sigma_{1}) \right\}$$

$$\cdot \left[ \frac{(\mu_{n}^{*}\sigma_{1})^{2}}{2} E_{6-} - F_{6+} + 0.5 e^{-\mu_{n}^{*}(\ell_{1}^{-}\ell_{u})} \left( \frac{(\mu_{n}^{*}\sigma_{1})^{2}}{2} E_{2-} + E_{2+}^{(\ell_{1}^{*})} \right) \right]$$

# 2.3 Examples

11

The analytical solution developed in the previous section will be used to predict the thermal behavior of solar ponds located in Montreal, Canada and Shiraz, Iran. The climatic data for Montreal was obtained from the Department of Meteorology of McGill University and the data for Shiraz from Akbarzadeh and Ahmadi (1980). Table 2.1 shows the data for the two locations.

, TABLE 2.1
CLIMATIC DATA FOR MONTREAL AND SHIRAZ

Location	Latitude Ambient Temperature (°C)			Solar Radiation $(\frac{W}{m^2})$			
•	(Degrees)	Average	T <sub>a</sub>	Amplitude $\overset{\sim}{\mathtt{T}}_{a}$	Average H	Amplitude H	
Montreal	45.45	5.5		15.0	150.0	110.0	
Shiraz	32.0 <b>4</b>	17.3	•	11.3	210.16	81.84	

In the following examples the rate of heat extraction is arbitrarily assumed to be as follows unless otherwise stated:

$$\overline{\overline{U}} = 0.2 \overline{\overline{H}}_{S}$$
 ,  $\widetilde{\overline{U}} = 0.5 \overline{\overline{U}}$  , and  $\delta_{u} = 90^{\circ} = 13$  weeks

The area of the pond is taken as 1 km<sup>2</sup> and the depth of the UCZ is set at 0.2 meter, which seems to be the minimum value achievable in practice (Crevier, 1980). The temperature of the heat sink is assumed to be the same as the average ambient temperature. Table 2.3 summarizes the results of the analytical solution for two considered locations.

( )

The results presented in Table 2.2 reveal the following facts:

- (1) The depth of the UCZ plays a very important role in the performance of a solar pond. Comparison of cases 8 and 10 shows that higher temperatures can be obtained when there is no UCZ, i.e., for the same operating temperatures a pond without UCZ yields higher efficiency. Therefore, control of UCZ thickness is certainly a must for good performance of a solar pond. UCZ has an effect on the average, amplitude, and phase lag of the LCZ temperature.
- (2) Thickness of the NCZ, which is the thermal insulator of a pond, will have an optimal value which yields maximum LCZ temperature (cases 1 19).
- (3) The depth of the storage layer has a stronger effect on the amplitude than on the average of the LCZ temperature. In fact the LCZ thickness should not have any effect on average temperature. The

SUMMARY OF THE RESULTS FOR ANALYTICAL SOLUTION

A = 1	Km <sup>2</sup> ,	2 =	0.2 m ,	<b>ū</b> = 3	30 MWt ,	ν = 15 <b>M</b> Wt	$\delta_{\rm u} = 13$ weeks
Location	Case	<sup>l</sup> 1 (m)	l (m)	T <sub>s</sub> (°C)	r̃s(°c)	δ (weeks)	Remarks
Montreal	1	0.8	1	34.07	28.46	5.59	$T^{M} = 62.53   T^{M} = 5.61$
	2	8.0	2	33.66	21.57	7.41	$T^{M} = 55.23   T^{m} = 12.09$
	<b>.</b> 3	0.8	3	33,13	16.96	8.5	$T^{M} = 50.09   T^{M} = 16.17$
,	4	8.0	. 5	31.48	11.70	9.71	$T^{M} = 43.18   T^{m} = 19.78$
	5	1.0	<b>1</b> ·	37.71	. 26.96	6.24	$T^{M} = 64.67   T^{M} = 10.75$
	6	1.0	2	37.09	19 76	7,89	$T^{M}_{,} = 56.85 \qquad T^{m} = 17.33$
	7	1.0	3	36.29	15.31	8.84	$T^{M} = 51.6$ $T^{m} = 20.98$
	8	1.2	. 1	39.33	24.88	6.72	$T^{M} = 64.21   T^{m} = 14.45$
e	9	1.2	1	46.25	24.88	6.72	$T^{M} = 71.13   T^{m} = 21.37$
•			. •		ì	<u> </u>	for $\ell_2 = \infty$
•	10	1.2	1 .	52.0	25.69	7.35	$T^{M} = 77.69 \qquad T^{m} = 26.31$
· 19	<b>₽</b>				`		for $\ell_{\mathbf{u}} = 0$

TABLE 2.2 (cont'd)

Location	Case	£ <sub>1</sub> (m)	l <sub>s</sub> (m)	τ̄ <sub>s</sub> ( <sup>o</sup> c)	. T <sub>S</sub> (°C)	δ <sub>s</sub> (weeks)	Remarks
Montreal	11	1.2 1	39.33	32.76	9.04	$T^{M} = 71.09   T^{m} = 6.57$ $\delta_{11} = 180^{O} = 26 \text{ weeks}$	
•	12	1.2	2	38.51	/ 17.94	8.22	$T^{M} = 56.45$ $T^{m} = 20.57$
	13	1.2	3	37.46	13.82	9.07	$T^{M} = 51.28   T^{M} = 23.64$
	14	1.4	1	39.37	22.56	7.09	$T^{M} = 61.93   T^{M} = 16.81$
	15	1.4	2	38.37	16.18	8.48	$T^{M} = 54.55$ $T^{m} = 22.19$
	16	1.4 .	3	37.1	12.45	9.25	$T^{M} = 49.55   T^{m} = 24.65$
	17	1.6	1	38.16	20.26	7.38	$T^{M} = 58.42 \cdot T^{M} = 17.9$
	18	1.6	2	37.01	14.49	8.68	$T^{M} = 51.5$ $T^{m} = 22.52$
	19	1.6	3	35.57	* 11.15	9.40	$T^{M} = 46.72   T^{m} = 24.42   .$
Shiraz	20	0.8	2	57.78	17.12	5.69	$T^{M} = 74.9   T^{M} = 40.66$
	21	1.0	. 2	63,07	15.97	6.01	$T^{M} = 79.04   T^{m} = 47.1$
	22	1.2	2	65.54	14.73	6.17	$T^{M} = 80.27   T^{m} = 50.81$
	23	1.4	· 2	65,78	13,49	6.25	$T^{M} = 79.27   T^{m} = 52.29$
	24	1.6	<b>.</b> 2	64.27	12.27	6.24	$T^{M} = 76.54   T^{M} = 52.0$
			•	No.			•

THE REPORT OF THE PARTY OF THE

decrease in LCZ average temperature with its thickness that can be observed in Table 2.2 is due to the fact that in our model, the bottom heat sink is assumed to be at a fixed depth. Making the pond deeper thus brings its bottom closer to the heat sink which increases conductive losses. Increasing LCZ thickness reduces the amplitude of the LCZ temperature but this requires more salt and for the locations where salt is expensive the economic advantage of a solar pond may very well disappear.

- (4) The thermal conductivity of the ground underneath a solar pond as well as the depth of the heat sink can affect the performance of a pond to a great extent. Comparison of cases 8 and 9 shows that if the depth of the heat sink tends to infinity, the pond will not suffer from bottom losses in the steady state operation and performs better than when the heat sink is at a finite depth.
- (5) The scheduling of the heat extraction also plays an important role in determining the thermal behavior of a pond. This question will be investigated in detail in Chapter IV; it is however clear from Table 2.2 that a different maximum pond temperature will be obtained if heat is extracted at different times (cases 8 and 11).
- (6) Comparison of the thermal behavior of the ponds located in Montreal and Shiraz (cases 1 - 19 and 20 - 24) reveals that because of higher insolation in Shiraz, ponds perform better there than in Mon-

treal. For the same operating LCZ temperature ponds will have smaller efficiency in Montreal than in Shiraz.

# 2.4 Static Efficiency

Definition: We shall define the static efficiency of a solar pond as the ratio of the average heat extracted to the average value of the solar radiation incident upon the pond surface :

Equation (2.20) can be rewritten as follows:

$$\vec{v} = \frac{\vec{x} \cdot \vec{k} \cdot \vec{F}}{\ell_1 - \ell_2} + \frac{\kappa_2}{\ell_2} (\vec{T}_s - T_w) + \frac{\kappa_1}{\ell_1 - \ell_2} (\vec{T}_s - \vec{T}_a)$$

where

$$F = \sum_{n=1}^{4} \frac{\eta_n}{\frac{\pi}{n}} (e^{-\mu_n^* \ell_u} - e^{-\mu_n^* \ell_1})$$

Therefore the static efficiency becomes :

$$\eta_{S} = \frac{\tau F}{\ell_{1} - \ell_{u}} - \frac{\kappa_{2}}{\ell_{2}} * \frac{(\bar{T}_{S} - T_{W})}{\bar{H}_{S}} - \frac{\kappa_{1}}{\ell_{1} - \ell_{u}} \frac{\bar{T}_{S} - \bar{T}_{a}}{\bar{H}_{S}}$$
(2.23)

The maximization of the static efficiency with respect to depth of NCZ for a given climatic condition can be performed by setting the derivative of the static efficiency with respect to the depth of the NCZ to be zero. The resulting non-linear equation can not be solved in closed form and a numerical solution technique must be used.

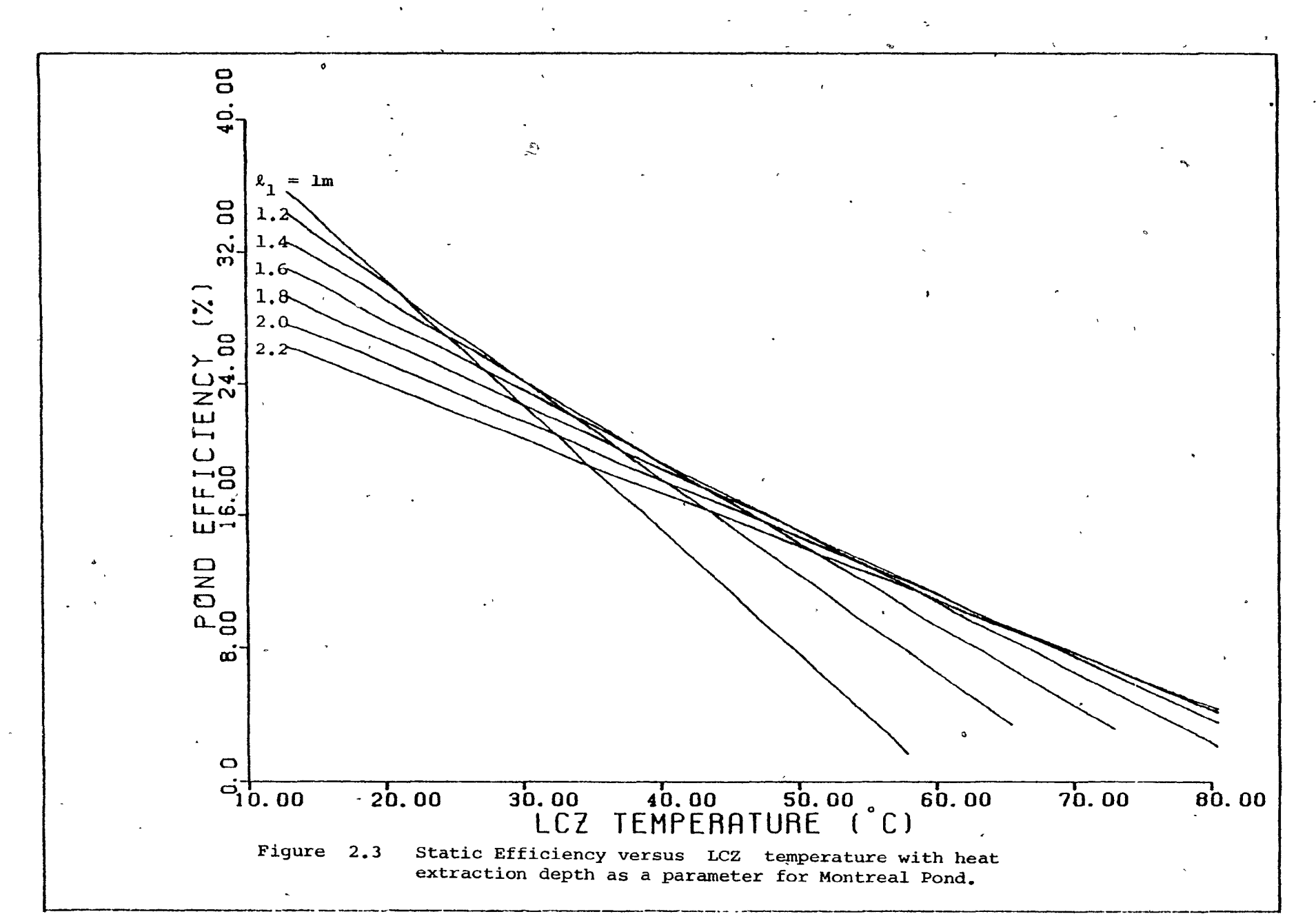
Figure 2.2 shows the variation of conduction losses, radiation penetrating to the bottom of the NCZ , and efficiency as a function of heat extraction depth. Figure 2.2 assumes a value of 0.25  $\frac{^{\text{O}}\text{C} \cdot \text{m}^2}{\text{W}}$  for the parameter  $\frac{\Delta}{\text{H}_S}$ , where  $\Delta$  T is the temperature difference between the LCZ and UCZ . This value of  $\Delta$  T /  $\overline{\text{H}}_S$  implies an average storage temperature of 43°C for Montreal conditions. The optimal NCZ thickness corresponds to an optimal compromise between its insulating properties, which would lead one to make it as thick as possible, and the amount of radiation that it absorbs and prevents from reaching the LCZ , which would be minimized by making the NCZ as thin as possible. Therefore there is an optimum value for  $\ell_1$  which maximizes efficiency. For the case at hand a value of 1.575 meters gives a maximum efficiency of 18.2% .

Maximization of efficiency with respect to depth of the heat sink is achieved when this thickness tends to infinity, as was observed in Table 2.2 .

Equation (2.23) shows that static efficiency is a linear function of  $\overline{T}_S$  and in Figure 2.3 this variation for different values of NCZ thickness is shown. Figure 2.3 suggests that the yield of a solar pond could be increased if it were possible to vary the thickness of the non-convecting zone as a function of the pond temperature and climatic conditions. The optimal value of the NCZ thickness is determined by the parameter  $\Delta$  T /  $\overline{H}_S$ . Assuming constant values for ambient temperature and solar radiation, Figure 2.3 indicates how the pond efficiency can be maintained at the optimum value as it heats up by making the NCZ depth equal to the value characterized by the straight line tangent to the optimal efficiency curve at the given pond temperature.

#### 2.5 Numerical Solution Using Finite Difference Technique

The analytical solution presented in the previous sections involves a large number of approximations. For example, when the thermal load can not be well approximated by a sinusoid or the pond surface is covered with ice, the analytical solution becomes far more complex. Simulation is required to determine the pond's thermal performance under realistic conditions. A reasonably accurate picture of its thermal regime can be obtained by using the finite difference technique, which is a standard method for thermal analysis. Here the pond's tempera-



ture is computed with respect to both time and depth. This procedure has the advantage of specifically including the start-up transient period and time required to reach steady state behavior. Variable thermal properties as a function of temperature and salinity can also be included in the model fairly easily.

This section begins by defining some of the finite difference operators, as well as relations between them and the differential operator.

Finite difference equations arise as approximations to ordinary and partial differential equations, the solution of which cannot easily be found analytically, especially in the case of coupled equations.

Let y = y(x) be a function of the real variable x. The first forward and backward difference operators are defined (Korn and Korn, 1968) by:

$$\Delta y \stackrel{\Delta}{=} y(x+h) - y(x)$$

$$\nabla y \stackrel{\Delta}{=} y(x) - y(x - h)$$

where  $h=\Delta \; x$  is a fixed increment of x . The central difference  $\delta$  is given by :

$$\delta y = y(x + 1/2 h) - y(x - 1/2 h)$$

Furthermore, the displacement operator (shift) and its inverse are defined by :

$$E y \stackrel{\triangle}{=} y(x + h)$$

$$E^{-1}y \stackrel{\Delta}{=} y(x - h)$$

Let us define the differential operator D , by the following relation :

$$D y \stackrel{\Delta}{=} \frac{d y}{d x}$$

The connection between the difference and differential operators is provided by Taylor's theorem:

$$E y = y(x + h) = y(x) + h D y(x) + \frac{h^2}{2!} D^2 y(x) + \dots$$

$$= (1 + hD + \frac{(hD)^2}{2!} + \dots) y(x) = e^{hD} y(x)$$

Therefore,

$$E = e^{hD}$$

The various operators can be shown (Korn and Korn, 1968) to have many relations among themselves, for example:

$$E = 1 + \Delta$$
 ,  $E^{-1} = 1 - \nabla$  ,  $\delta = E - E = 2 \sinh(1/2 \text{ hD})$ 

D = 
$$\frac{1}{h}$$
 Ln E =  $\frac{1}{h}$  Ln (1 +  $\Delta$ ) =  $-\frac{1}{h}$  Ln (1 -  $\nabla$ ) =  $\frac{2}{h}$  sinh 1/2  $\delta$ 

and,

$$D^{n} = \frac{1}{h^{n}} [\Delta - 1/2 \Delta^{2} + 1/3 \Delta^{3} - \dots]^{n}$$

Higher order difference operators are obtained by expressing them in terms of the shift operator and / or its inverse and then making use of the Binomial theorem.

Many difference approximations are possible for a given differential equation. The selection of a particular difference
relation is usually determined by the nature of the truncation error
associated with the approximation. The following difference relations
were used in our analysis.

First order difference for first differential operator :

Second order difference for first differential operator :

$$D y(x) = \frac{1}{2h} [-3 y(x) + 4 y(x + h) - y(x + 2h)] + 0(h^{2}) SFD$$

$$= \frac{1}{2h} [3 y(x) - 4 y(x - h) + y(x - 2h)] + 0(h^{2}) SBD$$
(2.27)

and for the second differential operator :

$$D^{2} y(x) = \frac{1}{h^{2}} [y(x+h) - 2 y(x) + y(x-h)] + 0(h^{2})$$
 CD

The diffusion equation of the form  $\alpha \frac{\partial^2 y(x, t)}{\partial x^2} = \frac{\partial y(x, t)}{\partial t}$  can be approximated as follows:

$$y(x, t+k) - y(x, t) = \frac{\alpha k}{h^2} \{ \epsilon [y(x+h, t+k) - 2y(x, t+k) + y(x-h, t+k)] + (1-\epsilon)[y(x+h, t) - 2y(x, t) + y(x-h, t)] \} + O(kh^2 - k^2)$$
 (2.28)

The above approximation is the weighted sum of the central differencing at times t+k and t; where  $k=\Delta$  t is the time increment step and  $\alpha$  is the coefficient of diffusivity. The parameter  $\epsilon$  is called the degree of implicitness. When  $\epsilon=0$ , the difference is said to

В

be fully explicit, and  $\varepsilon = 1$  fully implicit. It can be shown (Hildebrand, 1968) that the fully explicit differencing for the above diffusion equation is numerically stable if the following relation holds:

$$\frac{\alpha k}{h^2} \le 1/2$$

In case of a solar pond if we take h = 0.1 m the above stability criterion would restrict the time step, k, to 9.5 hours (for  $\alpha = 0.144 \times 10^{-6}$  m<sup>2</sup> / sec) which would make the computation numerically inefficient. We have used the Crank and Nicholson approximation ( $\epsilon = 1/2$ ) for which the solution of diffusion equation is unconditionally stable (Hildebrand, 1968).

The governing equations (2.10), (2.12), and (2.13) have been discretized using equations (2.24), (2.25) and (2.28). The resulting finite difference equations can be written as follows:

UCZ: for j = 1, m

$$T_0 = T_a(t + j \cdot k)$$
 (2.29)

NCZ: for i = 1,  $n_1$ 

where  $m = \frac{TMAX}{k}$  and TMAX is the simulation period and :

$$f_1 = \frac{\alpha_1 k}{2(h^2 + \alpha_1 k)}$$

$$f_2 = \frac{h^2 - \alpha_1 k}{h^2 + \alpha_1 k}$$

and  $n_1 = \frac{\ell_1 - \ell_u}{h}$  is the number of space intervals in the NCZ.

LCZ:

where  $i = n_1 + 1$  represents the storage layer (only one sublayer is considered for LCZ since it is a convecting zone). The other coefficients are as follows:

$$f_3 = \frac{\rho_S C_S l_S}{k} + \frac{k_1}{2h} + \frac{k_2}{2h}$$
,  $f_4 = \frac{k_2}{2h}$ ,  $f_5 = \frac{k_1}{2h}$ 

and

$$f_6 = \frac{{}^{\rho} s {}^{C} s {}^{k} s}{k} - {}^{\prime} f_4 - f_5$$

Finally, in the ground underneath the pond:

for 
$$i = n_1 + 2$$
,  $n_1 + 2 + n_2$ 

where  $n_2 = \frac{l_2}{h}$  is the number of space intervals in the ground and

$$f_7 = \frac{\alpha_2 k}{2(h^2 + \alpha_2 k)}$$
,  $f_8 = \frac{h^2 - \alpha_2 k}{h^2 + \alpha_2 k}$ 

and the boundary condition of : #

1-

$$j+1$$
 $T_{i+1} = T_W$ 
,  $i = n_1 + 2 + n_2$  (2.33)

The set of equations (2.30) - (2.32) constitutes a system of simultaneous equations with a coefficient matrix of tridiagonal structure. These equations in compact form can be written as follows:

$$j+1$$
A  $\underline{T} = \underline{b}$  for  $j = 1$ , m

where T is the vector of temperatures at nodal points;

A and <u>b</u> are coefficient matrix and right hand side vector respectively, given by the following:

1 - f<sub>1</sub> 1 1

1 Tn1+n2+2

 $T_{n_1+1}^{j+1}$ 

 $T_{n_1+2}^{j+1}$ 

<u>T</u>j+1

60

The solution to the aforementioned simultaneous equations can be obtained either directly or iteratively. A direct solution technique was chosen because the coefficient matrix has a tridiagonal structure and does not change with time. Therefore using LU decomposition (Stewart, 1973), the matrix A is decomposed into a lower and upper diagonal matrix where solution at each time can easily be obtained by a forward and backward substitution. The algorithm can be written as follows:

The accuracy of the finite difference scheme discussed in this section was verified by using it to solve several boundary value problems for which analytical solutions were available, including the analytical solution of solar pond model presented in the previous sections.

## 2.5.1 Comparison of Numerical and Analytical Solutions

The numerical solution by finite difference was tested for the same conditions as in case 12 of Table 2.2. The results of the simulation are compared with those of the analytical solution in Table 2.3. A time step of one week and spatial increment of 10 cm were considered. It can be seen from Table 2.3 that results of the difference scheme are in good agreement with the analytical solution.

TABLE 2.3

COMPARISON OF ANALYTICAL AND NUMERICAL SOLUTION

1 .	Analytical	Numerical (Finite Difference)		
T <sub>S</sub>	38.51	38.01		
Ťs (°C)	17.94	18.35	,	
δ <sub>S</sub> (weeks)	8.22	8.0		

Simulations showed that the steady state behavior is reached after four years of operation (assuming that steady state is reached when the difference between temperatures for two consecutive years is less than 0.5  $^{\circ}\text{C}$ ).

### 2.5.2 Effects of Ice Coverage and Sun's Declination Angle

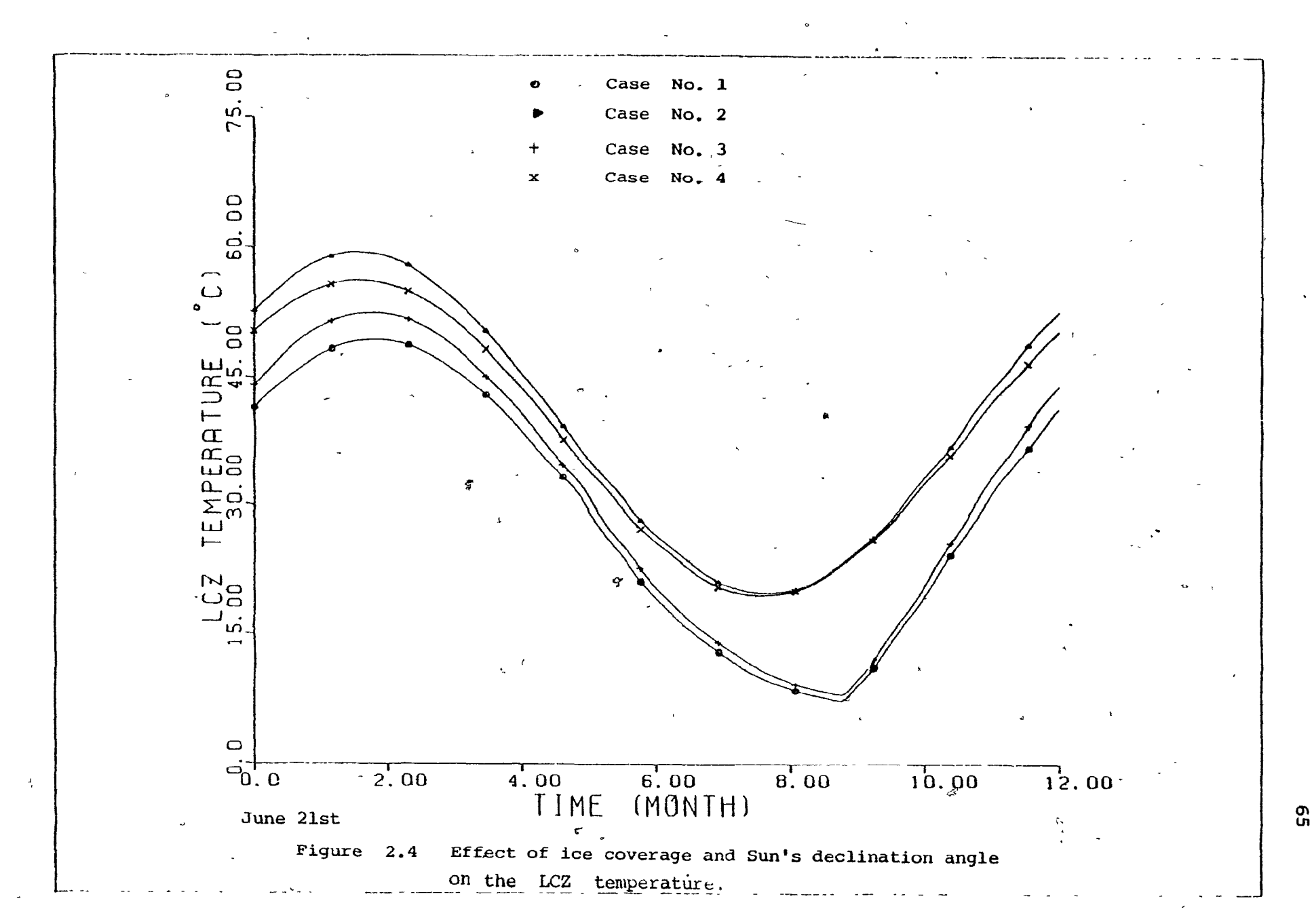
The following simulations were carried out to determine the effects of ice coverage of the pond surface and also variation of the sun's declination angle. The four curves shown in Figure 2.4 correspond to the following conditions:

Curve No. 1 represents the thermal behavior of a pond which is covered with ice whenever the ambient temperature falls below - 2 °C (the freezing point of 3% brine); it is assumed that ice is blocking 80% of the solar radiation.

Curve No. 2 corresponds to a pond model taking into account the variation of the sun's declination angle throughout the year, but assumes no ice coverage.

Curve No. 3 assumes a varying declination angle and ice coverage.

Curve No. 4 finally corresponds to a pond with no ice coverage and a fixed declination angle taken to be that occurring at the spring equinox (Rabl and Nielsen, 1975).



The average, amplitude, and phase lag of the above mentioned cases are summarized in Table 2.4. Comparison of cases 2 and 4 shows that assumption of constant sun's declination angle does not affect the LCZ temperature considerably and it is only a conservative assumption. Ice coverage of the pond surface as it was expected yields lower LCZ temperatures because of lower radiation during ice coverage. (It should be noted that ice coverage of the pond's surface will reduce the upward conduction losses since the UCZ remains at the equilibrium temperature between ice and UCZ brine).

TABLE 2.4

COMPARISON OF LCZ TEMPERATURES FOR CURVES IN FIGURE 2.4

Curve No.	1	2	3	4	,
T <sub>s</sub> (°c)	28.23	39.68	30.23	38.01	
T <sub>s</sub> (°C)	21.2	19.68	22.34	18.35	
δ <sub>s</sub> " (weeks)	9	8	9	8	

\_\_\_\_

in,

#### CHAPTER III

### OPTIMIZATION OF A SOLAR POND POWER PLANT

#### PART I: STATIC OPTIMIZATION

#### 3.1 Introduction

As pointed out by E.I.H. Lin (1982), Solar Pond Power Plant (SPPP) system simulation and optimization has barely been addressed in the literature. Adequate attention was not paid to the subject. In terms of the economics of a SPPP, the effect of the pond's performance alone (as defined in a previous chapter) may be misleading. It is actually the performance of the entire pond system, including the power generation equipment, that should be translated into pond energy economics. This chapter presents a basis for the systematic simulation and optimization of a Solar Pond Power Plant (SPPP).

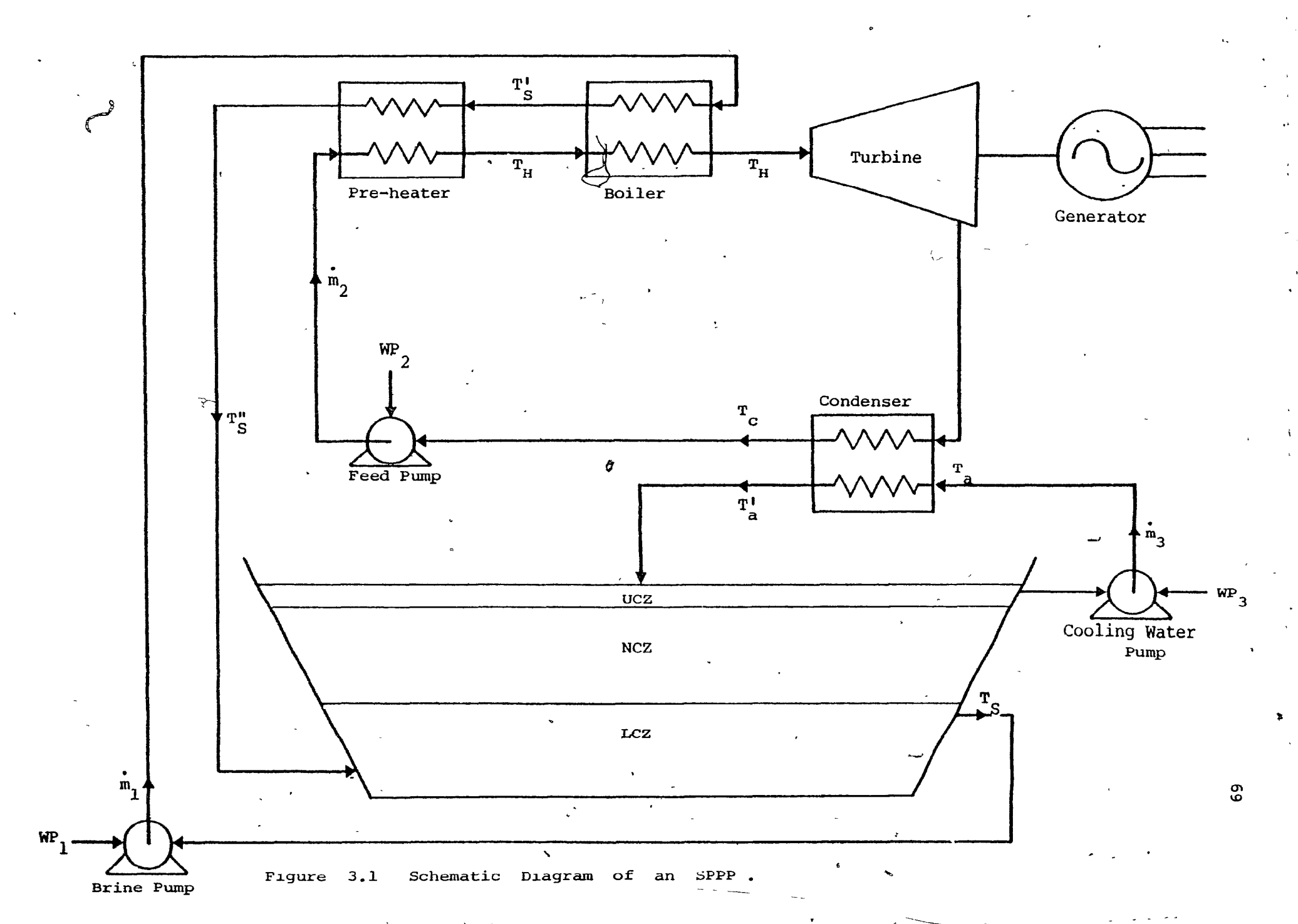
# 3.2 A Solar Pond Power Plant (SPPP)

A source of heat, even at moderate temperatures, can be converted to mechanical or electrical power. The process will be economically viable, if the calorie cost is sufficiently low. Solar ponds, being usually a cheap solar collector and having built-in storage, are attractive devices for electric power generation. Unlike

the temperatures obtained in fossil-fuel combustion, those obtained from solar ponds are relatively low. For this reason a low temperature turbine with motive (working) fluid other than steam should be used in a SPPP (Bronicki, 1972). Organic fluids, such as Freon, with boiling points lower than that of water can be used as working fluids in the Rankine Cycle heat engine (Bronicki, 1982).

Before going into modeling of the SPPP elements we first describe how it works in principle. A pump extracts hot brine from the LCZ on one side of the pond and propels it through an evaporator and preheater before returning it to the other side of the pond. In the evaporator, the hot brine turns an organic liquid into vapor. The vapor expands in a turbine, which drives a generator producing electric power. In the condenser the vapor turns into liquid. A feed pump returns the condensed liquid into the pre-heater and then back to the boiler to complete the cycle. Cooling water, which may be pumped from the UCZ of the pond or any other convenient cold sink, cools the condenser.

In order to predict the performance of an SPPP, one has to model the solar pond, heat exchangers, auxiliary pumps, and the power cycle which converts the thermal energy into useful shaft work. The resulting model equations can then be used to optimize the power genera-



tion costs. The cost optimization procedure has been decomposed into two steps:

- (a) The examination of the system components and the formulation of their mathematical models and governing equations in terms of thermodynamic, geometric and economic parameters.
- (b) The solution of the mathematical model using an optimization program with the help of a digital computer.

Steps (a) and (b) above will be performed for static conditions of solar radiation and ambient temperature. If these conditions are chosen in such a way as to represent the average for the period when the pond is in operation, basic system parameters such as turbine inlet and outlet pressures, heat exchangers and pond surface areas and depth of NCZ, can be determined by this procedure.

## 3.3 Power Cycle Analysis

The thermodynamic processes which occur, even in the most simple thermal engines, are usually so complicated that it is necessary to assume a theoretical model in which the various events are idealized. This assumption facilitates the analysis and predictions of non-ideal deviations.

A repeated sequence of thermodynamic processes represents a cycle, in which the operation of the heat engine may be described In each process of the cycle, changes in thermodynamic and simulated. properties, such as pressure, temperature, density, internal energy, enthalpy, and entropy are occurring as the working fluid moves from one state to another. Thermodynamic cycles can be represented graphically on P-V (pressure-volume), T-S (temperature-entropy), or P-H (pressureenthalpy) diagrams. The temperature-entropy diagram of a Rankine Cycle is illustrated in Figure 3.2. The working fluid is pressurized from a pressure of  $P_1$  to  $P_2$  via a feed pump (isentropic compression, 1 - 2); it then absorbs sensible heat in the pre-heater (isobaric heating, 2 - 3) and passes through a boiler, where most of the external heat is added to the cycle, (isothermand isobaric heat absorption, 3 - 4). At this point, if necessary, the vapor may be further heated at constant pressure (superheating) . The vapor then expands across the turbine blades where its internal energy is transformed into mechanical energy (isentropic expansion, 4-5). Now if the expansion does not end up in the two phase region, where both liquid and vapor exist, (see Figure 3.2) , some sensible heat has to be removed before the vapor turns into liquid while passing through the condenser (heat rejection, 5 - 1). The working fluid finally enters the hotwell to repeat the cycle. The dashed lines appearing in Figure 3.2 show the deviation from ideal isentropic expansion and compression.

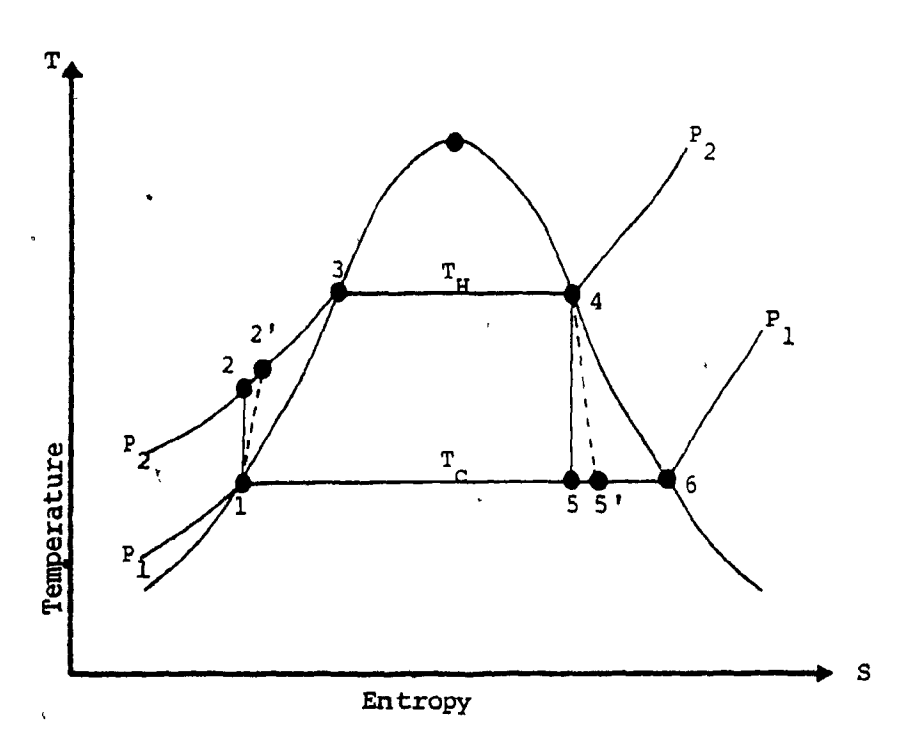


Figure 3.2 A power cycle on the Temperatureentropy diagram.

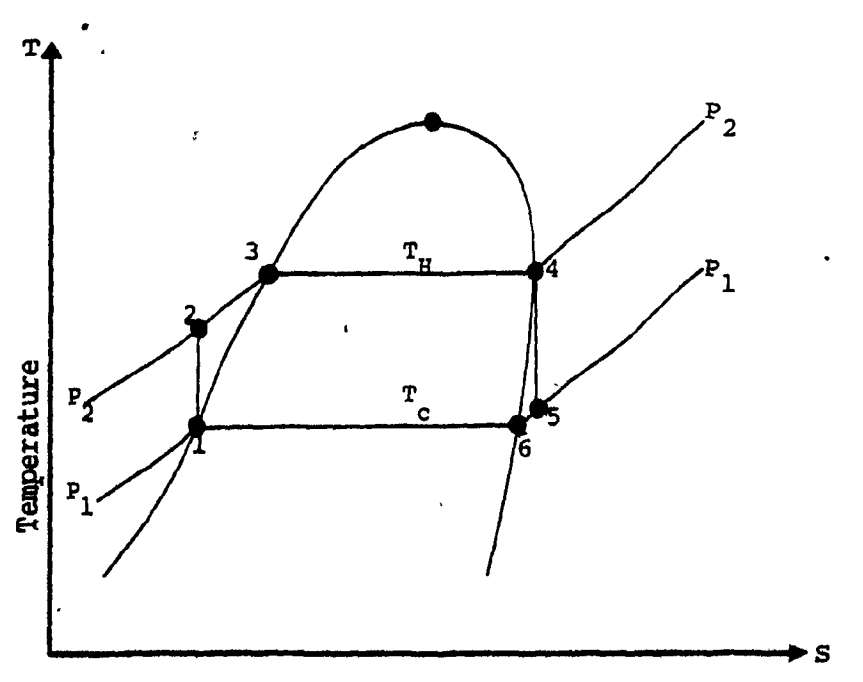


Figure 3.3 Temperature-entropy diagram with positive slope of saturated vapor line.

(<sup>...</sup>,

<u>(</u>;

....

(

...

Realizing that the motive fluid plays a major role in the heat engine performance, care was taken to develop a mathematical model of the Rankine Cycle engine which could take its characteristics into account. The model should also be suitable for use with an optimization procedure.

Power cycle analysis requires that the numerical values of the thermodynamic properties of the working fluid be available at different stages in the cycle. Extracting these properties from tables and / or charts is not practical for computerized analysis. The Generalized Thermodynamic Properties method (Pradhan and Larson, 1980) requires very little data input for power cycle analysis, but has the disadvantage of being less accurate than the chart method (prediction of the thermodynamic properties by this method can be in error by as much as 18%; and the resulting average thermal efficiency deviation by 10% (Levi, (1979)).

The method used here is based on approximating the thermodynamic properties of the working fluid on the saturated liquid and vapor lines as a function of boiler and condenser temperatures. All required properties for cycle analysis such as enthalpy, entropy, pressure, volume are expressed as polynomial functions of the temperatures. These polynomials were developed so as to be valid in the expected range of operating temperature  $(0 - 100^{\circ}\text{C})$ . The polynomial curve fitting

procedure was carried out as follows for each of the required properties: The property data was extracted from tables (not necessarily at equal intervals) for a given liquid; then, a polynomial of the collowing form was fitted to the data:

$$f(T) = \sum_{i=0}^{n} a_{i} T^{i}$$

where f represents the property, T is the temperature, n is the degree of polynomial, and a is the vector of unknown coefficients.

Using least squares technique, the solution of the following minimization problem yields the coefficients:

$$\min_{a} \ \underline{r}^{T} \ \underline{r} = \sum_{j=1}^{m} (f_{j} - \hat{f}_{j})^{2} = \|F - \hat{F}\|^{2} . \tag{3.1}$$

where  $\hat{f}_j$  is the predicted or calculated value of the dependent variable (property) for the jth data point. m is the total number of considered points and  $\underline{r}$  is the residuals vector. A minimum is obtained when the gradient of (3.1) vanishes. This leads to a system of linear equations which can be solved by direct or an iterative method.

This method is applicable to any fluid for which sufficient data is available in the form of charts or tables. For the required properties we found that a fourth order polynomial was adequate to represent that property in the range of considered temperatures (average error of 2%).

Thermodynamic properties of points not lying on the saturated lines can be calculated for the following cases:

is negative (see Figure 3.2), then isentropic expansion will make the state of the fluid penetrate into the two-phase region. The quality factor,  $X_{5S}$ , (the quality factor is a measure of the amount of vapor present in the liquid-vapor mixture) can be calculated as follows:

$$x_{5S} = \frac{S_5 - S_{1f}}{S_{6g} - S_{1f}}$$

where  $S_5 = S_4$  for ideal isentropic expansion. The indices f and g refer to the liquid and vapor states respectively and S represents entropy. Having determined the quality factor the enthalpy of point 5 can be determined from the following expression:

$$H_5 = H_{1f} + X_{5S}(H_{6q} - H_{1f})$$

- (2) In case of a positive slope of the saturated vapor line (Figure 3.3) the following steps should be executed:
- (a) The temperature of point 5 can be determined as follows: the low-pressure specific heat,  $C_{\mathbf{p}}^{0}$ , obtained experimentally either from calorimetric data or from spectroscopic data, is usually approxi-

الميمين المامينية mated in the literature (Perry and Chilton, (1973)) by a quadratic function of temperature:

$$c_{\mathfrak{p}}^{0} = a_{0} + a_{1} T + a_{2} T^{2}$$
 (3.2)

For the range of operating pressure of the power cycle considered here, the effect of pressure on the specific heat can be ignored (Perry and Chilton, (1973)). The entropy difference between points 5 and 6 (Figure 3.3) can be expressed analytically as a function of temperature (obtained from the first law of thermodynamics for isobaric process):

$$s_5 - s_6 = \int_{T_6}^{T_5} (\frac{c_p^0}{T}) dT$$

Integration of the above equation when  $C_p^0$  is substituted from equation (3.2) yields:

$$a_0 L_n \frac{T_5}{T_6} + a_1 (T_5 - T_6) + a_2 (T_5 - T_6)^2 = S_5 - S_6$$

The above nonlinear equation can be solved numerically for the temperature of point  $S(\mathbf{T}_S)$  .

(b) The enthalpy of point 5 can then be calculated as follows:

$$H_5 = H_6 + \int_{T_6}^{T_5} c_P^O dT$$

therefore,

$$H_5 = H_6 + a_0 (T_5 - T_6)^{\circ} + a_1 (T_5 - T_6)^2 + a_2 (T_5 - T_6)^3$$

The superheating could have also been considered in a similar way as step (b) above.

We are now ready to write down the main equations for the power cycle analysis. The amount of heat added, the heat rejected, the work done by the turbine and the feed pump, and finally the cycle efficiency are given by the following relations:

$$Q_{h}$$
 = heat added to the cycle =  $m_{2}^{2} (H_{4} - H_{2})$  (3.3)

$$Q_R$$
 = rejected by the cycle =  $\dot{m}_2 (H_5 - H_1)$  (3.4)

$$W_{\text{tur}} = \text{work done by turbine} = m_2 (H_4 - H_5) \cdot n_t$$
 (3.5)

$$W_{fp} = \text{work done by feed pump.} = \frac{1}{m_2} (H_2 - H_1) / \eta_{fp}$$
 (3.6)

$$rac{1}{cy}$$
 = cycle efficiency =  $rac{W_{tur} - W_{fp}}{Q_n}$ 

where m<sub>2</sub> is the mass flow rate of the working fluid, n<sub>t</sub> and n<sub>fp</sub> are turbine and feed pump efficiencies respectively. The work required by the feed pump can also be approximated (from the first law of thermodynamics for isentropic process) as follows:

$$W_{fp} = \dot{m}_2 \cdot v_{1f} \cdot (P_2 - P_1) / \eta_{fp}$$
 (3.7)

where  $v_{lf}$  is the specific volume of the saturated liquid at the turbine outlet temperature,  $P_2$  and  $P_1$  are the inlet and outlet turbine pressures.

The pond performance should match the cycle specifications: for example, brine entering the vaporizer at average temperature  $\bar{T}_S$  and flow rate  $m_1$  should be able to vaporize the working fluid at a temperature of  $T_H$ . The heat added to the cycle will be supplied by hot brine extracted from the LCZ of the pond. This thermal heat can be written in the following form:

$$\bar{\mathbf{U}} = \hat{\mathbf{m}}_{1} C_{S} (\bar{\mathbf{T}}_{S} - \bar{\mathbf{T}}_{S}^{t}) = \frac{\tau F \bar{\mathbf{H}}_{S} A}{2_{1} - 2_{u}} - (\frac{K_{1}}{2_{1} - 2_{u}} + \frac{K_{2}}{2_{2}} + 2 U_{e} / \frac{\pi}{A}) \cdot (\bar{\mathbf{T}}_{S} - \bar{\mathbf{T}}_{a}) A$$

$$(3.8)^{*}$$

The above equation represents the stationary behavior of the pond for the average excitation developed in Chapter II. Edge losses have also been incorporated here (Crevier, (1980)).

#### 3.4 Heat Exchangers

The electric power generated by an SPPP is greatly dependent on the heat exchangers' performance. A finite temperature difference across a heat exchanger is required for heat to flow through However, since we start with a rather small temperature difference between pond and ambient, we do not wish to reduce the temperature difference available to the thermal cycle itself through excessive heat exchanger temperature drops. A small temperature drop across the heat exchangers calls for a large surface area exchanger, representing an important cost item in the system costs. Therefore a trade-off is mandatory between the objectives of optimal physical efficiency, which would theoretically require heat exchangers of infinite area, and the objective For this reason the function to be of total system cost minimization. minimized was chosen as the unit cost of electric energy generated by an SPPP (¢ / KWh) . The size chosen for the exchangers, and consequent temperature drop, is therefore determined from an optimization procedure. A proper design of the heat exchangers should also yield the optimum The heat exchanger parameters which can vary in our pumping power. analysis are :

surface area, terminal temperatures, and mass flow rates. Constant overall heat transfer coefficients are assumed and parasitic losses in the exchangers are ignored because they are small compared to total parasitic system losses.

(£

The heat exchangers considered in our analysis are assumed to be of the counterflow type. The energy balance equation for the boiler can be given by (Rohsenow and Hartnett, 1973):

$$Q_{B} = \dot{m}_{1} C_{S} (\bar{T}_{S} - \bar{T}_{S}^{*}) = \dot{m}_{2} (H_{4} - H_{3})$$
 (3.9)

and the surface area required by the boiler can be determined by the following expression:

$$A_{B} = \frac{Q_{B}}{U_{B} \cdot (LMTD)_{B}}$$
 (3.16)

where U<sub>B</sub> is overall heat transfer coefficient of the boiler and (LMTD)<sub>B</sub> is the logarithmic mean temperature difference (Rohsenow, 1973) of the boiler evaluated from the following relation:

Power required to overcome pressure loss due to friction including sudden expansion and contraction.

$$(LMTD)_{B} = \frac{\bar{T}_{S} - \bar{T}_{S}^{H}}{Ln \left(\frac{\bar{T}_{S} - T_{H}}{\bar{T}_{S}^{H} - T_{H}}\right)}$$

Similar expressions can be written for the pre-heater and condenser: the energy balance of the pre-heater can be given by:

$$Q_{p} = \dot{m}_{1} C_{s} (\bar{T}_{s}^{"} - \bar{T}_{s}^{"}) = \dot{m}_{2} (H_{3} - H_{2})$$
 (3.11)

The required surface area of the preheater:

$$A_{p} = \frac{Q_{p}}{U_{p} (LMTD)_{p}}$$
 (3.12)

where

0

$$(\text{LMTD})_{p} = \frac{(\vec{T}_{s}" - T_{H}) - (\vec{T}_{s}" - T_{C})}{\vec{T}_{s}" - T_{H}}$$

$$= \frac{\vec{T}_{s}" - T_{H}}{\vec{T}_{s}" - T_{C}}$$

and finally the heat rejected by the condenser and its required surface area are given by the following expressions:

$$Q_C = \dot{m}_3 C_3 (\ddot{T}_a' - T_a) = \dot{m}_2 (H_5 - H_1)$$
 (3.13)

and,

$$A_{C} = \frac{Q_{C}}{U_{C} \cdot (LMTD)_{C}} = \frac{Q_{C}}{\overline{T}_{a}^{i} - \overline{T}_{a}}$$

$$L_{n} \left(\frac{\overline{T}_{a}^{i} - \overline{T}_{a}}{\overline{T}_{a}^{i} - \overline{T}_{c}}\right)$$
(3.14)

For a working fluid with positive slope of saturation vapor curve

(Figure 3.3) a feed-back heat exchanger (an additional area of condenser is required for removing some sensible heat) should be considered.

The total heat to be extracted from the pond is the sum of equations (3.9) and (3.11):

$$\vec{U} = Q_B + Q_P = \vec{m}_1 C_S (\vec{T}_S - \vec{T}_S^*) = \vec{m}_2 (H_4 - H_2) = Q_A$$
 (3.15)

#### 3.5 Auxiliary Pumps

for pumping the fluids through the heat exchangers. Only the power required for pumping brine from the LCZ of the pond, as well as cooling water from the UCZ or any other convenient source, and the power required for pumping the motive fluid are considered here.

Ø

The electric power required by a pump can be calculated as follows (ASHRAE, 1975 [ ...

$$W_{P} = \frac{\dot{m} (\Delta P)}{\rho \eta_{mp}}$$
 (3.16)

where  $\dot{m}$  is the mass flow rate,  $\rho$  is the specific density of the is the efficiency of the pump and its motor, and  $\Delta P$  is the pressure drop given by:

$$\Delta P = \rho g h_g \qquad (3.17)$$

where g is the acceleration due to gravity, and h, is the head loss, which can be written as follows:

$$h_{\ell} = h_{f} + h_{O} + h_{s}$$
 (3.18)

where  $h_{f}$  is the head loss created by viscous effects,  $h_{0}$  is the head loss due to obstacle to the flow pattern (such as valves, orifices, pipe corners or bends, etc.) , and  $h_a$  is the static head. Head loss due to viscous effects (friction) can be obtained from the Darcy-Weisbach equation (Streeter, 1961):

$$h_{f} = f \frac{L}{d} \frac{v^2}{2q} \qquad (3.19)$$

where L and d are the length and diameter of the pipe respectively,

f is the friction factor, and V is the fluid velocity given by the

following expression:

$$V = \frac{4 \text{ m}}{\pi d^2 \rho}$$
 (3.20)

Determination of h<sub>0</sub> requires the knowledge of the exact piping plan and specific obstacles to the flow, but since its value is proportional to the second power of velocity and the exact piping plan is not known we have arbitrarily increased friction losses by 20% to account for these losses. Therefore, using equations (3.17) - (3.20), equation (3.16) can be rewritten as follows:

$$W_{p} = 1.2 \frac{8fL \stackrel{\cdot \cdot 3}{m}}{d^{5} \cdot \pi^{2} \cdot \rho^{2} \cdot \eta_{mp}} + \frac{\stackrel{\cdot \cdot \cdot 3}{m gh_{s}}}{\eta_{mp}}$$
(3.21)

The above equation is used for the brine and cooling water pumps. The friction factor, f, is here considered dependent on the flow rate m; it is recomputed at each step of the optimization process so as to satisfy the Von Karman equation (Streeter, 1961):

$$\sqrt{f}$$
 = 4.06 log (Re  $\sqrt{f}$ ) - 0.6 (3.22)

where the Reynolds number Re is given by:

$$Re = \frac{4 \text{ m}}{\pi \text{ d} \mu_{\text{f}}}$$
 (3.23)

with  $\mu_{ extsf{f}}$  being the fluid viscosity.

### 3.6 Optimization

The models presented previously for solar pond, power cycle, heat exchangers, and auxiliary pumps will be put together in this section to formulate an optimization problem from which the optimal components size and operating conditions can be obtained. The function to be minimized was chosen as the unit cost of electric energy (¢ / KWh).

The net electric power generated by a SPPP can be expressed as follows:

$$W_{nt} = W_{tur} \cdot \eta_{G} - \sum_{i=1}^{3} W_{pi}$$
 (3.24)

where  $W_{\rm Pl}$  and  $W_{\rm P3}$  are the electric power required by the brine and cooling water pumps as given by equation (3.21), where the corresponding quantities of each pump is substituted.  $W_{\rm P2}$  is the power required by the feed pump given by equation (3.6), and  $n_{\rm G}$  is the generator efficiency.

Total installation costs consist of the following items:
solar pond, heat exchangers, turbine, generator, pipes, and pumps.
Other costs such as land, control equipment, instrumentation, and working fluid are not taken into account for this analysis. Therefore, the system installation costs can be given by:

( )

( k

The annual expenses can be determined by first calculating the capital recovery factor as follows (Benson, 1980):

$$CRF = \frac{(1+1)^{\frac{N}{p}}}{(1+1)^{\frac{p}{p}}-1} \dots$$

where N is the plant lifetime (in years), and I is the interest rate. Then adding to CRF the annual operation and repair costs (as a fraction of the total capital cost), the total expenses on a yearly basis are:

$$E_{tot} = C_{tot} \cdot (CRF + 0 + r)$$

Assuming a 10% interest rate and 20 years lifetime (Tabor, 1981)

yields a CRF of 11.7%. Adding to this figure a 7% 0 and r

cost results in a total annual cost of 18.7% of the total capital

costs. Therefore the cost per kilowatt-hour of electric energy can be expressed as follows:

$$\frac{c}{kwh} = \frac{E_{tot}}{t_{f}}$$

$$\int_{t_{0}}^{t} w_{nt} \cdot dt$$
(3.25)

where the integration is carried out over one year  $(t_f - t_0 = 1 \text{ year})$ .

The optimization problem in a compact form can be stated as follows:

Minimize 
$$C_{kwh} = f(\underline{x})$$

subject to;

0

$$\underline{\mathbf{g}}(\underline{\mathbf{x}}) = \underline{\mathbf{0}} \tag{3.26}$$

$$\underline{\mathbf{a}}^{\mathbf{L}} \leq \underline{\mathbf{h}}(\underline{\mathbf{x}}) \leq \underline{\mathbf{a}}^{\mathbf{U}}$$

and '

$$\bar{x}_{\mathrm{m}} < \bar{x} < \bar{x}_{\mathrm{m}}$$

where the vector  $\underline{x}$  consists of the following parameters:

$$\underline{\mathbf{x}}^{T} = [A, \ell_{1}, A_{B}, A_{C}, A_{P}, (m_{1}, i = 1, 3),$$

$$\bar{T}_{s}, \bar{T}'_{s}, \bar{T}''_{s}, T_{H}, T_{C}, \bar{T}'_{a}]$$

The equality constraints,  $\underline{q}(\underline{x}) = \underline{0}$ , are the energy balance equations marked with asterisks on the previous pages of this chapter.

In addition the inequality-constraints should be imposed to respect physical constraints (for example the heat exchanger effectiveness should be less than unity and greater than zero). The vectors a and a are the upper and lower bounds on the inequality constraints. Upper and lower bounds are also imposed on the variables to respect physical and practical constraints and at the same time help the optimization routine for better convergence. Therefore we are dealing with a minimization problem, (3.26), having a nonlinear objective function, equality and inequality constraints, and bounds on the variables. It is worth mentioning again that this optimization will not yield a minimum cost nor a maximum electric power; it is rather a trade-off between these two objectives which yields the minimum unit a cost of electric energy.

The analytical solution of the problem, (3.26), is not possible because of the number of variables involved (14), nonlinear objective and constraints, and also the fact that the objective function.

can not be given in a closed form. Therefore a numerical technique had to be used with the help of a digital computer.

The Generalized Reduced Gradient (GRG) package (Lasdon et al., 1975) was used to find the optimal solution of (3.26). Scaling, which is almost always necessary for optimization problems, was required because not all the functionals, i.e., objective and constraints, have the same sensitivity to the variables. For the case at hand, balancing the derivatives by diagonal scaling (Gill et al., 1981) of the variables provided satisfactory results: the vector of unknowns actually used in the computations is the vector Z given by:

$$Z = D \cdot x$$
  $D = a diagonal matrix$ 

and,

$$d_{jj} = \frac{2|g_{j}|}{[1 + |f(\underline{x})|]}$$

where g is the derivative of  $f(\underline{x})$  with respect to the jth variable.

### 3.6.1 Flow Diagram of the Optimization

The flow chart presented in Figure 3.4 summarizes the processes involved in the optimization.

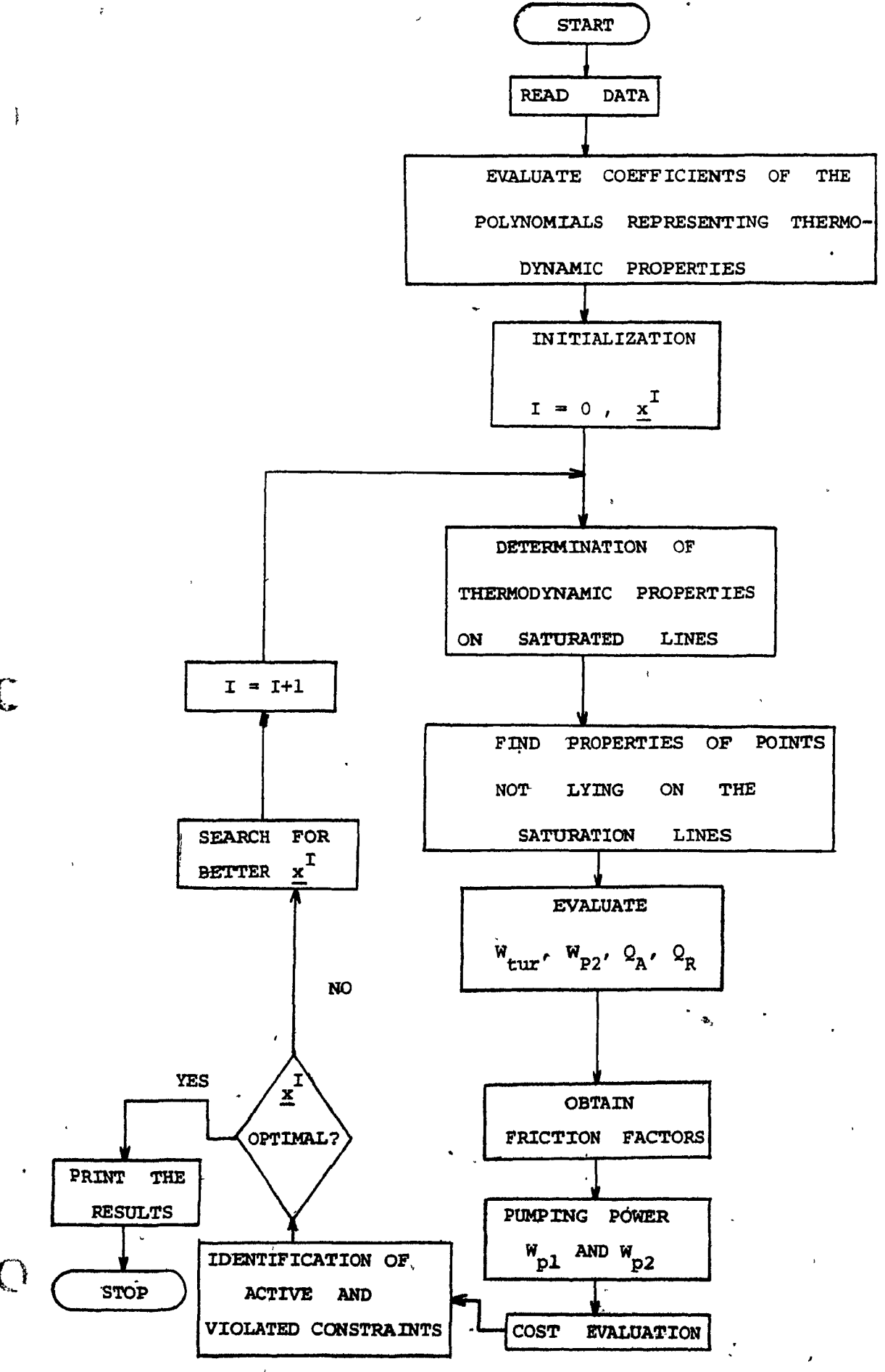


Figure 3.4 The flow diagram for the simulation.

The input data are climatic information (insolation and ambient temperature), latitude of the pond site, conductivity and diffusivity of brine and soil, data of the working fluid for cycle The next step in the simulation would be the computation of the coefficients of polynomials representing thermodynamic properties of the working fluid.\* At this time an initial guess is provided for Then the power cycle analysis is carried out for the optimization. the initial guess and quantities such as heat supplied to and rejected by cycle, work of turbine and feed pump are determined. numbers for the flows in brine and cooling water pipes are calculated, from which the friction factor in these pipes can be found by solving nonlinear equation (3.22) numerically. The pumping power of brine and cooling water pumps are then calculated . The next step is the determination of the required surface area for each heat exchanger. The cost function is evaluated and violated constraints are then If the optimality conditions are met the program identified . prints the optimal solution, otherwise a better solution will be searched by the GRG package until the optimal solution is obtained or the number iteration exceeds its specified limit.

i)

See Appendix B .

# 3.6.2 "Numerical Results and Discussions

In this section estimates of the possible cost of a SPPP will be made in an attempt to judge its economic performance.

The optimization of a SPPP system will be carried out for two different climatic conditions namely, Montreal and Shiraz.

Some system component costs are those published by other investigators, (Tabor, 1981, Ophir and Nadav, 1982), whereas other costs were obtained from Montreal area suppliers. A list of the component costs appears in Table 3.1. The climatic conditions for the two considered locations are those listed in Table 1.2.

The first example will be the optimization of unit energy cost for an SPPP with a net electric power of 5 MW. This formulation adds one more equality constraints to the already existing ones.

Optimization results for the Montreal pond with two working fluids appear in Table 3.2. Power generation is assumed to be carried out during the entire year using the UCZ as the heat sink. The thickness of

It is worth mentioning here that heat rejection to UCZ will not disturb the NCZ. Crevier, 1982 showed experimentally that circulating hot brine from LCZ through pipes placed in UCZ resulted in surface temperature increase of only 1°C. Increased surface evaporation rate resulting from depositing heated water on the pond surface was reported by Nielsen, 1982.

TABLE 3.1

# COMPONENT COSTS OF A SPPP

COMPONENT	COST
Pond:	
NaCl salt*	10 \$ / ton
Liner	5 \$ / m <sup>2</sup>
Wave damper	2 \$ / m <sup>2</sup>
Excavation	3 \$ / m <sup>3</sup>
Heat exchanger:	200 \$ / m <sup>2</sup>
Generator :	500 \$ / kw
Turbine :	500 \$ / kw
Pumps :	400 \$ / kw

Assuming proximity to a salt supply.

the UCZ was assumed to be 0.2 meter, which seems to be the minimum attainable thickness in practice (Crevier, 1980). The thickness of LCZ was arbitrarily set to three meters, which will be validated by simulation. For the Montreal pond it was assumed that the pond is covered with ice whenever the ambient temperature was less than  $-2^{\circ}\text{C}$ , which is the freezing point of the 3% brine (by weight) assumed in the UCZ. The surface of the pond was assumed to be at ambient temperature whenever this temperature was greater than  $-2^{\circ}\text{C}$  and remain at  $-2^{\circ}\text{C}$  (the equilibrium temperature between 3% brine and ice) whenever the ambient temperature fell below  $-2^{\circ}\text{C}$ . Ice on the pond surface was assumed to block 80% of the solar radiation.

It can be seen from Table 3.2 that a SPPP with refrigrant 113 yields a cheaper unit energy cost than F-11. Therefore the motive fluid chosen for a SPPP affects not only the power conversion subsystem: the performance and operating conditions of the entire system can be changed by altering the fluid. The disadvantages of F-11 as motive fluid are its lower pressure at condensing temperature (3.67 psia), which may introduce air leakage problems, and the positive slope of its saturated vapor curve, which calls for a feed-back heat exchanger. The latter drawback is not, as serious as the first one because this slope for F-113 is very close to zero.

A simulation of the pond temperature evolution for three years revealed that the assumed thickness of the lower convecting zone

TABLE 3.2
SUMMARY OF THE RESULTS FOR A 5 MW SPPP IN MONTREAL

()

ITEM	F - 113	F - 11	
Pond :			
Surface area (Km <sup>2</sup> )	3.54	3.82 1.63 59.63	
Heat extraction depth (m)	1.68		
Temperature of LCZ (OC)	62.11		
Efficiency (%)	12.16	12.96	
Heat Exchanger Area (10 m 2):			
Vaporizer (boiler)	2.585	2.83	
Condenser	2.63	3.22	
Pre-heater	0.185	.173	
furbine :			
Inlet pressure (psia)	19.54	37.16	
Outlet pressure (psia)	3.67	9.3	
. Inlet temperature (°C)	56.3	<b>`53.</b>	
Outlet temperature ( <sup>O</sup> C)	11.52	11.48	
Mass Flow Rates (kg/sec) :		•	
Brine	3576	3810	
Working fluid	, 349	362	
Cooling water	3230	3658	
Gross Power (MW) :	5.58	5.67	
System Efficiency (%):	0.94	,8718	
Energy Cost (¢/kwh):	33 <b>.</b> 77	36.67	

results in a temperature variation of  $\pm 14^{\circ}$ C around the average 62.11°C), which is of the same order of magnitude as that reported by French, 1982.

(I

The cost of generated power is however of  $33.77 \ c$  / kwh which is much more than those reported by Tabor (1981) and Ophir and Nadav (1982) , where the estimates vary between 5.3 to  $13.5 \ c$  / kwh . This unacceptable cost led us to investigate the possibility of using a cold source at a temperature lower than that of the UCZ of the pond, which will be discussed in Chapter V .

appear in Table 3.3. The first column corresponds to an optimization with salt cost of 10\$ / ton whereas the second column assumes free salt. The latter case is not far from reality because of the existence of salt lakes near Shiraz. The energy cost of a SPPP in Shiraz is less than half of the Montreal pond, while the insolation is only 50% larger than that of Montreal. The explanation may lie in the difference between the latitudes of the two locations. The pond area is also smaller by a factor of two. Here for the case of free salt, the cost per kilowatt hour is in the same order as those reported by Tabor, (1981). The installation cost of 5000 \$/kw is also in good agreement with that of French, (1982).

TABLE 3.3

SUMMARY OF THE RESULTS FOR A 5 MW SPPP IN SHIRAZ

()·

ITEM	SALT AT \$10/TON	FREE SALT	
Pond :	•	v	
Surface area (Km²)	1.62	1.63	
Heat extraction depth (m)	1.52	1.583	
Temperature of LCZ ( <sup>O</sup> C)	84.75	86.28	
Efficiency (%)	16.08	15.75	
leat Exchanger Area (10 <sup>4</sup> m <sup>2</sup> ) :			
Vaporizer (boiler)	1.7222	1.63	
, Condenser	1.94	1.77	
Pre-heater	.1527	.148	
turbine :	* %	<b>u</b>	
Inlet pressure (psia)	37.57	39.153	
Outlet pressure (psia)	6,04	6,036	
Inlet temperature ( <sup>O</sup> C)	78.8	80.0	
Outlet temperature (OC)	23.4	23.33	
ass Flow Rate (kg/sec) :	•		
Brine	<b>3188</b>	3281	
Working fluid	291	286.5	
Cooling water .	<b>3139</b>	3547	
cross Power (MW <sub>e</sub> ):	∕ 5 <b>.56</b>	5.61	
ystem Efficiency (%):	1.465	1.45	
nergy Cost (¢/kwh):	16.88	11.4	

#### CHAPTER IV

# OPTIMIZATION OF A SOLAR POND POWER PLANT

#### PART II : OPTIMAL HEAT EXTRACTION AND STORAGE DEPTH

#### 4.1 Introduction

In the previous chapter the optimal sizes of the system's components as well as optimal operating conditions were obtained under stationary (average) excitations. The objectives of this chapter are to determine the optimal heat extraction time table and thickness of LCZ. Two different approaches will be presented, namely, an approximate semi-analytical evaluation, followed by a mathematical programming method. Before describing these methods it is necessary to mention some results from the previous chapter which have been used to assist the present simulations.

#### 4.2 Assumptions

A number of simulations which were carried out preliminary to obtaining the results described in Chapter III revealed that optimum heat exchanger effectiveness 1 remained almost constant as long as cost

$$\varepsilon \stackrel{\overline{q}}{=} \frac{q^{c}}{q^{c}}$$

Heat exchanger effectiveness  $\varepsilon$  is defined as the ratio of the maximum possible rate of heat transfer to the actual rate of heat transfer (Thomas, (1981)):

coefficients were kept constant. It was also observed that the optimum temperature drop across the boiler and condenser  $(\overline{T}_S - \overline{T}_A) - (T_H - T_C)$  was in the range of  $11 - 12^{\circ}C$  (for the two locations considered), which is in good agreement with the value of  $10^{\circ}C$  reported by Tabor (1982). (For example in the case of the Montreal pond, Table 3.2,  $\Delta T_1 = \overline{T}_S - \overline{T}_A = 56.61$  and  $\Delta T_2 = T_H - T_C = 44.78$ , therefore  $\Delta T = \Delta T_1 - \Delta T_2 = 11.83^{\circ}C$ ). The small difference, in the value of  $\Delta T$ , between our result and that of Tabor (1981), could have been caused by our use of different parameters for heat exchangers (i.e., cost coefficient, overall heat transfer coefficient, etc.). In particular, Tabor did not mention

For example consider a counter-flow heat exchanger as shown in Figure 4.la and its temperature profile in Figure 4.lb. The energy balance can be given by :

$$q_{\tilde{c}} = m_{\tilde{c}} C_{\tilde{c}} (T_{\tilde{c}0} - T_{\tilde{c}i}) = m_{\tilde{h}} C_{\tilde{h}} (T_{\tilde{h}i} - T_{\tilde{h}0})$$

The maximum rate of heat transfer, q , would occur if the outlet temperature of the fluid with a smaller value of capacity rate (mc) were to be equal to the inlet temperature of the other fluid, therefore :

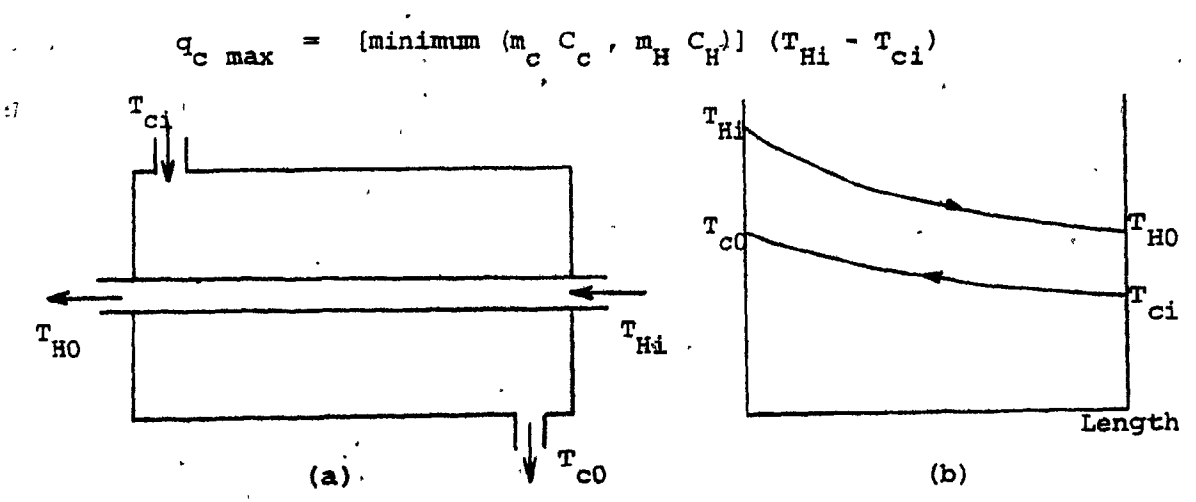


Figure 4.1 Schematic diagram of a counter-flow heat exchanger.

<sup>1 (</sup>cont'd)

the overall heat transfer coefficient of his heat exchanger. It was also found in the previous chapter that the electric power required by the pumps, circulating brine and cooling water, can be approximated as follows:

$$W_{p1} + W_{p2} \approx K_{p} (\dot{m}_{1} + \dot{m}_{3})$$
 (4.1)

where K is the pump power factor (KJ / Kg). Its value was found to be 0.081 KJ / Kg for an assumed static head of six meters. A pump power factor of 0.13 KJ / Kg was obtained for a static head of 10 meters: this is in good agreement with the value of 0.12 estimated by Coffay (1980), in a Westinghouse study for an OTEC plant optimized to produce fresh water. For simplicity, we shall assume equal flow rates for brine and cooling water. This approximation can be justified by the results of Chapter III (see Tables 3.2 and 3.3) where a small difference is seen to exist between these two quantities. French (1982) also reports equal flow rates.

#### 4.3 Semi-Analytical Solution

In this section an approximate solution of the governing equations of the solar pond thermal behavior in steady state for sinusoidal excitations will be presented in terms of unknown sinusoidal heat

extraction rate and thickness of LCZ. The equation of the electric power generated by the SPPP will then be derived and the unit electric energy cost will be minimized with respect to the unknowns. An analytical solution of this optimization problem is not possible because the objective function as well as the constraints are non-linear. The numerical solution can be obtained by either exhaustive enumeration or an optimization routine.

# 4.3.1 Approximate Analytical Solution of the Pond Governing Equations

An approximate solution of the governing equations (2.10), (2.12), and (2.13) can be obtained if the heat stored in the NCZ and ground can be ignored. This is a good assumption in many practical cases, since the LCZ often provides a rather large part of the total storage capacity. A lumped parameter solution can be obtained by solving equations (2.10) and (2.13) while neglecting heat storage capacities and using the boundary conditions of (2.11) and (2.14); then substituting the results into (2.12) yields the following first order differential equation:

$$\rho_{s} C_{s} \ell_{s} \frac{d T_{s}(t)}{dt} = \frac{\tau F H_{s}(t)}{\ell_{1} - \ell_{u}} - (\frac{K_{1}}{\ell_{1} - \ell_{u}} - \frac{K_{2}}{\ell_{2}}) T_{s}(t) + \frac{K_{1}}{\ell_{1} - \ell_{u}} T_{a}(t) + \frac{K_{2}}{\ell_{2}} T_{w} - U(t) - 2 U_{e} \sqrt{\pi/A} (\bar{T}_{s} - \bar{T}_{a})$$

U

Substitution of equations (2.5) - (2.8) for  $H_s(t)$ ,  $T_a(t)$ , U(t), and  $T_s(t)$  in equation (4.2) and then separating for average and amplitude components, the following expressions can be obtained for the average, amplitude and phase lag of the LCZ temperature:

$$\bar{T}_{s} = \frac{\frac{\tau F \bar{H}_{s}}{K_{1}} + \frac{K_{2}}{K_{1}} \frac{\ell_{1}^{-\ell_{u}}}{\ell_{2}} T_{w} - \frac{\ell_{1}^{-\ell_{u}}}{K_{1}} \bar{U} + (1 + 2U_{e} / \pi/A \frac{\ell_{1}^{-\ell_{u}}}{K_{1}}) \bar{T}_{a}}{1 + \frac{K_{2}}{K_{1}} \frac{\ell_{1}^{-\ell_{u}}}{\ell_{2}} + 2 U_{e} / \frac{\pi}{A} \frac{\ell_{1}^{-\ell_{u}}}{K_{1}}}$$

$$\tilde{T}_{s}' = \frac{\tilde{T}_{a}(\cos \delta_{a} - b \sin \delta_{a}) + \frac{\ell_{1} - \ell_{u}}{K_{1}} \tilde{y} (b \sin \delta_{u} - \cos \delta_{u}) + \frac{\tau F \tilde{H}_{s}}{K_{1}}}{(1 + b^{2}) \cos \delta_{s} + (1 - b) \frac{K_{2}}{K_{1}} \frac{\ell_{1} - \ell_{u}}{\ell_{2}}}$$
(4.4)

and

$$\delta_{s} = -\arcsin\left(\frac{\frac{\frac{K_{2}}{K_{1}}}{\frac{\ell_{1}-\ell_{u}}{\ell_{2}}}}{\sqrt{\frac{(\gamma-b)^{2}+(1+b\gamma)^{2}}{(1+b\gamma)^{2}}}}\right) + \arctan\frac{\frac{1+b\gamma}{\gamma-b}}{(4.5)}$$

\ where

$$b = \frac{\ell_1 - \ell_u}{K_1} \rho_s \cdot C_s \cdot \ell_s \cdot \omega$$

$$\gamma = \frac{\frac{\tau \ \text{F} \stackrel{\circ}{\text{H}}_{\text{s}}}{K_{1}} - \frac{\ell_{1} - \ell_{u}}{K_{1}} \stackrel{\circ}{\text{U}} \cos \delta_{u} + \stackrel{\circ}{T}_{a} \cos \delta_{a}}{-\frac{\ell_{1} - \ell_{u}}{K_{1}} \stackrel{\circ}{\text{U}} \sin \delta_{u} + \stackrel{\circ}{T}_{a} \sin \delta_{a}}$$

If the depth of the heat sink from the pond bottom tends to infinity and edge losses are ignored then, the results obtained here will be the same as those reported by Zangrande (1979).

From the approximate formulation contained in equation

(4.2), one can estimate the time required by a pond to approach the steady state as follows. From the complementary solution of equation

(4.2) the time constant can be given by the following expression:

$$\tau_{p} = \frac{\rho_{s} C_{s} \ell_{s}}{\frac{K_{1}}{\ell_{1} - \ell_{u}} + \frac{K_{2}}{\ell_{2}}}$$

The pond will reach its steady state operation after approximately three times the value of this time constant.

## 4.3.2 Formulation of the Net Electric Power

Thermodynamics teaches that the maximum efficiency with which heat can be converted into mechanical or electrical energy is given by Carnot's Law:

$$\eta_{c} = \frac{W_{\text{mec}}}{U} = \frac{1 - \frac{T_{c}}{T_{H}}}{T_{H}}$$

where  $W_{mec}$  is the mechanical power of the turbine and other symbols have their previous meanings. It should be noted that the temperatures,  $T_{c}$  and  $T_{H}$ , are in absolute degrees. Therefore the maximum electric power can be expressed as follows:

$$W_{e \text{ max}} = \eta_G \left(1 - \frac{T_C}{T_H}\right) U$$

where  $\eta_G$  is the generator efficiency. No real heat engine can give the ideal efficiency of the theoretical Carnot engine. In addition the heat exchangers walls induce a loss of temperature which causes an even lower efficiency. The simulations of Chapter III showed that for the considered working fluid (Refrigrant 113) only 64% of the above power can be realized (Tabor, 1981 gives a value of 65% but he is not mentioning any particular working fluid).

As was mentioned earlier in this chapter, we have found that there is an optimum temperature change experienced by brine and cooling water. Moreover electric power is needed for the auxiliaries, in particular, for pumping the fluids through the heat exchangers. Therefore the net electric power can be given by:

$$W_{nt}(t) = 0.64 \eta_G \left(1 - \frac{T_a(t) + d_1}{T_s(t) - d_2}\right) U(t) - (W_{pl} + W_{p3})$$
 (4.6)

a a p C

where d<sub>1</sub> and d<sub>2</sub> are the optimum temperature changes of cooling water and brine. The last term on the right hand side of the above equation represents electric power required by circulating pumps. The pumping power can be calculated as follows: the heat extracted from the LCZ can be given by:

$$U(t) = \dot{m}_1 C_s (T_s - T_s^i) = \dot{m}_1 C_s \Delta T$$
 (4.7)

where  $\Delta T$  is the temperature change experienced by brine and its value is taken as the optimum value obtained from the optimization of Chapter III. Assuming equal flow rates for brine and cooling water and using equations (4.1) and (4.7) the pumping power can be expressed in the following form:

$$W_{p1} + W_{p2} = \frac{2 K_{p}}{C_{s} \Delta T} U(t)$$
 (4.8)

As a last approximation, for the practical operating temperature of LCZ (0  $\leq$  T<sub>S</sub>  $\leq$  100°C), the term  $\frac{1}{T_{\rm S}(t)-d_2}$  in equation (4.6) can be well approximated by a linear function of T<sub>S</sub>(t) as follows:

$$\frac{1}{T_s(t) - d_1} = e_0 + e_1 T_s(t)$$
 (4.9)

where  $e_0$  and  $e_1$  can be obtained by a linear least squares technique.

# 4.3.3 Formulation of the Optimization Problem

The unit energy cost, equation (3.25), can be rewritten in the following form :

$$c_{\text{KWh}} = \frac{0.187 (c_{\text{tl}} + c_{\text{t2}} \cdot l_{\text{s}})}{\int_{t_0}^{t_f} w_{\text{nt}}(t) dt}$$

where  $C_{t1}$  and  $C_{t2}$  are installation costs independent and dependent on the thickness of the LCZ respectively. Substituting equation (4.6) for  $W_{nt}(t)$  and using equations (4.8) and (4.9), the above equation can be transformed into the following:

$$J = \frac{-1}{0.187 (C_{t1} + C_{t2} \cdot l_s)} \int_{t_0}^{t_f} \{0.64 \eta_G [1 - (T_a(t) + d_1)]$$

$$\cdot (e_0 + e_1 T_s(t)] U(t) - \frac{2 K_p}{C_s \Delta t} U(t)\} dt$$

where.

$$J = \frac{-1}{C}$$
KWh

We define the optimization problem in the following form :

minimize 
$$J = \int_{t_0}^{t_f} f[(U(t), l_s, T_s(t)]dt]$$

$$U(t), l_s \qquad (4.11)$$

Using equations (2.5) - (2.8) for  $H_S(t)$ ,  $T_a(t)$ , U(t), and  $T_S(t)$ , the above optimization, after carrying out integration and some algebraic manipulations, reduces to the following expression :

$$\begin{array}{lll} \underset{\bar{\mathbf{U}},\bar{\mathbf{U}},\delta_{\mathbf{U}},k_{\mathbf{S}}}{\min \mathbf{minimize}} & \mathbf{J} & = & \frac{-(\mathbf{t_{f}}-\mathbf{t_{0}})}{0.187(C_{\mathbf{t}1}+C_{\mathbf{t}2}-l_{\mathbf{S}})} \{0.64\,\eta_{\mathbf{G}}\,\{\bar{\mathbf{U}}-\bar{\mathbf{U}}(\mathbf{T_{a}}+d_{\mathbf{1}})\\ & \cdot (\mathbf{e_{0}}+\mathbf{e_{1}}\,\bar{\mathbf{T}_{\mathbf{S}}}) - 0.5\,\mathbf{e_{1}}\,\bar{\mathbf{U}}\,\bar{\mathbf{T}_{\mathbf{S}}}\,\bar{\mathbf{T}_{\mathbf{a}}}\,\cos(\delta_{\mathbf{S}}-\delta_{\mathbf{a}})\\ & -0.5(\mathbf{e_{0}}+\mathbf{e_{1}}\,\bar{\mathbf{T}_{\mathbf{S}}})\,\bar{\mathbf{U}}\,\bar{\mathbf{T}_{\mathbf{a}}}\,\cos(\delta_{\mathbf{U}}-\delta_{\mathbf{a}}) & (4.12)\\ & -0.5(\mathbf{T_{a}}+d_{\mathbf{1}})\,\mathbf{e_{1}}\,\bar{\mathbf{T}_{\mathbf{S}}}\,\bar{\mathbf{U}}\,\cos(\delta_{\mathbf{U}}-\delta_{\mathbf{S}})] - \frac{2\,K_{\mathbf{D}}}{C_{\mathbf{S}}\,\Delta\mathbf{T}}\,\bar{\mathbf{U}}\,\} \end{array}$$

where  $T_S$ ,  $T_S$ , and  $\delta_S$  are given by equations (4.3) - (4.5). The above minimization is subjected to  $t_S$  following constraints and bounds on the variables:

Some of the upper and lower limits are artificially imposed on the variables to help the optimization routine to converge (none of the bounds should be active constraints at the solution).

#### 4.4 Examples

The solution of the optimization problem presented in the previous section can be obtained by either exhaustive enumeration method or an optimization routine. Montreal and Shiraz are again the two considered locations for which we seek optimal heat extraction rates and LCZ thicknesses (other parameters such as pond area, depth of NCZ, costs of the components etc., are taken to be the same as those appeared in Tables 3.2 and 3.3).

The UCZ is considered to be the source of cooling water, but the following approximation has been made for the Montreal pond because of surface icing; the truncated sinusoidal function shown with dashed lines in Figure 4.2 (which represents the temperature of the UCZ) is approximated by a sinusoidal function which has the same average and minimum values as the truncated one. This function will be considered as the cooling water temperature for the Montreal pond.

4

Although the optimal average heat extraction term was determined in Chapter III, for the sake of comparison optimization will be carried out on this term again. Table 4.1 summarizes the results obtained for the two considered locations. The results show that optimal average heat extractions for Montreal and Shiraz are 20.8 and 34.88 W/m² respectively while values of 18.24 and 33.00 W/m² were obtained in Chapter III. Since the optimal

O

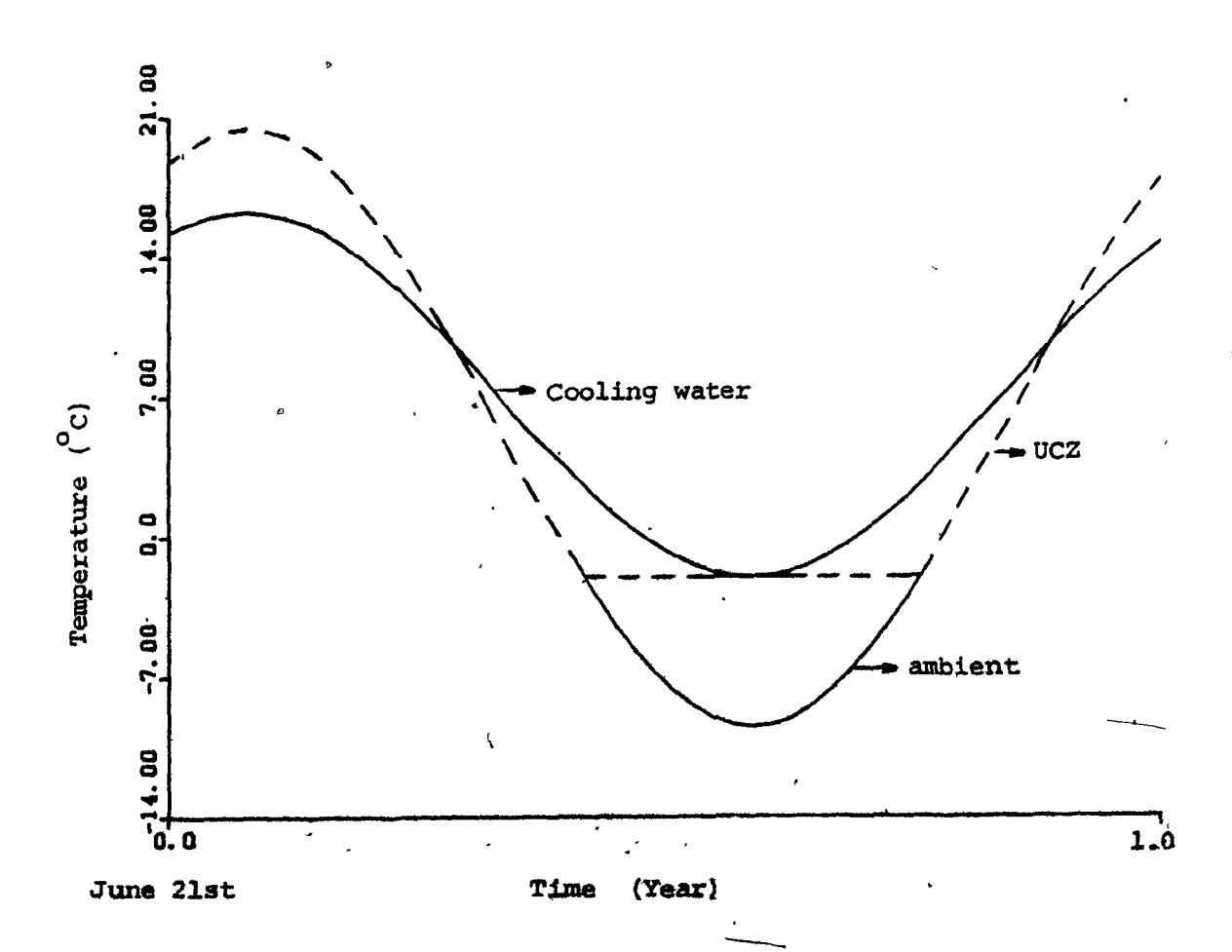


Figure 4.2 Ambient, cooling water, and UCZ temperatures for Montreal Pond.

storage depth is small (0.5 meter for the cases at hand), the aforementioned discrepancy can be expected, because smaller storage depth causes a higher amplitude of oscillation of the LCZ temperature. It is therefore more economical to extract heat at a higher average temperature than the one obtained under constant excitations (optimization of Chapter III). In addition, the amplitude of the heat extraction has an optimal value equal to the average for case 1 (Table 4.1), because it would be cheaper not to produce power during the entire year than having a larger LCZ depth to keep the system generating power during winter in spite of the very low insolation. The Shiraz pond does not present this problem because of the relatively smaller variation of its solar radiation.

The electric energy cost for the Montreal pond, 21.68 ¢/KWh is about 35 per cent lower than that obtained in Chapter III (see Tables 3.2 and 4.1). This reduction in cost is evidently caused by the smaller LCZ depth, which makes use of the system during the warmer part of the year only. On the other hand the Shiraz pond is capable of producing cheaper energy (9.07 ¢/KWh) during the entire year even with a small storage depth.

A number of optimization runs were carried out to find the effect of fixing the lower limit of the LCZ thickness (in all runs this became an active constraint) at a value larger than 0.5 meter.

TABLE 4.1

SIMMARY OF THE RESULTS FOR OPTIMAL HEAT EXTRACTION AND STORAGE DEPTH

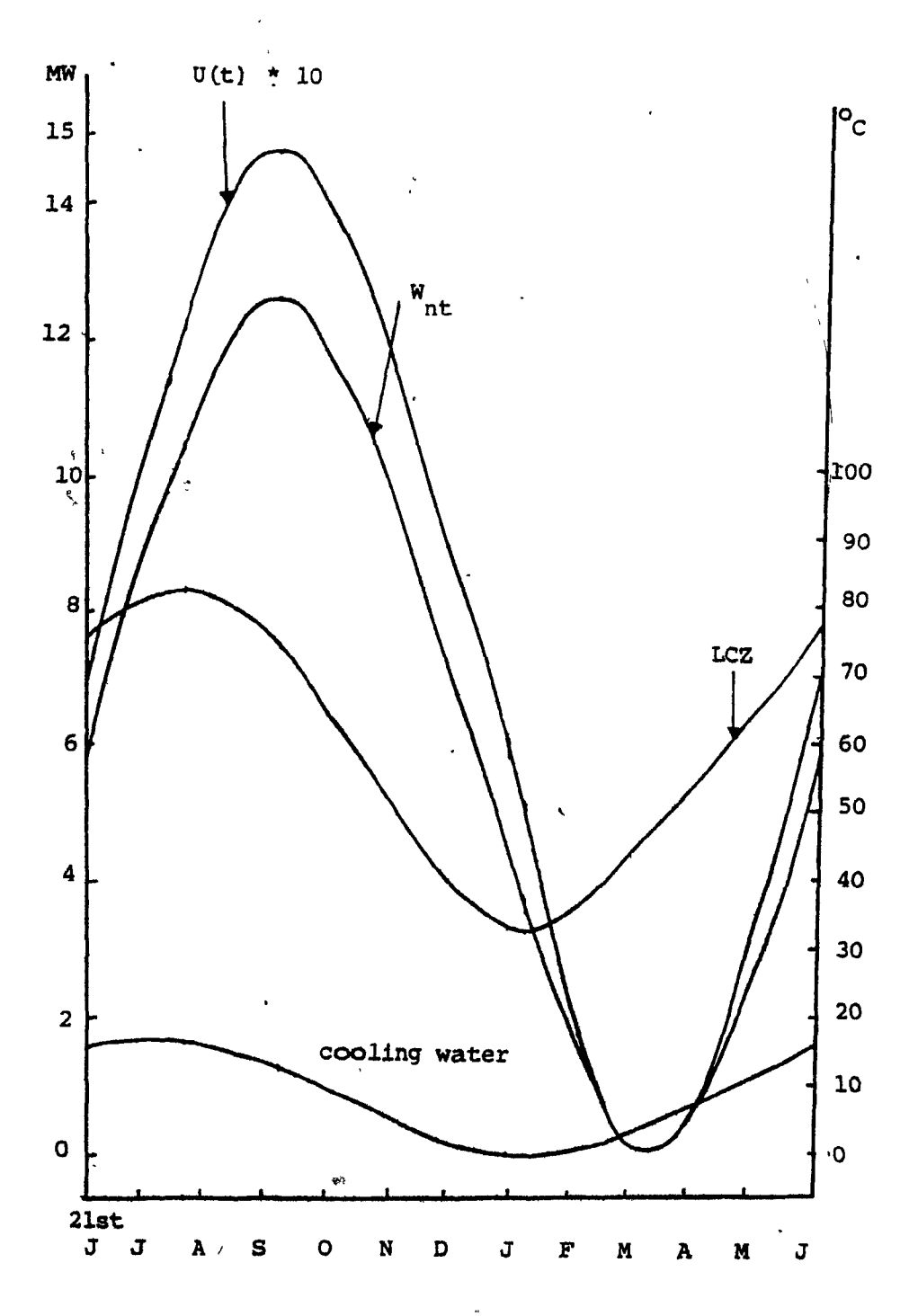
Location	.s (m) :	Ū (₩/m²)	บี้ (พ/m <sup>2</sup> )	• 6 u (Radian)	Ts oc)	T s cc)	δ <sub>S</sub> (Radian)	Electric Energy Cost (¢/KWh)	Cases
Montreal	0.5	20=8	20.8	1.618	57.08	<b>25.</b> 06	0.633	21.68	1
	0.5	34.88	14.61	1.08	81.9	15.	0.6488	9.07	2
	1.5	34.24	15.47	1.625	83.	13.8	0.86	9.39	3
Shiraz*	3.5	33.0 <sub>.</sub>	0.0	^ N/A	87.0	7,8	1,546	10.38	4
,	. 4.5	33.0	0.0	N/A	87.0	6.44	1.55	10.8	5
4	ı		•	1					

Free salt is assumed for these minimizations:

$$K_{\rm p} = 0.081 \frac{\rm kJ}{\rm kg}$$
 ,  $d_{\rm l} = d_{\rm l} = 6 ^{\circ} \rm C$  ,  $\eta_{\rm G} = 0.9 ^{\circ} \rm max$   $min$   $t_{\rm s} = 0.5 \, \rm m$  for cases 1 and 2  $min$   $t_{\rm l} = 1.5$  , 3.5 , 4.5 for cases 3 , 4 , and 5 .

The results of some of these runs are also summarized in Table 4.1 (cases 3 - 5). It can be seen that for deep storage depth ( > 3.5 meters) the heat extraction will be constant, and its value is exactly the same as that obtained in Chapter III.

Figures 4.3 and 4.4 show the time variations of the LCZ and cooling water temperatures, heat extraction rates, and net electric powers generated by SPPP for cases 1, 2, and 5 of Table It can be seen that operating strategies for optimal electric power generations are different for these two locations. power generation for the Montreal pond happens in late September while for Shiraz it is in December. The minimum power extraction occurs in March and early June respectively for Montreal and Shiraz. results for Shiraz are quite similar to the ones reported by French, 1981, for a hypothetical Salton Sea pond. Finally, Figure 4.5 shows the variation of the unit energy cost for the Montreal pond as a function of amplitude and phase lag of heat extraction, while keeping average heat extraction and LCZ thickness at their optimal values. The cost contours are also shown in this figure. Similar cost contours are shown for Shiraz pond in Figure 4.6. It can be seen that minimum cost occurs for heat extraction with an amplitude of about 14.5 W/m², which peaks in early October. The results mentioned in this section were obtained by using the GRG computer optimization The exhaustive enumeration method also gave similar results. package.



O

Figure 4.3 LCZ and cooling water temperatures, heating extraction and net electric power for Mon-treal pond.

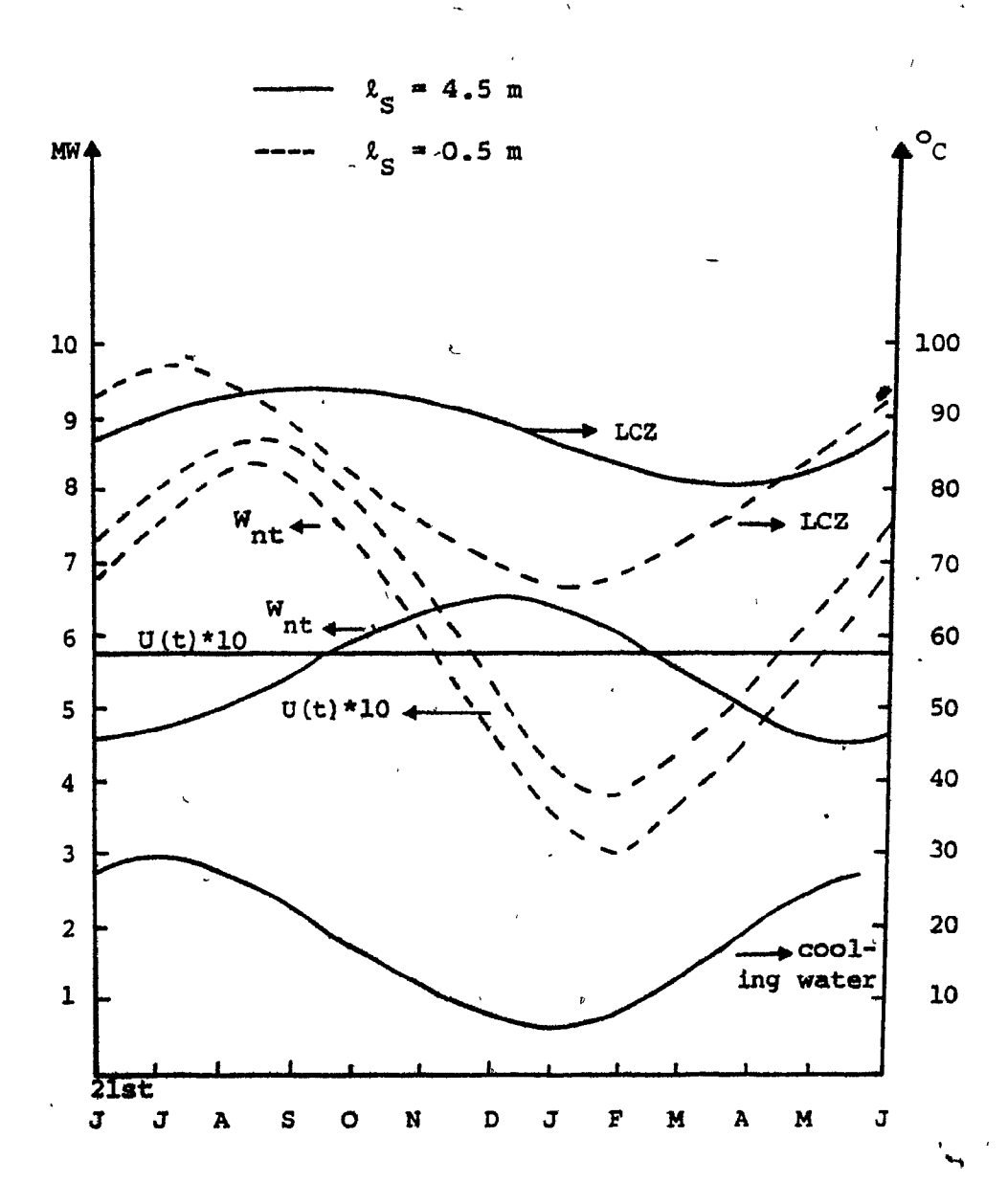
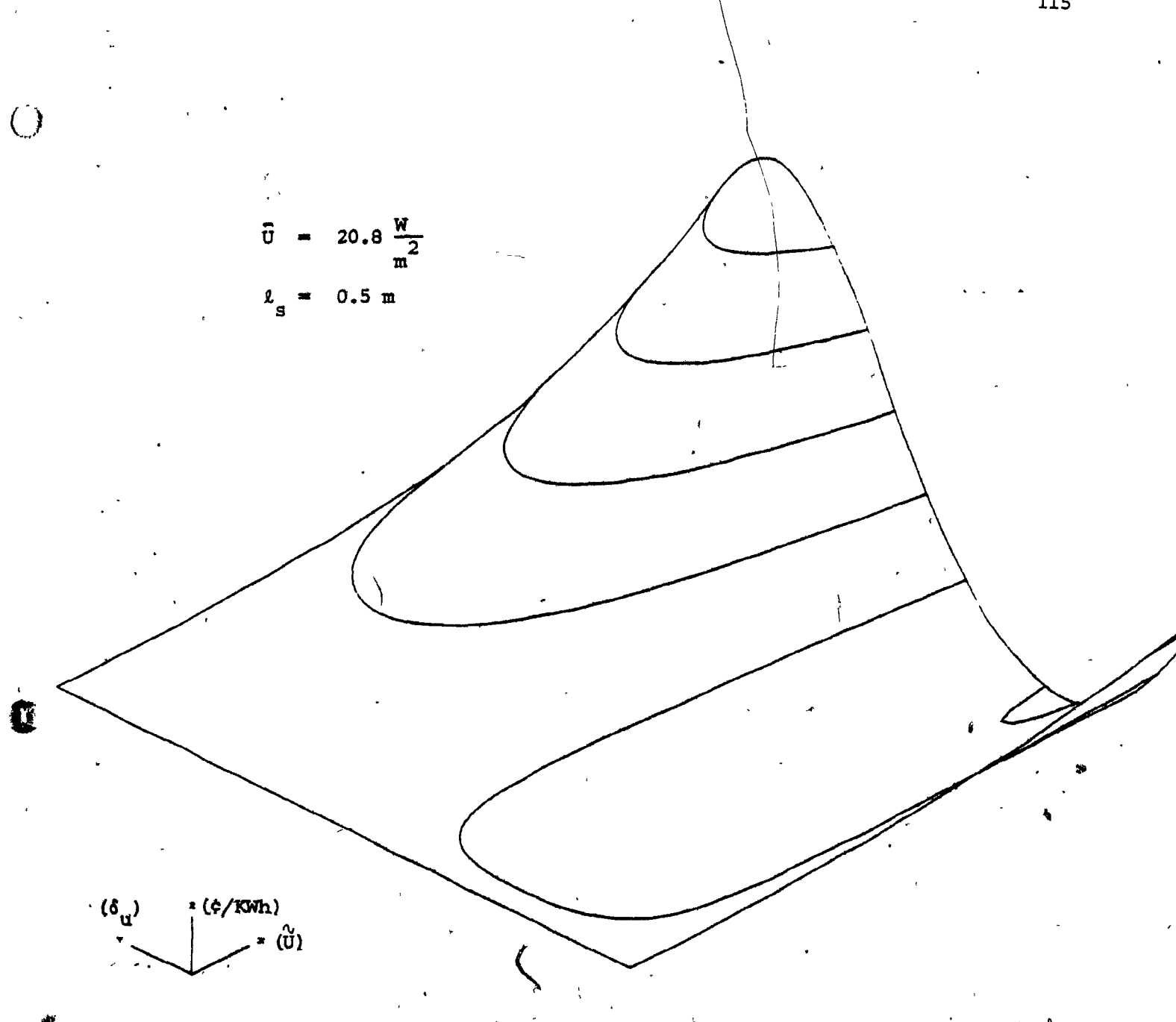
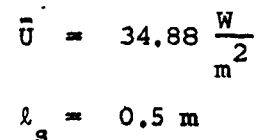


Figure 4.4 LCZ and cooling water temperatures, heat extraction and net electric power for Shdraz pond.



CONTOURS AT MULTIPLES OF 2

Electric Energy Cost as a function of phase lag . and amplitude of heat extraction for Montreal Pond.  ${f 9}$ 



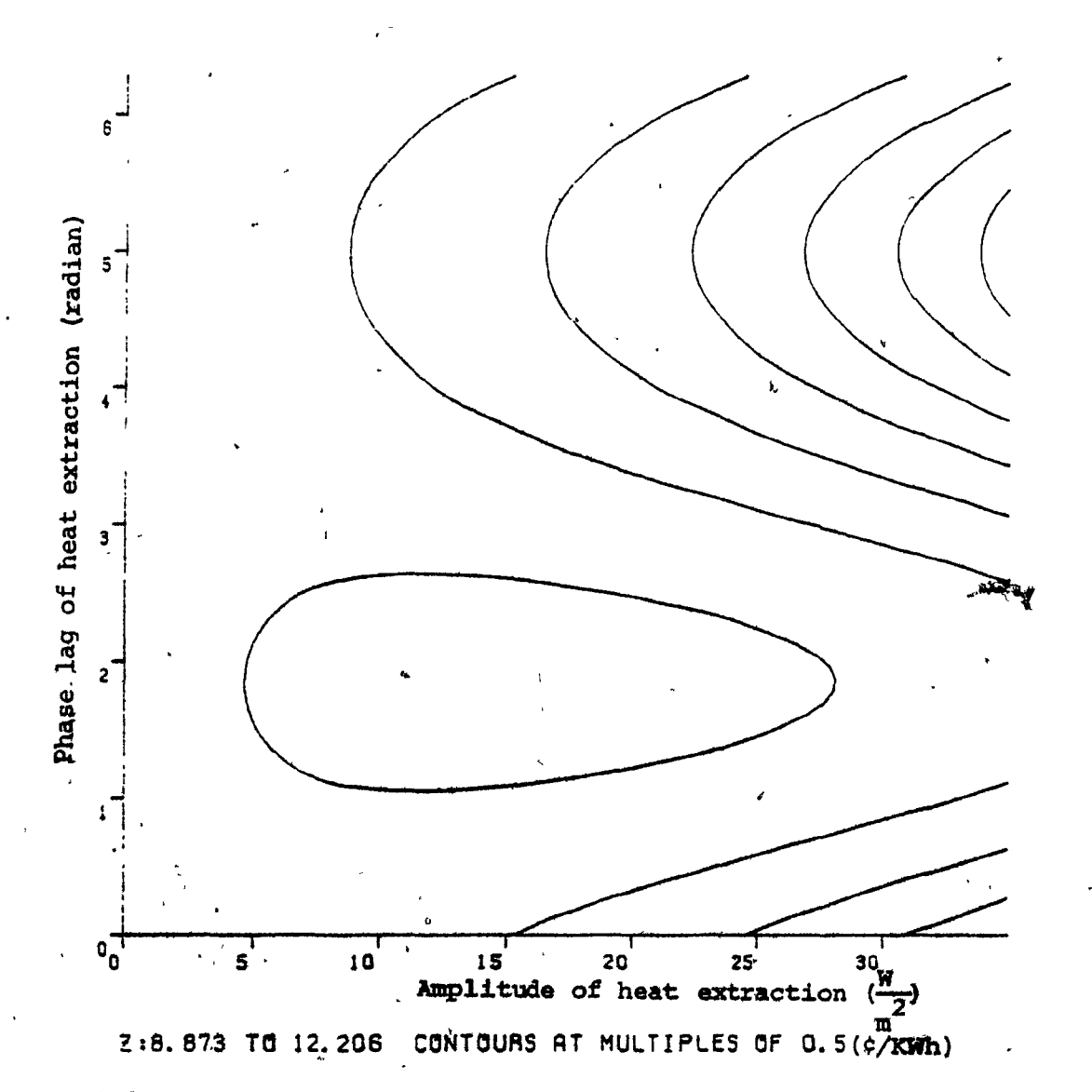


Figure 4.6 Contours of Energy Cost as a function of phase lag and amplitude of heat extraction for Shiraz Pond.

# 4.5 Mathematical Programming Method

(

In the previous sections the optimal heat extraction schedule as well as the thickness of the LCZ were obtained under sinusoidal excitations. If the radiation, ambient, and UCZ temperatures can not be well approximated by sinusoidal functions the semi-analytical method presented earlier can no longer be used. In this section the optimization will be cast into an optimal control problem and the solution will be obtained by mathematical programming techniques through discrete optimal control.

# 4.5.1 Optimal Control Formulation

Consider the governing equations of the pond's thermal behavior, equations (2.10), (2.12), and (2.13). These equations can be discretized in space only by replacing first and second space derivatives (terms of the form  $\frac{\partial}{\partial x}$  and  $\frac{\partial^2}{\partial x^2}$ ) by difference operators. In a compact form the following set of ordinary coupled differential equations would result:

$$\underline{\underline{\mathbf{T}}} = \underline{\mathbf{A}} \underline{\mathbf{T}} + \underline{\mathbf{e}}_{n+1} U(t) + \underline{\mathbf{v}}(t)$$

where  $\underline{T}$  is the  $(m \times 1)$  vector of nodal temperatures, A is the coefficient matrix (tridiagonal structure), v(t) is the vector of

except the n+1 is an m x 1 vector whose elements are zero except the n+1 , which is unity (position n+1 refers to LCZ temperature). Therefore the optimal control problem can be stated in the following form:

minimize 
$$= \frac{1}{C_{t1} + C_{t2} l_s} \int_{t_0}^{t_f} W_{nt}(t) dt = \int_{t_0}^{t_f} L[T_{n+1}(t), U(t), l_s, t] dt$$

$$(4.14)$$

subject to:

$$\frac{\dot{T}}{T} = A T + \underline{e}_{n+1} U(t) + \underline{v}(t) \qquad \underline{T} (t = t_0) = \underline{T}^0. \quad (4.15)$$

and

$$0 \le v(t) \le v^{max}$$

$$0 \le T_{n+1} \le T_{n+1}^{max}$$

where  $W_{nt}(t)$  is the net electric power given by equation (4.6) and bounds on the variables take into account the physical realizability. It should be noted that  $T_{n+1}(t)$ , the LCZ temperature, is a function of the LCZ thickness and other parameters.

An analytical solution of the above problem based on the Maximum / Minimum Principle (Athans and Falb, 1966) is probably possible, but the nonlinearities involved would make it exceedingly complex. The complexity would not be reduced even if we wanted to use the lumped parameter model, equation (4.2), in the problem at hand. If we accept the fact that most optimal control problems must be solved numerically (Bryson, 1972) using a digital computer, one can always regard the determination of U(t) (to  $t \in t$  as equivalent to the determination of U(0), U(1), .... U(N-1), the discrete equivalent of U(t).

It is convenient to rewrite the problem stated in equations (4.14) and (4.15) as follows:

minimize 
$$T_{m+1}$$
 (t<sub>f</sub>) (4.16)  $U(t), l_g$ 

subject to :

$$\frac{\dot{\mathbf{T}}}{\dot{\mathbf{T}}} = \mathbf{A} \, \frac{\mathbf{T}}{\mathbf{T}} + \frac{\mathbf{e}}{\mathbf{n}+1} \, \mathbf{U}(\mathbf{t}) + \frac{\mathbf{v}}{\mathbf{t}}(\mathbf{t}) \qquad \frac{\mathbf{T}}{\mathbf{T}} \, (\mathbf{t} = \mathbf{t}_0) = \frac{\mathbf{T}^0}{\mathbf{t}} \qquad (4.17).$$

$$\dot{T}_{m+1} = L (T_{n+1}(t), U(t), l_s, t)$$
  $T_{m+1}(t = t_0) = 0$  (4.18)

where m is the total unknown nodal temperatures and  $T_{m+1} = \frac{1}{C_{KWh}}$ 

The numerical solution consists of successively finding a U(i) sequence which satisfies the optimality conditions. The class of functions chosen for approximating U(t) is the class of step-functions, where U(t) is constant per interval. The overall interval, [t<sub>0</sub>, t<sub>f</sub>], for the case at hand is divided into 52 intervals (corresponding to 52 weeks of the year), in each of which U(t) is constant. Each interval is divided into subintervals (usually each interval is divided in half) for better accuracy of the numerical integration of the system differential equations. It should be mentioned that the system of differential equations (4.17), representing pond thermal behavior, are first solved for steady state operation using finite difference; and then equation (4.18) is solved using an IMSL<sup>1</sup> subroutine (a subroutine called DVERK which is based on the fifth and sixth orders Runge-Kutta method).

# 4.6 Examples

The optimal heat extraction and storage depth will be calculated using mathematical programming. We have first tried an

International Mathematical and Statistical Library.

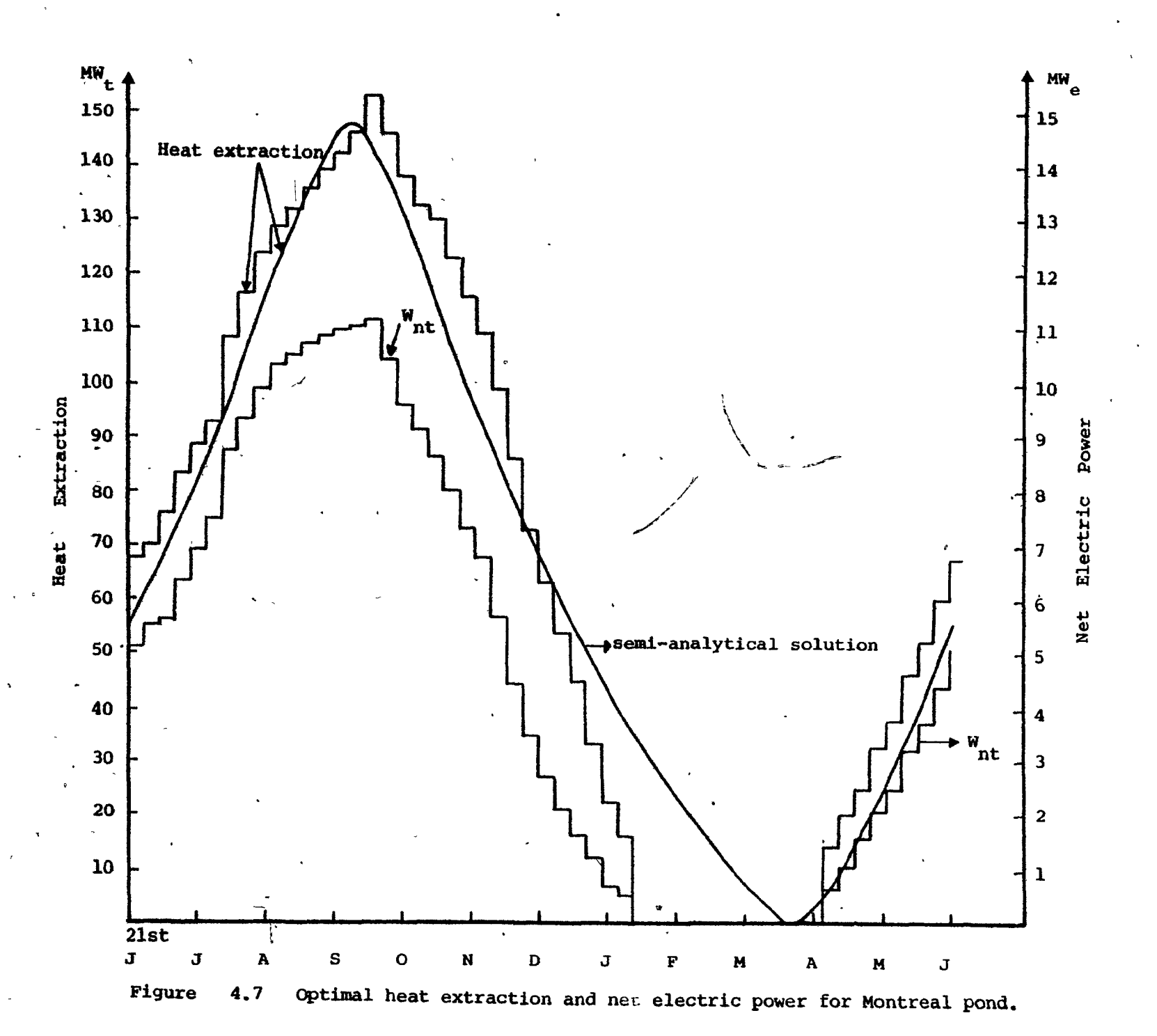
optimal control problem with a known analytical solution (Speyer and Bryson, (1968)) to test the GRG package in handling discrete optimal control problems. The results obtained were in excellent agreement with the analytical solution for the 30 intervals of stepfunctions. It is assumed that ice on the surface of the Montreal pond will block 80% of radiation. The cooling water temperature is also assumed to follow ambient temperature whenever the latter is above  $-2^{\circ}$ C (freezing point of 3% brine in the UCZ) and remains at  $-2^{\circ}$ C whenever the ambient temperature falls below  $-2^{\circ}$ C.

The optimal heat extraction and electric power generation for the Montreal pond using Mathematical programming is shown in Figure 4.7. For the purpose of comparison the result of the semi-analytical solution is superimposed on this figure. An energy cost of 20.97 ¢ / KWh was obtained here, which is slightly less than that

Find the optimal program, U(t), over the interval t [0, 1] which minimizes:

Minimize J = 1/2  $\int_{0}^{3} U^{2}(t) dt$  subject to:  $\dot{x} = A \times + b U(t)$  and U(t)  $x_{2}(t) + 4t^{2} - 12t + 8 \ge 0$ ,

where:  $A = \begin{bmatrix} 0 & 1 & 0 \\ 0 & 0 & 1 \\ 0 & 0 & 0 \end{bmatrix}$  and  $b = \begin{bmatrix} 0 \\ 0 \\ 1 \end{bmatrix}$ and  $x(t=0) = \begin{bmatrix} 1.6 & -1 & 0 \end{bmatrix}^{T}$ ,  $x(t=3) = \begin{bmatrix} 0 & -1 & 0 \end{bmatrix}^{T}$ 

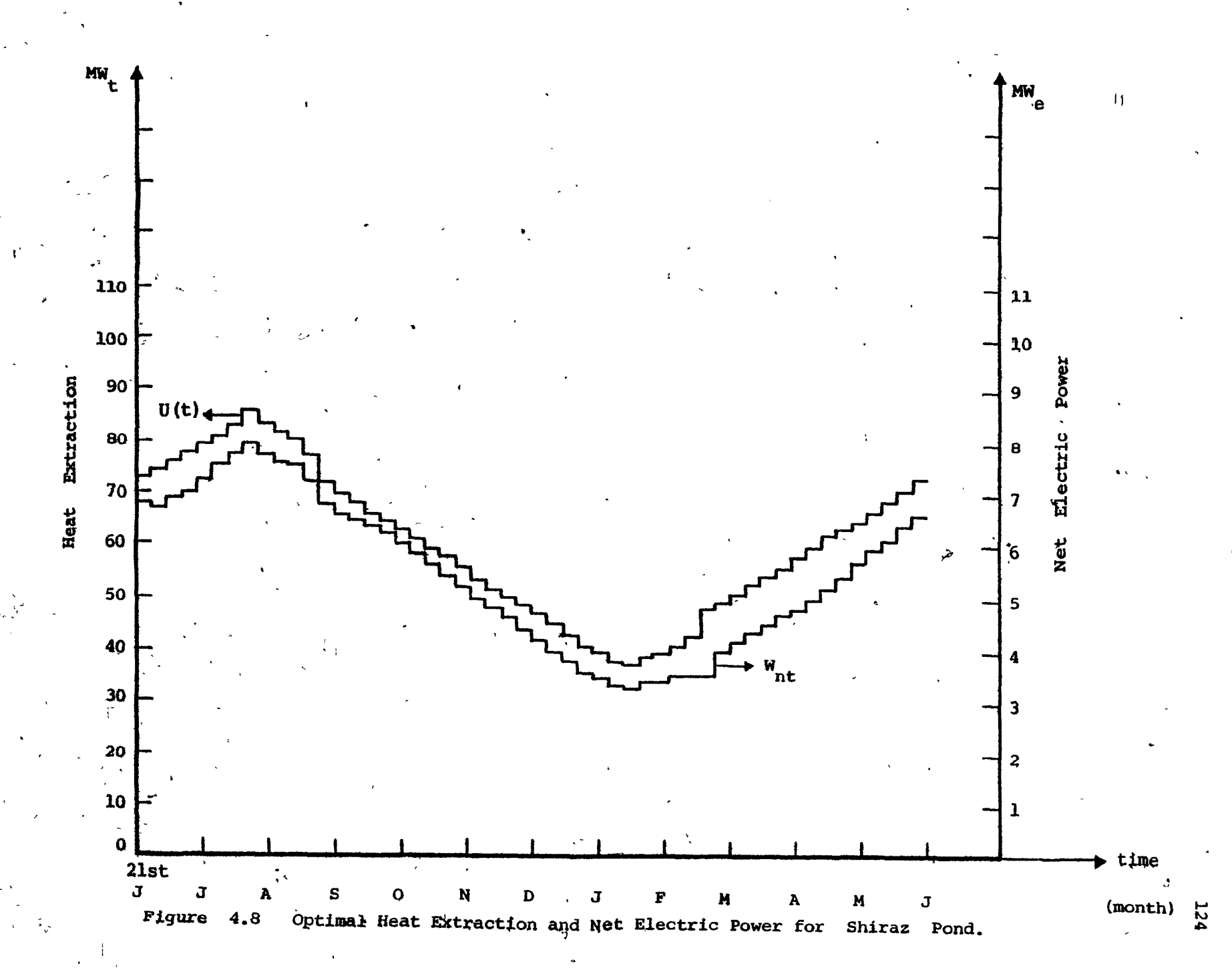


of semi-analytical solution (21.68 ¢ / KWh). It should be noted that the actual difference in energy cost for these methods should be even larger because the effective insolution considered in the mathematical programming solution was lowered by ice absorption.

It can be seen from Figure 4.7 that the SPPP will not produce electric power for three months. The optimal storage depth has the same value (0.5 meter) as in the semi-analytical solution.

The optimal heat extraction and net electric power generated by SPPP for Shiraz are depicted in Figure 4.8. The optimal heat extraction obtained by mathematical programming is in good agreement with that of the semi-analytical method. The energy cost of 8.5 ¢ / KWh is comparable with 9.07 ¢ / KWh of the semi-analytical solution.

Therefore it can be concluded that the optimal heat extraction is really a sinusoid for locations where no ice coverage of the pond surface occurs and all excitations can be well approximated by sinusoidal functions. It is interesting to mention that the CFU time required for mathematical programming (using Fortran H compiler on Amdahl V7) was on the average five minutes while the corresponding time for semi-analytical solution was around two seconds.



#### CHAPTER V

### COST REDUCTION TECHNIQUES

### 5:1 Introduction

The unacceptable energy cost for the Montreal pond led us to consider possible cost reduction techniques. The present chapter deals with concepts that may result in electric energy cost reduction of an SPPP in northern climates. We have seen how LCZ thickness affects the LCZ temperature profile. The amplitude of the variation of the LCZ temperature can be reduced by increasing the LCZ depth, but, the salt requirement will then also increase, which is an important item in SPPP capital costs. For this reason, a floating pond equipped with a deep saltless storage zone is first proposed.

The cooling water temperature plays an important role in cycle efficiency and of course in energy cost (¢ / Kwh) of an SPPP. The possibility of using an ice storage pit to provide a lower cooling temperature than that of the UCZ will also be investigated in this chapter.

### 5.2 The Floating Solar Pond

The possibility of making the NCZ of a solar pond float over a layer of fresh water is investigated. Such a construction

would greatly reduce salt costs in ponds equipped with deep LCZ and may eventually permit the construction of solar ponds as floating structures in natural bodies of water. It would also permit the location of large solar ponds close to densely built urban centers, where they could not otherwise be installed because of space limitations.

### 5.2.1 Floating Structure

It is proposed (Crevier and Moshref, 1981) to separate the NCZ from the fresh or sea water underneath by an impermeable membrane stabilized by weights and buoys attached to it. A possible design for a floating solar pond appears in Figure 5.1 . It is inspired from the "lake storage" concept developed at the Studsvick Energy Research and Development Center in Sweden (Morgan, 1978) . A flexible, insulating envelope, open at the top, encloses a part of a lake or a bay This "diving bell" is anchored to the bottom of the lake to resist the upward pressure created by the difference in density between the warm water inside and the cold surrounding water. NCZ floats at the surface; this layer is contained by a structure consisting of a flexible bottom membrane stabilized by weights and buoys assemblies, and maintained on the sides by a rigid floating hull. This layer will naturally stabilize, itself at a depth where the bottom

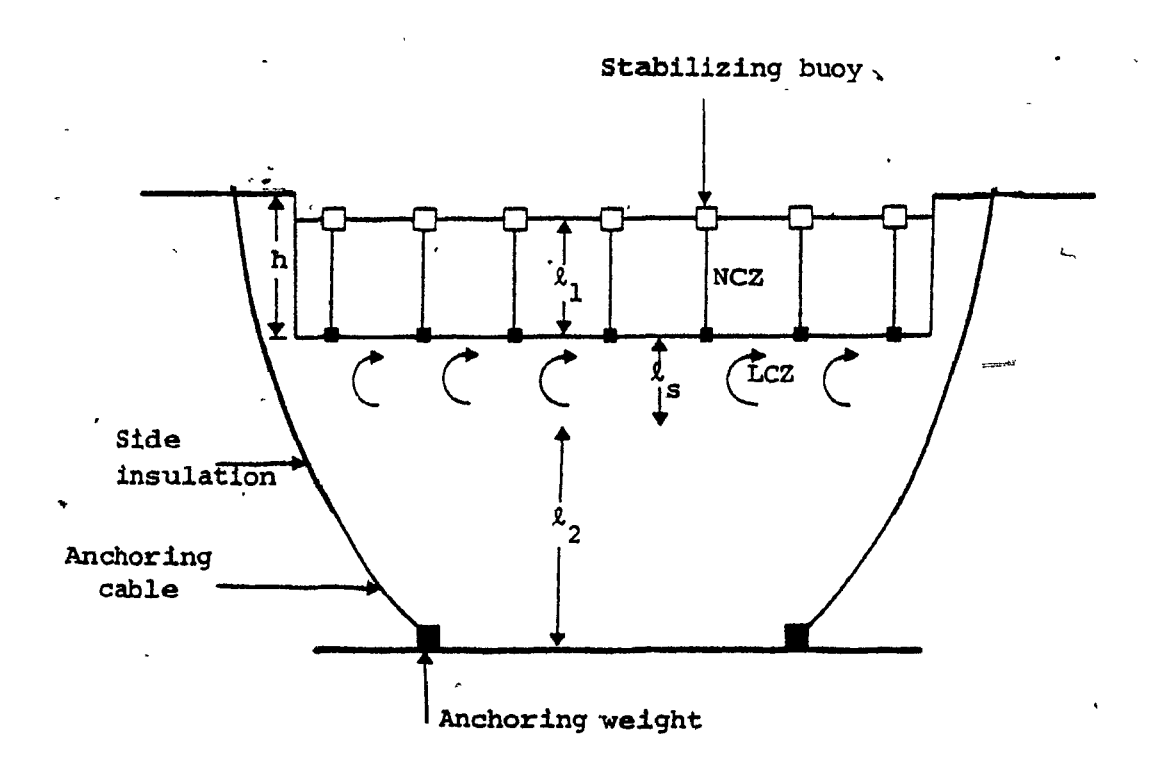


Figure 5.1a Water Based Floating Pond.

0

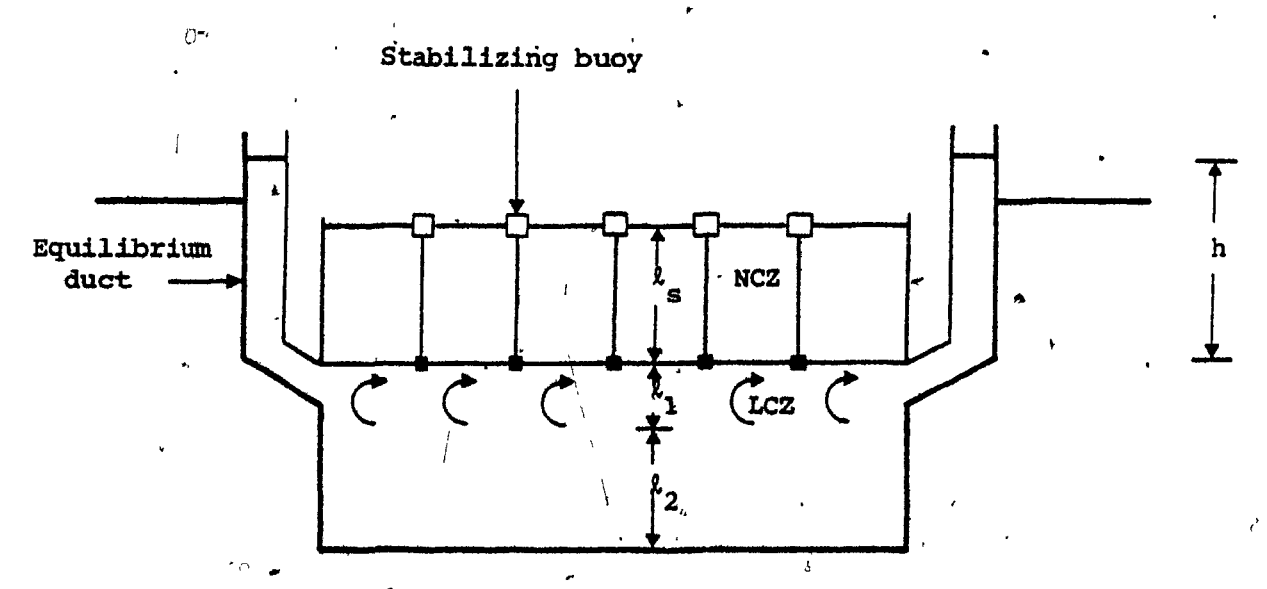


Figure 5.1b Land Based Floating Pond.

Figure 5.1 Schematic Diagram of Floating Solar Pond.

membrane will be under equilibrium pressure. The membrane can be either transparent or opaque. In the case of a transparent membrane; a convective, or storage layer can be induced by placing at some distance under the floating NCZ an opaque, not necessarily impermeable, membrane absorbing the radiation reaching this depth. The layer of water between this membrane and the floating NCZ will thus be heated from underneath and constitute the convecting layer of the floating solar pond. Two possible difficulties may arise from the use of a transparent membrane:

- (a) loss of transparency of the membrane due to accumulation of debris,
- (b) degradation of the transparent membrane by ultraviolet radiation.

A variation on this design would consist in having only one, opaque membrane at the bottom of the upper insulation layer and to induce a forced circulation of water in the LCZ, which would then be heated from above instead of from below. This would eliminate the above problems, and in addition reduce the membrane costs and of course increase electric power requirements for auxiliary pumps.

It is interesting to note that the mathematical model of a floating solar pond is exactly the same as that of the ordinary salt gradient pond if the buoys are made of transparent material. It

should however be noted that the transparency of the membrane does not enter into account, since any radiation reaching the bottom of the NCZ is considered trapped in the pond.

# 5.2.2 Stabilization of the NCZ over Fresh Water (Uniform Concentration)

The heavier salt water of the NCZ can be prevented to sink into the fresh water of the LCZ by the following means:

- (1) The two layers are separated by a transparent plastic membrane.
- (2) The pressures are equalized on both sides of the membrane by equilibrium ducts.
- (3) The membrane is stabilized by a combination of buoys and weights.

In the absence of buoys and weights, the flat bottom configuration shown in Figure 5.1 would not be stable for the following reason. Let us, as a first approximation, neglect the fact that there exists a density gradient in the non-convecting layer, and assume that this layer contains salt water of uniform density  $\rho_1$  (average

density between UCZ and the bottom of NCZ) , larger than the density  $\rho_2$  in the LCZ . Let, as before, the depth of the NCZ layer be  $\ell_1$  , and the height of the fresh water in the equilibrium ducts above the membrane be h . If a pressure equilibrium exists, then :

$$\rho_1 \ell_1 = \rho_2 h \tag{5.1}$$

If now a disturbance causes a local downwards buckling of depth dy of the flexible bottom, the downwards pressure at the lowest point of the deformation will be:

$$P_{d} = \rho_{1} g(l_{1} + dy)$$
 (5.2)

where g is the acceleration due to gravity. The upwards pressure can be expressed as follows:

$$P_{u} = \rho_{2} g(h + dy)$$

If we let P be the net pressure (positive upwards), then :

$$P_n = P_d - P_d = -(\rho_1 - \rho_2) g dy$$
 (5.3)

This pressure is thus directed downwards, which will intensify the

buckling. For the same reasons, an upwards buckling would also tend to be amplified, and the flat bottom configuration is unstable.

Assume now that  $n_i$ : stabilizing buoys are attached to the bottom of the membrane as in Figure 5.1, in such a way that when the weights attached to the buoys are at a depth  $\ell_1$ , the buoyancy of the immersed part of the buoys exactly compensates the downward pull of the weights. If, however, n contiguous weights and buoys sink to a depth  $\ell_1 + dy$ , the total upward pull exerted on the attachment points to the membrane will be:

$$F = n A_b \rho_1 g dy \qquad (5.4)$$

where  $A_b$  is the cross-sectional area of one buoy. If there is one buoy per  $A_m$  square meters of the pond, this force is equivalent to an upwards pressure  $P_b$  of magnitude :

$$P_{b} = \frac{F}{n A_{m}} = (\frac{A_{b}}{A_{m}}) \rho_{1} g dy$$
 (5.5)

By virtue of equation (5.3), the total upwards pressure exerted on the membrane at the bottom of the disturbance constituted by the  $\, n \,$  depressed buoys is then :

$$\underline{P} = (\frac{A_b}{A_m}) \rho_1 g dy - (\rho_1 - \rho_2) g dy \qquad (5.6)$$

This net upwards pressure  $\underline{P}$  will be positive for :

$$\left(\frac{\mathbf{A}_{\mathbf{b}}}{\mathbf{A}_{\mathbf{m}}}\right) > \left(\rho_{1} - \rho_{2}\right) / \rho_{1} \tag{5.7}$$

In other words, for a NCZ of uniform density, the fraction of the pond area occupied by the stabilizing buoys must be larger than the fractional difference in density between the NCZ and LCZ, which would be approximately 10 per cent for the solar pond. The size of the individual buoys and their spacing must be such that the membrane's capacity to withstand local deformation is not exceeded; while deformations covering a larger area will be stabilized by the buoys.

# 5.2.3 Stabilization of the NCZ over Fresh Water (Linear Salt Gradient)

Let us assume that a linear salt gradient exists in the NCZ as follows:

$$\rho(y) = \rho_1 + (\rho_2 - \rho_1) \frac{y}{k_1}$$

where  $\rho_1$  and  $\rho_2$  are densities in UCZ and the bottom of NCZ re-

spectively. For a disturbance of dy the downwards pressure can be expressed by (see Figure 5.2) :

$$P_{d} = \int_{0}^{\rho(y)} \rho(y) g dy = \rho_{1} g (\ell_{1} - dy) + \frac{\rho_{2} - \rho_{1}}{2 \ell_{1}} g (\ell_{1} - dy)^{2}$$
(5.8)

The upwards pressure can be written as :

$$P_{u} = \rho_{3} g (h - dy)$$
 (5.9)

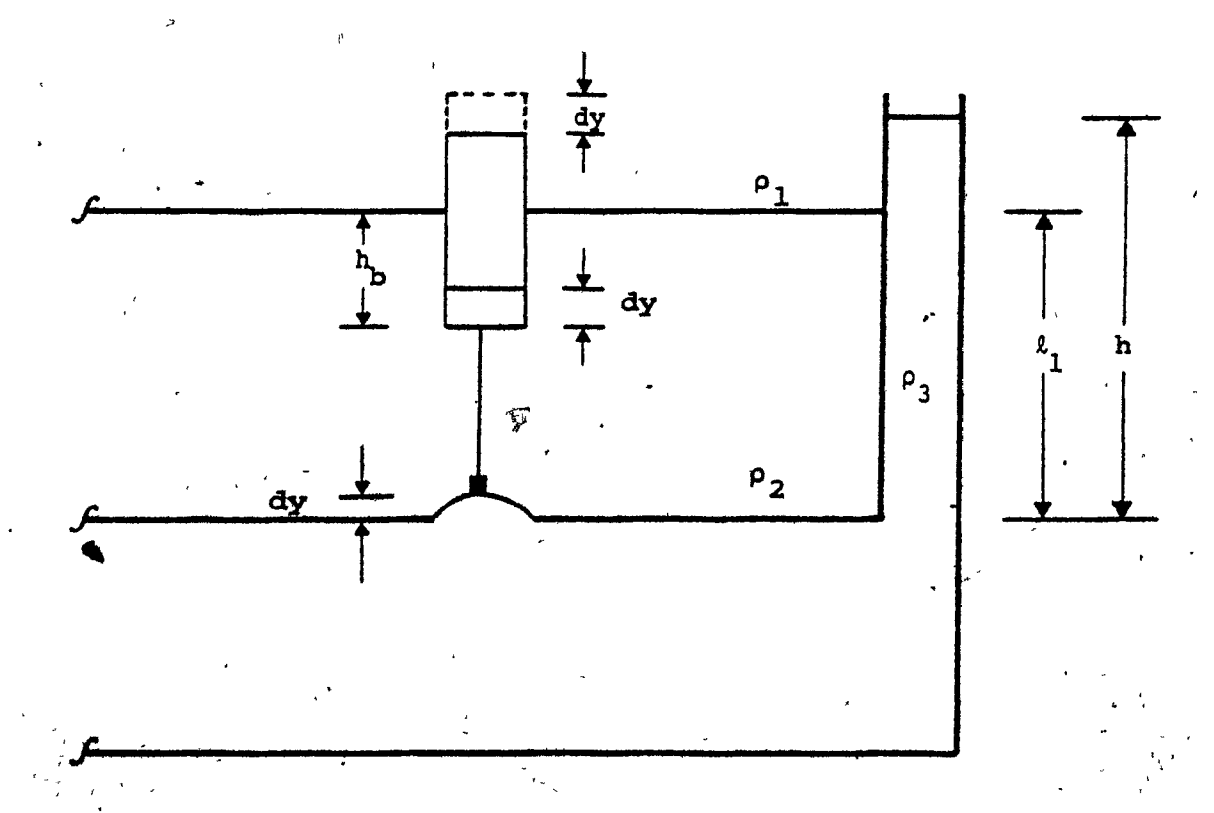


Figure 5.2 Close-up of the membrane deformation.

where  $\rho_3$  is the density of water in equilibrium duct. The net upwards pressure, using equations (5.8) and (5.9), is given by:

$$\underline{P} = P_{u} - P_{d} = \rho_{3}^{*} hg - \frac{\rho_{1} + \rho_{2}}{2} l_{1} g + (\rho_{2} - \rho_{3}) dy g$$

$$- \frac{\rho_{2} - \rho_{1}}{2 l_{1}} dy^{2} g$$
(5.10)

but,

$$\rho_3 h = \frac{\rho_1 + \rho_2}{2} \ell_1 \quad \text{equilibrium condition } (P_u |_{dy = 0}) = P_d |_{dy = 0}$$

Therefore, equation (5.10) simplifies into the following form :

$$\underline{P} = [(\rho_2 - \rho_3) dy - \frac{\rho_2 - \rho_1}{2 \ell_1} dy^2] g$$
 (5.11)

For small dy, the disturbance will be intensified:

$$\frac{\partial P}{\partial dy}\Big|_{dy = 0} = g (\rho_2 - \rho_3) > 0$$

The force which is applied to one buoy, from its attachment weight, can be expressed as:

$$F = g A_b \int_{b}^{h_b} \rho(y) dy$$

$$h_b - dy$$

The above equation upon a simple integration and simplification yields:

$$F = -g A_b dy \left[\rho_1 + \frac{\rho_2 - \rho_1}{\ell_1} \left(h_b - \frac{dy}{2}\right)\right]$$
 (5.12)

The equivalent pressure for n buoys will be :

$$\begin{array}{ccc} P_{\text{eq}} & \stackrel{*}{=} & \frac{F}{A_{\text{m}}} \end{array}$$

Therefore the net pressure can be given by the following, using equations (5.11) and (5.12):

$$P_{\text{net}} = P + P_{\text{eq}} = g \left[ \binom{\rho_{2} - \rho_{3}}{2} dy - \frac{\rho_{2} - \rho_{1}}{2 \ell_{1}} dy^{2} \right]$$

$$- g \frac{A_{b}}{A_{b}} dy \left[ \rho_{1} + \frac{\rho_{2} - \rho_{1}}{\ell} (h_{b} - \frac{dy}{2}) \right]$$

To stabilize the membrane, the net pressure should be negative. The stability can be obtained if the following is satisfied:

$$\frac{\partial P_{\text{net}}}{\partial dy} \Big|_{dy = 0} < 0$$

or,

$$\frac{\mathbf{A}_{\mathbf{b}}}{\mathbf{A}_{\mathbf{m}}} > \frac{\rho_2 - \rho_3}{\rho(\mathbf{h}_{\mathbf{b}})} \tag{5.13}$$

where

$$\rho(h_b) = \rho_1 + (\rho_2 - \rho_1) \frac{h_b}{2}$$

As an example, for  $h_b = 0.5l_1$ , the inequality of (5.13) reduces to the following:

$$\frac{\mathbf{A}_{\mathbf{b}}}{\mathbf{A}_{\mathbf{m}}} > \frac{\mathbf{\rho}_{2} - \mathbf{\rho}_{3}}{\mathbf{\rho}_{1} + \mathbf{\rho}_{2}}$$

which for typical values of  $\rho_1$ ,  $\rho_2$ ,  $\rho_3$ , gives the same condition as in equation (5.7), i.e., the fraction of the pond area occupied by the stabilizing buoys must be greater, or equal to .10 per cent.

### 5.3 Optimization of a Floating SPPF

The model developed in Chapter II can be used to simulate the floating pond with the difference that the physical properties of the ground and LCZ would be replaced by that of fresh or sea water. Most of the cost of a floating pond would reside in the hull and the membrane isolating the salt gradient layer. Hull costs will be minimum when a section of a natural body of water is isolated to make up the pond, and maximum when the hull must enclose the entire pond. Here it will be assumed that the length of hull required is equal to one half of the perimeter of a circular pond of the considered area, at a cost of \$100 /  $m^2$  of hull area. This cost consists in material costs (inner impermeable liner, \$10 /  $m^2$ ; insulation, \$15 /  $m^2$ ; outer grid, \$25 /  $m^2$ ) and labour costs of \$50 /  $m^2$ . The cost of membrane, weights, and buoys are assumed to be \$10. for a square-meter area of the pond.

An optimization, similar to the one presented in Chapter III, will be carried out for a floating SPPP for Montreal conditions. The life time of the plant is here assumed to be ten years because of uncertainty in the long term performance of the membrane. The results are summarized in Table 5.1. A comparison between the present simulation and that of Table 3.2 shows that the energy cost of a floating SPPP (FSPPP) is about 12% lower than that of an ordinary SPPP. Since the in-

TABLE 5.1
SUMMARY OF THE RESULTS FOR A 5 MW FLOATING SPPP IN MONTREAL

ITEM	Floating SPPP (F-113 Working Fluid)
Pond:	
Surface area (Km <sup>2</sup> )	3.56
Heat extraction depth (m)	1.72
Temperature of LCZ ( <sup>O</sup> C)	63,32
Efficiency (%)	. 11.80
Heat Exchanger Area (10 <sup>4</sup> m <sup>2</sup> ) :	٠
Vaporizer (boiler)	2.19
Condenser	2.33
Pre-heater	1644
· ou	
Turbine:	
Inlet pressure (psia)	20.26
Outlet pressure (psia)	3,68
Inlet temperature (°C)	57.45
Outlet temperature (°C)	11.63
Mass Flow Rate (Kg/sec):	
Brine	3136
Working Fluid	339
Cooling Water	3386
Gross Power (MW <sub>e</sub> ):	" 5.562Ž
System Efficiency (%):	0.9351
Energy cost (¢ / KWh) :	29.6

stallation cost of FSPPP is smaller than that of an SPPP it is economical to operate the pond at a higher average LCZ temperature.

Other parameters and operating conditions are only marginally different from those of Table 3.2.

The concept of a floating SPPP seems to have its merits despite of the still high energy cost. Making the NCZ float on a layer of fresh water would eliminate a major fraction of the pond cost in areas where salt is expensive. Making use of this principle in natural bodies of water would permit the construction of large solar ponds close to densely populated urban areas, where land costs would be prohibitive. The water-based floating pond has no excavation cost in addition to reduced salt costs (Crevier and Moshref, 1981) . saltless LCZ would also facilitate the extraction of heat from the pond by preventing corrosion in the heat exchangers, where water from the LCZ is circulated. The existence of buoys would probably reduce the costs of the required wave dampers. Environmental and structural problems should however be given careful consideration before the concept is declared viable.

### 5.4 Ice Storage as a Heat Sink for SPPP

### 5.4.1 Introductory Remarks

One possible way of improving the efficiency of the power plant

would be to lower the heat sink temperature, i.e., increase the temperature difference between source and sink. For a given climate, the LCZ temperature and associated source temperature can be controlled by the pond's geometry and heat extraction rate. On the other hand the sink temperature is usually determined by that of the available cooling medium (air or water). In this section, the possibility of using an ice storage for cooling the turbine working fluid will be investigated.

Storage of sawed blocks of river and lake ice in pits, caves, and insulated buildings was commonly done both commercially and privately by generations of our ancestors. With the advent of mechanical refigeration, engines driven by heat or electricity could produce ice in commercial volume almost any where, at any time, and the labor-intensive cutting and storage of natural ice largely disappeared. Present-day energy costs and supply problems, coupled with the development of relatively low energy techniques for recreational snow-making, have provided the stimulus and the means for resurrecting the production and storage of natural ice and snow.

Canada and the northern part of the United States can benefit from significant periods of sub-freezing winter weather, where large amounts of naturally forming ice can be found. It is therefore proposed here, to harvest the ice and snow during the winter. This

ice storage will serve as a heat sink for SPPP during the warmer part of the year.

### 5.4.2 Structure and Mechanism of Ice Storage

It is assumed that a pit, having a volume  $V_i$  yet to be determined, is excavated in the ground close to the solar pond. This reservoir will have a water-tight membrane liner (if impermeable soil can be found this liner can be eliminated). Snow and naturally forming ice, collected during winter, are stored in it and will be used as a cooling medium whenever the upper convective zone of the pond is at a temperature larger than zero degree Celcius. The ice storage will be covered, with an insulating blanket to minimize melting. During any subfreezing night the blanket can be opened on two sides to provide air passage, and the cooling water returning from the SPPP condenser can be sprayed over the ice and re-frozen.

### 5.4.3 Sizing of the Ice Storage

La Bran in the

Suppose the ice storage at the end of the harvesting period contains  $M_{0}$  and  $M_{10}$ , Kg of water and ice respectively, and let us

assume that the well mixed water underneath is at equilibrium temperature  $T_i$ . This water will be pumped with a flow rate of  $m_3$  to the condenser; the warmer water is returned to the top of the reservoir to be re-cooled to zero  $^{\circ}$ C by the remaining ice. If melted ice is added at a rate of  $m_{\widetilde{W}}$  per unit time, the following heat balance can be written for the system:

$$\dot{m}_3 C_w (T_1' - T_1) = \dot{m}_w h_{sl} + q_t + q_b$$
 (5.14)

where h<sub>sl</sub> is the latent heat of fusion of ice, q<sub>t</sub> and q<sub>b</sub> are the heat gains from top and bottom (side heat gain is ignored), and T<sub>i</sub> is the temperature of the water returning from the condenser. Conservation of mass will give the following:

$$M_{i}(t) + M_{w}(t) = Constant$$

or

$$\frac{dM_{w}(t)}{dt} = -\frac{dM_{1}(t)}{dt}$$

where  $M_{i}(t)$  and  $M_{i}(t)$  are the amount of ice and water at any given time. Therefore, using equation (5.14), equation (5.15) after integration can be written as:

$$M_{i}(t) = -\left(\frac{m_{3} C_{w} (T_{i}^{*} - T_{i}) + q_{t} + q_{b}}{h_{sl}}\right) t + c$$
 (5.16)

where the constant of integration, c , can be obtained from the initial and final conditions:

$$M_{i} (t = t_{0}) = M_{i0}$$
 and  $M_{i} (t = t_{f}) = 0$  (5.17)

q and q will be estimated for steady state operations; the bottom losses, as in the solar pond, can be given by:

$$q_{b} = \frac{\kappa_{2}}{\ell_{2}} (T_{w} - T_{1}) A_{1}$$
 (5.18)

where A is the ice storage area yet to be determined. The top losses can be formulated as follows:

$$q_t = U_0 A_i (\bar{T}_a - \bar{T}_i)$$
 (5.19)

where  $U_0$ , the overall heat transfer coefficient for the insulating blanket, can be given by (Rohsenow, 1973):

$$\frac{1}{v_0} = \frac{1}{h_{fr}} + \frac{t_1}{K_1}$$

where h is the free convection heat transfer coefficient; t and

 $K_1$  are the thickness and thermal conductivity of the insulating blanket respectively. A value of 67  $\frac{W}{m^2 \cdot c}$  is awsumed for  $h_{fr}$ .

which is an average free convection heat transfer coefficient for flat surfaces (Rohsenow, 1973). Using equations (5.16) - (5.19), the amount of ice that should be stored in order to last through the summer can be given by the following:

$$M_{i0} = \frac{\dot{m}_{3} c_{w} (T_{i}^{i} - T_{i}) + (\frac{K_{2}}{\ell_{2}} (T_{w} - T_{i}) + U_{0} (\bar{T}_{a} - T_{i})) A_{i}}{h_{s\ell}} (t_{f} - t_{0})$$
(5.20)

The minimum volume required for ice storage (neglecting the initial water,  $\rm M_{\omega Q}$  , in the ice storage) .

$$v_i = \frac{M_{i0}}{\rho_i}$$

where  $\rho_1$  is the density of ice; if the ice storage is assumed to be an inverted pyramid of top area of  $A_1$  and slope of 1:2, it can be shown that:

$$V_{i} = \frac{\lambda_{i}}{12}$$
 (5.21)

Therefore the required area,  $A_{\hat{1}}$ , can be calculated from the following expression :

$$\frac{\rho_{i} \quad h_{se}}{12 \ (t_{f} - t_{0})} \quad A_{i} = \left[ \frac{K_{2}}{\ell_{2}} \left( T_{w} - T_{i} \right) + U_{0} \left( \overline{T}_{a} - T_{i} \right) \right] A_{i} - \dot{m}_{3} C_{w} \left( T_{i}^{*} - T_{i} \right) = 0$$

(5.22)

The cost of ice storage can be determined if the amount of heat rejected by SPPP is known. This can be achieved by adding equation (5.22) as an equality constraint to the functional equalities of the optimization problem described in Chapter III. The cost of ice storage consists of that of the insulation blanket and of the excavation (the insulation is considered to be  $$8 / m^2$$  of ice storage surface area).

### 5.4.4 Static Optimization of SPPP with Ice Storage

The first case considered will be that of an SPPP having ice storage as heat sink for the Montreal climate. The static optimization, assuming the average excitations presented in Chapter III, will be used to size the ice storage as well as the pond and other equipments, under average operating conditions. Equation (5.22) should be added to the other equality constraints of Chapter III. The results of this optimization is summarized in Table 5.2. (The LCZ thickness of 3 meters has again been assumed). Although the re-

TABLE 5.2

# RESULTS OF STATIC OPTIMIZATION

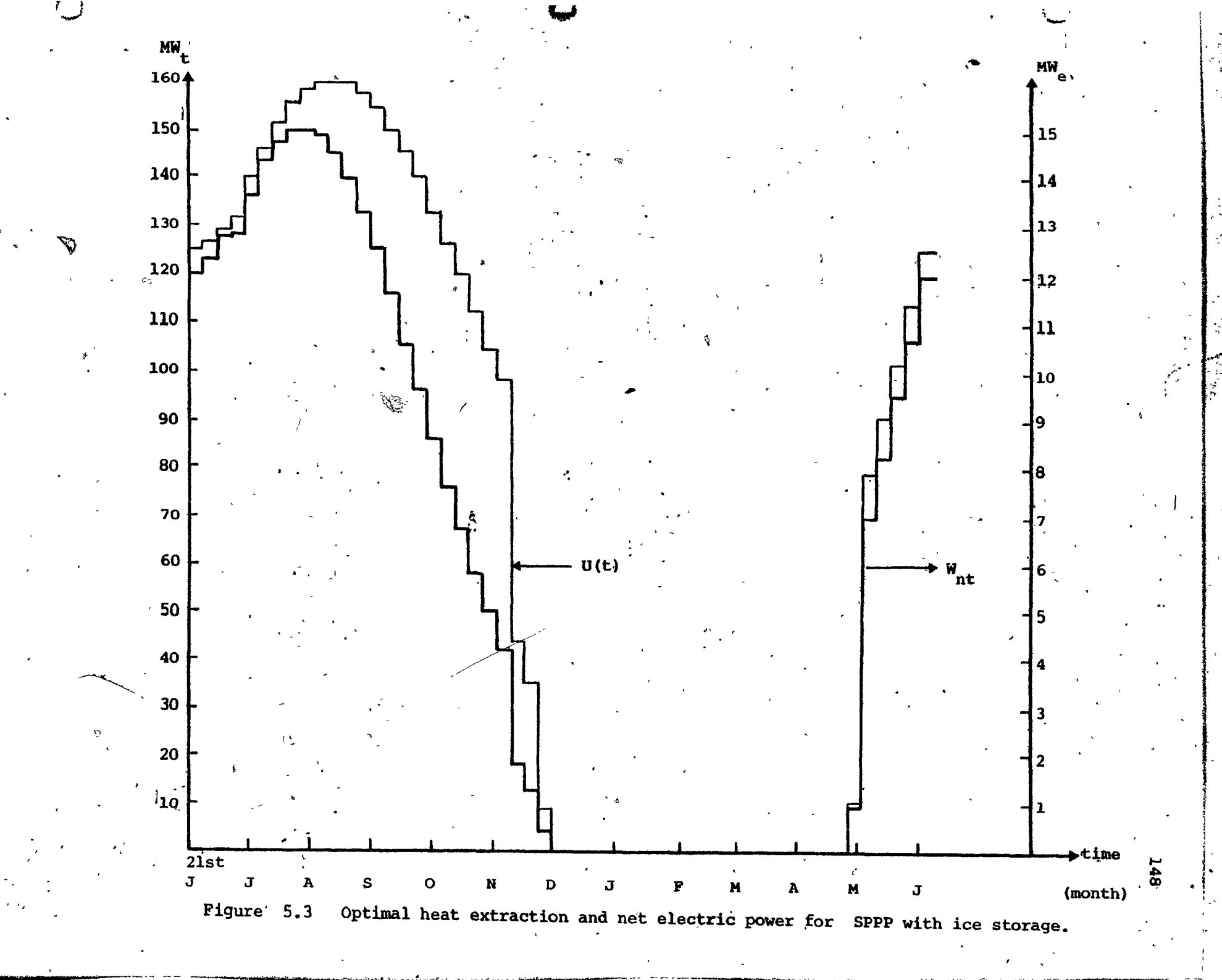
# FOR A 5 MW SPPP WITH ICE STORAGE

ITEM	SPPP	WITH	ICE	STORAGE
Pond:				
Surface area (Km²)		, з.	26	
Heat extraction depth (m)	1	1,.	7	
Temperature of LCZ (°C)		64.	56	· .
Efficiency (%)		11.	345	
Heat Exchanger Area (10 <sup>4</sup> m <sup>2</sup> ) :				
Vaporizer (boiler)		1.	98	
Condenser		2.	124	
Pre-heater	_	٠.	15	•
Turbine:		,		
Inlet pressure (psia)	,,	21.	23	
Outlet pressure (psia)	•	2.	<b>8</b> 7	-
Inlet temperature (°C)		58.	96	•
Outlet temperature (°C)		6.3	15	, <b>&amp;</b>
Mass Flow Rate (Kg / sec) :	•		,	,
Brine	, .	3474	4	
Working fluid (F-113)		, 290	0	``
Cooling water (ice storage)	•	2708	3	•
Ice Storage Volume (m <sup>3</sup> ):	•	2.2	2 <b>x</b> :	106
Gross Power (MW ) :	`\$	5.	525	
System Efficiency (%):		. 1.	.022	•
Energy cost (¢/Kwh) :	•	31.	9	

quired areas of pond and heat exchangers are smaller than those of Table 3.2, the energy costs have not been reduced substantially (31.9¢ / Kwh compared with 33.77¢ / Kwh). Because of ice storage, the cycle efficiency as well as system efficiency have increased about 9%.

## 5.4.5 Optimal Heat Extraction and LCZ Thickness of SPPP with Ice Storage

In the next case, we tried to find the optimal heat extraction and depth of LCZ by the discrete optimal control technique (mathematical programming) presented in Chapter IV . The results are very encouraging and interesting. The optimal storage depth of 0.5 meter and energy costs of 16.23¢ / Kwh were obtained. heat extraction and net electric power are presented in Figure 5.3 . The energy cost, despite the added expense of the ice storage costs. (excavation and insulation costs) is 22 % lower than that obtained in Chapter IV for the Montreal pond. The present optimization showed that the residual heat in the pond for the time which is not producing electric power is considerable. It has been shown (Moshref and Crevier, 1982) that if this residual heat can be sold, for example, to heat a park of greenhouses (for the months of December and January) then, the energy cost



can be as low as 8.5 ¢/Kwh which should be economically attractive in the near future.

In conclusion, the solar pond can be used for the efficient generation of electric power in the northern climates (latitude  $\simeq 45^{\circ}$ ) if the pond construction and operation are as follows:

- (1) Permit operation during the warmer part of the year only, and make use of the residual heat available in the winter for purposes other than electric power generation.
- (2) Use accumulated ice to reduce the temperature of the cooling medium of the SPPP during the warmer part of the year.
- (3) Reduce the pond's thermal inertia so as to permit a rapid increase in temperature in the spring. This last modification obviously brings about a substantial reduction in pond construction costs.

### CHAPTER VI

### REVERSE. OPERATION: UNDERGROUND STORAGE

### 6.1 Introduction

As discussed in the previous chapters and as demonstrated in practice (Chinery et al (1983)) the ground provides some storage of heat under the pond. This heat can be recuperated from the ground during the winter time. The present chapter will examine means of enhancing the thermal storage properties of easily excavated soils by driving the heat deeper underground through a network of horizontal pipes. It is also proposed here to use the heat stored under the pond for the operation of a heat engine during the winter time and use the LCZ brine as a heat sink, in a manner which will be described later on..

# 6.2 Pipe Storage System

The ground may be used as a medium for interseasonal storage of sensible heat. The ground can be charged with heat during the warmer part of the year via circulation of hot brine from the LCZ through a network of buried horizontal pipes.

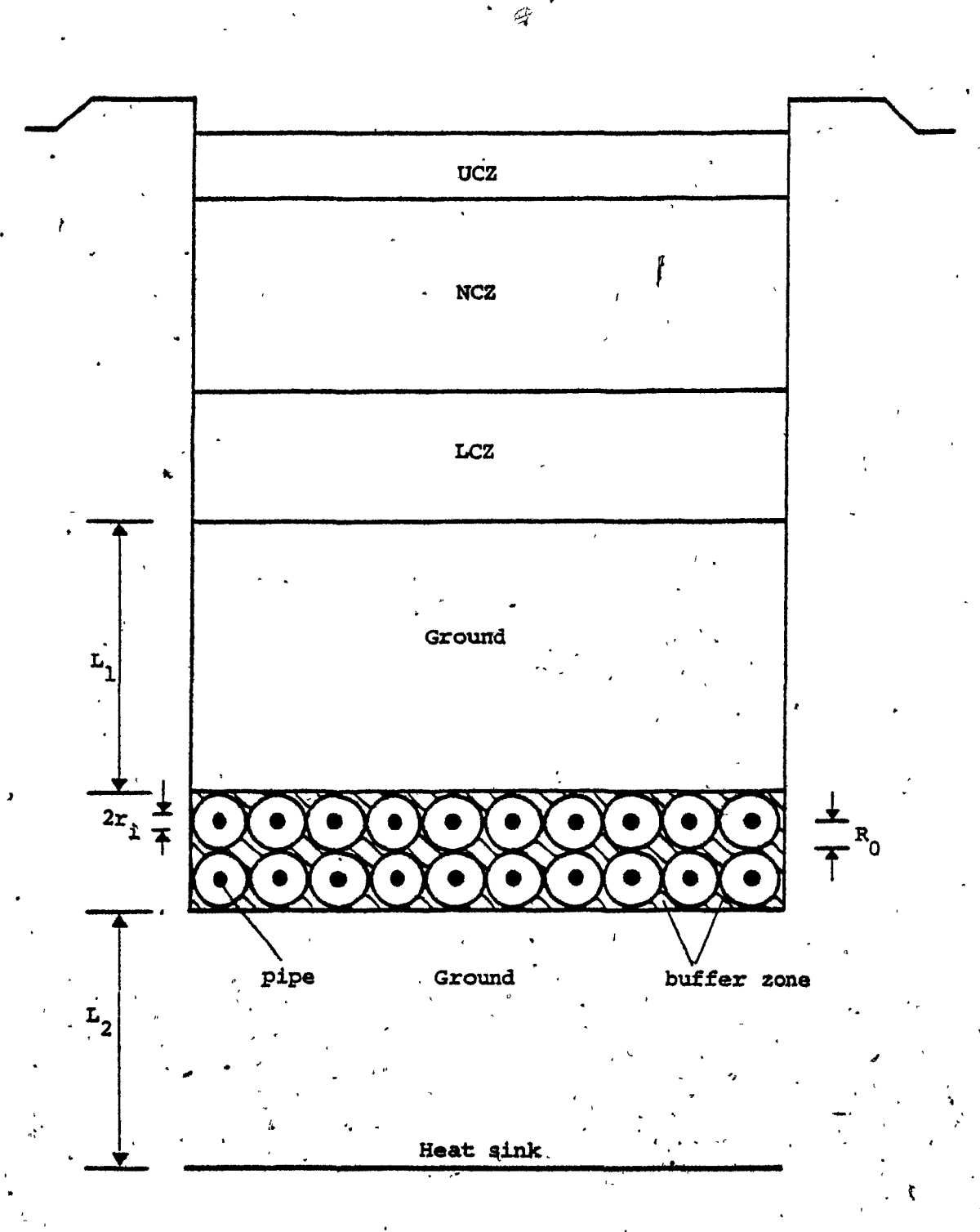
This section and the following two sections (excluding 6.3.4) are adapted from Crevier (1981), and are mentioned here for completeness and reference purposes.

As an alternative pipes could carry a heat transfer fluid (for example, air) warmed by heat extracted from the pond through a heat exchanger. Direct circulation of brine in pipes has over air circulation the advantage of not requiring an additional heat exchanger and would thus result in a higher efficiency. It would however represent a larger pollution hazard since a brine leak in one of the underground pipes would be almost impossible to locate and repair.

It will be assumed in the following mathematical model that the heat extracted from the LCZ, as a first priority, is used to generate electric power. Any surplus is sent into the underground storage.

### 6.3 Mathematical Model

Since heat will flow vertically near the pond's bottom, and radially near the pipes, the problem is characterized by a two-dimensional geometry even if edge effects are neglected. The problem has been reduced here to the numerical modelling of two coupled single dimensional heat flows, as illustrated in Figure 6.1. The two heat flow regions are coupled through a buffer zone where infinite conductivity is assumed. This region appears shaded in Figure 6.1.



( )

Figure 6.1 Cross Section of Ground Storage Solar Pond.

### 6.3.1 The Pond Model

The mathematical model for the pond NCZ, LCZ, and the ground section bounded by the bottom of the LCZ and buffer zone is exactly the same as that given in Section 2.3 with the difference that the boundary condition of the region 2 should be given by:

$$T_2 (l_1 + l_s + L_1, t) = T_3(t)$$
 (6.1)

In the above equation the temperature of the buffer zone,  $T_3$ , is considered, in a first approximation, as a fixed boundary condition when computing the vertical temperature distribution. The buffer zone provides the coupling between vertical and radial heat flows.

### 6.3.2 The Buffer Zone Model

The vertical and radial heat flows are coupled by the following artifice: It is assumed that the thermal conductivity of the shaded area "buffer zone" is infinite. This region is assumed to have the thermal inertia of soil, and its temperature change during one integration time step is determined by the amount of heat that it exchanges with the vertical pipes and horizontal regions. These heat exchanges are in turn determined by the derivatives of temperature with respect to depth and radius at the boundaries of the two regions with the buffer zone. Therefore a heat balance can be written for this zone as follows:

$$(n_c n_r) (4 R_0^2 l_p - \pi R_0^2 l_p) (\rho_3 C_3) \frac{dT_3}{dt} = n_c (2 R_0) l_p) K_6 \frac{\partial T_6}{\partial x}|_{x=l_1+l_3+l_1} + 2n_r R_0$$

$$\left| \begin{array}{c} -n_{\mathbf{g}} (2R_{\mathbf{0}} \ \ell_{\mathbf{p}}) K_{\mathbf{2}} \frac{\partial T_{\mathbf{2}}}{\partial \mathbf{x}} \Big|_{\mathbf{x} = \ell_{\mathbf{1}} + \ell_{\mathbf{g}} + \mathbf{L}_{\mathbf{1}}} - (n_{\mathbf{c}} \ n_{\mathbf{r}}) (2\pi R_{\mathbf{0}} \ \ell_{\mathbf{1}}) K_{\mathbf{4}} \frac{\partial T_{\mathbf{4}}}{\partial \mathbf{r}} \Big|_{\mathbf{r} = R_{\mathbf{0}}} \right|$$

$$(6.2)$$

where  $n_r$  and  $n_c$  are the number of pipes in the rows and columns of the pipe network respectively;  $\ell_p$  is the length of pipe.

## 6.3.3 The Pipe Storage Model

The pipe storage model consists in the cylindrical earth volumes surrounding the regularly spaced heat transfer pipes: these volumes have a radius of R<sub>0</sub> equal to half the interpipe distance, as shown in Figure 6.1. They are assumed to behave in identical fashion. Only one such region is therefore needed to analyze the model. Isotherms in this region would appear as circles concentric to the pipe. The only heat transfer process considered is conduction. The effect of convecting air or ground water in the neighbourhood of the pipes is neglected. The conduction equation for this region can be given by:

$$K_4 \frac{\partial^2 \mathbf{r}_4}{\partial \mathbf{r}^2} + \frac{1}{\mathbf{r}} K_4 \frac{\partial \mathbf{r}_4}{\partial \mathbf{r}} = \rho_4 C_4 \frac{\partial \mathbf{r}_4}{\partial \mathbf{t}} \qquad \mathbf{r}_1 < \mathbf{r} < \mathbf{R}_0$$
 (6.3)

The boundary conditions are provided by the buffer zone temperature, and the temperature of the inside pipe as follows:

$$T_4(R_0, t) = T_3(t), T_4(t_1, t) = T_5(t)$$
 (6.4)

The pipe temperature,  $T_5$  , in turn can be calculated as follows :

$$(n_c n_r) \rho_5 C_5 (\pi r_1^2 \ell_p) \frac{dT_5}{dt} = (n_c n_r) (2 \pi r_1 \ell_p) K_4 \frac{\partial T_4}{\partial r}\Big|_{r=r_1} + U_1(t)$$
(6.5)

where  $T_5$  is the inside pipe temperature which is assumed to be the average value of its inlet and outlet temperature.  $r_i$  is the pipe radius, and  $U_1(t)$  is the rate of heat extraction / injection to the pipe network. Finally the heat conduction for the ground layer, which is bounded by the buffer zone and heat sink, can be given by:

$$K_6 \frac{\partial^2 T_6}{\partial x^2} = \rho_6 C_6 \frac{\partial T_6}{\partial t}.$$
 (6.6)

and the boundary conditions of :

$$T_6 (l_1 + l_s + L_1 + 2 n_r R_0, t) = T_3(t)$$

$$T_6 (l_1 + l_s + L_1 + 2 n_r R_0 + L_2, t) = T_w$$
(6.7)

The governing equations and their boundary conditions, equations

(3.12) - (3.15) and (6.1) - (6.7) can be solved numerically using the finite difference technique described in Chapter II.

### 6.3.4 Numerical Solution using Finite Differences

The governing equations developed in the previous section and in Chapter II can be solved by the finite differences technique. Using first order differencing for the first differential operator resulted in a numerically unstable solution when a time step of one week Since this solution, will ultimately be used in an optiwas used. mization program we did not reduce the time step (since this would have made the solution computationally inefficient) . stead a second order differencing, quadratic approximation, for the first differential operator. Therefore the governing equations when discretized constituted a set of simultaneous linear equations. ever the coefficient matrix was no longer in the tri-diagonal structure. At each time step the system of equations was solved using the sparse matrix package, SPARSPK, developed by George and Liu, (1981), the University of Waterloo...

### 6.4 Model Validation

The model developed in the previous section must be modified so as to give results compatible with those of a conventional pond model in the absence of heat injection or extraction through the The modification is necessary for the following underground pipes. The accuracy of the model is probably acceptable in regard to radial heat flows to and from the pipes, since the length of the paths followed by the heat through the buffer zone (with infinite conductivity) would then be small compared to the distances  $L_1$  and  $L_2$ , as well as to the outer radius  $R_{\Omega}$  . When heat is injected into the . pipes from the LCZ, the model will however tend to exaggerate the flow of heat since the buffer zone "short-circuits" the heat resistance of the pipe storage zone in the vertical direction. effect has been corrected by decreasing the thermal conductivities in the ground layers above and below the buffer zone in a manner that will make, in the absence of heat flows in the pipes, the average LCZ and inner pipe temperatures be identical to those obtained in the pond without the pipe network. This was achieved by making the thermal resistance per unit area of earth layer 'L, equal to the resistance' of a layer of thickness  $L_1 + R_0$  of earth actually present under the empond, and similarly by setting the resistance of layer L, equal to a layer of thickness  $L_2 + R_0$  of real earth. Therefore the thermal conductivities  $K_2$  and  $K_6$  are given by :

$$\tilde{K}_2 = K_2 \frac{L_1}{L_1 + R_0}$$
 ,  $\tilde{K}_6 = K_6 \frac{L_2}{L_2 + R_0}$  (6.8)

Solution of the mathematical model showed that the above modifications, equation (6.8), induces an exact correspondence in the average temperatures of the two models (ponds with underground storage pipes and ordinary ponds) in the absence of any heat injection or extraction from the pipes. The amplitudes of the temperature variations in the lower convective zonesswere also in excellent agreement  $(\leq \pm 0.5 \text{ deg. C})$ .

# 6.5 Reverse Operation

It was seen in Chapters IV and V that the pond could not produce any electric power for many months during low insolation periods. If the LCZ is eliminated during low insolation by, say, storing this volume of concentrated brine in an auxiliary pond (or evaporation pond), it may be possible to produce electric power by using the pipe storage network as a heat source and brine in the auxiliary pond as a heat sink, in the following manner. The high concentration brine (LCZ) stored in the evaporation pond could be used to radiate heat during the night, while being protected from solar radiation by an opaque, white layer of fluid (for example foam used by fire fighters floated over it during the day time). This procedure would take advantage of the large thermal emissivity of water, which is approximately 0.96°,

(Kreith (1976)) and of the very cold effective night sky temperature during the winter (- 40 °C) to efficiently radiate heat away. addition the free and forced convection at the surface of the evaporation pond would enhance the cooling of the brine (brine of 21 % concentration freezes at - 18 °C , Ashrae (1974)) . Therefore the heat deposited into the evaporation pond from the power plant condenser would be easily dissipated: as demonstrated in Appendix C , the temperature of brine in the evaporation pond can be maintained below - 10 °C. Thus it is proposed to operate the SPPP with underground storage as follows: during the warmer part of the year the heat extracted from the pond, as a first priority, will be used to run the SPPP and any excess heat will be sent to underground pipe storage. During very low insolation periods, the LCZ will be extracted entirely and stored in an auxiliary pond. The heat will then be extracted from the pipe storage network and brine from the auxiliary pond will serve as a heat sink for the SPPP . It should be mentioned here that for the period of reverse operation (LCZ acting as a sink) , we will consider different heat exchangers, turbine, and working fluid, because the operating temperature of the SPPP will be then quite different from those encountered during ordinary operation.

6.6 Optimal Heat Extraction and Injection in SPPP with Underground Storage

Important factors in the operation of an SPPP with enhanced

earth storage will be the rate and schedule according to which heat is extracted from the pond LCZ and injected into the pipe network, and also the schedule of the heat recovery from this region. In the next section, we use the mathematical model of enhanced ground storage and the procedure described in Chapter IV (discrete optimal control) to find the optimal heat extraction and injection.

# 6.6.1 Formulation of Discrete Optimal Control for SPPP with Ground Storage

The SPPP with underground pipe network generates electric power according to two distinct modes, depending on the season.

First, during the warmer part of the year, the LCZ acts as a heat source and is responsible for vaporizing the working fluid; at the same time heat is extracted from the pond to charge the underground pipes. Second, in winter time, the heat extracted from the pipe storage acts as a heat source and the LCZ (which is stored in an auxiliary pond) acts as a heat sink. Therefore the net electric power can be given by the following equations, using assumptions of Section 4.2.

$$W_{nt}(t) = \begin{cases} W_{1}(T_{s}, U, t) & t_{0} \leq t < t_{1} \\ W_{0}(T_{6}, U_{1}, t) & t_{1} \leq t \leq t_{f} \end{cases}$$
 (6.9)

The function W<sub>1</sub> above is the same as that given in equation (4.6) and

W has the same form as W but with the difference that LCZ and UCZ temperatures should be replaced by the inside pipe and auxiliary point temperatures respectively.  $t_1$  and  $t_f$  mark the beginning and termination of reversed operation. Therefore

$$W_1(t) = 0.64 \eta_G \left(1 - \frac{T_a(t) + d_1}{T_g(t) - d_2}\right) U(t) - (W_{p1} + W_{p3})$$
 (6.10)

and

$$W_0(t) = 0.64 \eta_G \left(1 - \frac{T_{aux} + d_1}{T_5(t) - d_2}\right) U_1(t) - (W_{p1} + W_{p3})$$
 (6.11)

where T<sub>5</sub>(t) is the inside pipe temperature and U<sub>1</sub>(t) the rate of heat extraction from the pipe network. It should be noted that we have not included explicitly the flow rate at which the heat is injected into the pipe storage. Instead we will impose a constraint that requires the inside pipe temperature to be smaller or equal to the LCZ temperature during the time in which heat is injected.

Using the unit energy cost equation (4.14), the optimization problem for the SPPP with underground storage takes the following form:

$$\min_{\mathbf{U},\mathbf{U}_{1}} \mathbf{J} = \frac{-1}{c_{t1} + c_{t2} \, l_{s}} \left[ \int_{0}^{t_{1}} \mathbf{W}_{1}(t) \, dt + \int_{t_{1}}^{t_{f}} \mathbf{W}_{0}(t) \, dt \right]$$
 (6.12)

s.t.

$$\underline{\dot{\mathbf{T}}} = \mathbf{A} \, \underline{\mathbf{T}} + \underline{\mathbf{e}}_{n+1} \, \mathbf{U}(\mathbf{t}) + \underline{\mathbf{e}}_{q+1} \, \mathbf{U}_{1}(\mathbf{t}) + \underline{\mathbf{v}}(\mathbf{t}) \tag{6.13}$$

and

$$W_0(t) > 0$$
 ,  $W_1(t) > 0$  (6.14)  $U(t) > 0$  ,  $U_1(t) > 0$ 

$$T_{n+1}(t) - T_{q+1}(t) \ge 0$$
 if  $U_1(t) \ne 0$  for  $t_0 < t \le t_1$  (6.15)

entl and equal are mxl vectors with zero in all positions, except for "ones" in the n+l and q+l positions respectively (indices n+l and q+l refer to storage layer and inside pipe temperatures respectively). T is the mxl vector of unknown nodal temperatures. Equation (6.15) imposes the constraint that the LCZ temperature be greater than or equal to the inside pipe temperature during the injection period.

Once again, as in Chapter IV, the above problem has been solved numerically by discretizing U(t), the heat extraction from the LCZ, and the heat injected or extracted from pipe storage  $U_1(t)$ . The class of functions chosen for approximation of U(t) and  $U_1(t)$  are step-functions, which take on a constant value in a given time interval. Now, the overall interval,  $[t_0, t_f]$ , contains for this

case 91 unknowns (U(t) is assumed to be zero during the reverse operation; otherwise, the total number of unknowns would be 104)

The objective function, defined in equation (6.12); has been transformed into a form similar to that appearing in equations (4.16) - (4.18) of Chapter IV. The system of differential equations (6.13), representing the thermal behaviour of the pond and the ground, are first solved for steady state operation using finite differences for each interval; then equation (6.12) is integrated from  $t_0$  to  $t_f$  to obtain the value of the objective function for the considered heat extraction schedule. The optimization of the parameters defining the heat extraction schedule (i.e., the rate of heat extraction during each time interval) is performed by repeatedly computing the value of the objective function for different extraction schedules, using the generalized reduced gradient technique.

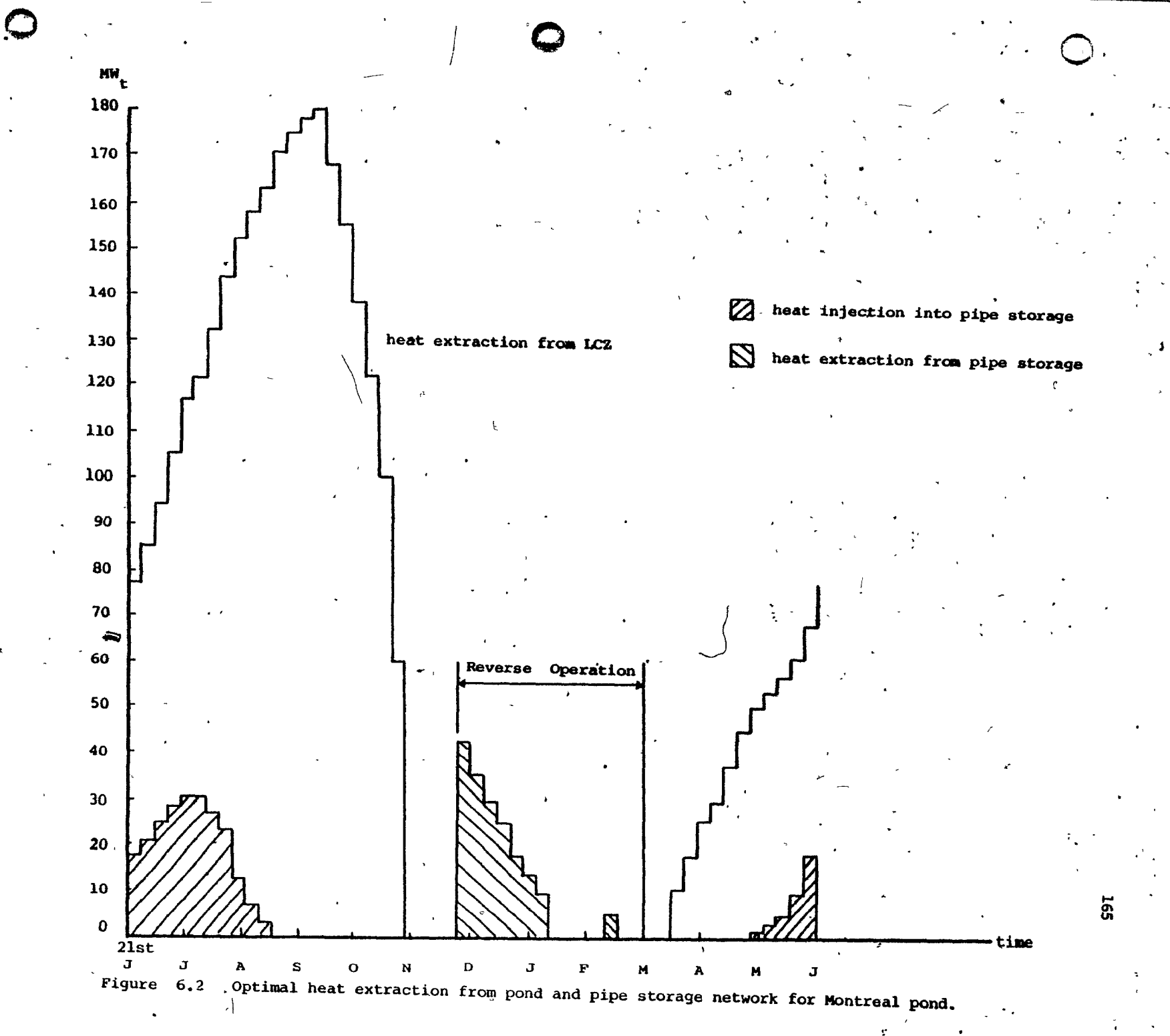
The added costs which were considered for SPPP with underground storage consisted of those of the pipe network and trenches. To obtain the cost of the trenches we assumed that placing the pipe network required an additional two meters of excavation per unit area of pond for a cost of  $3 / m^3$ . A cost of 3.75 / m of pipe was considered for the pipe network (Crevier, (1981)).

Using an IMLS subroutine based on Runge-Kutta method.

# 6.7 Example

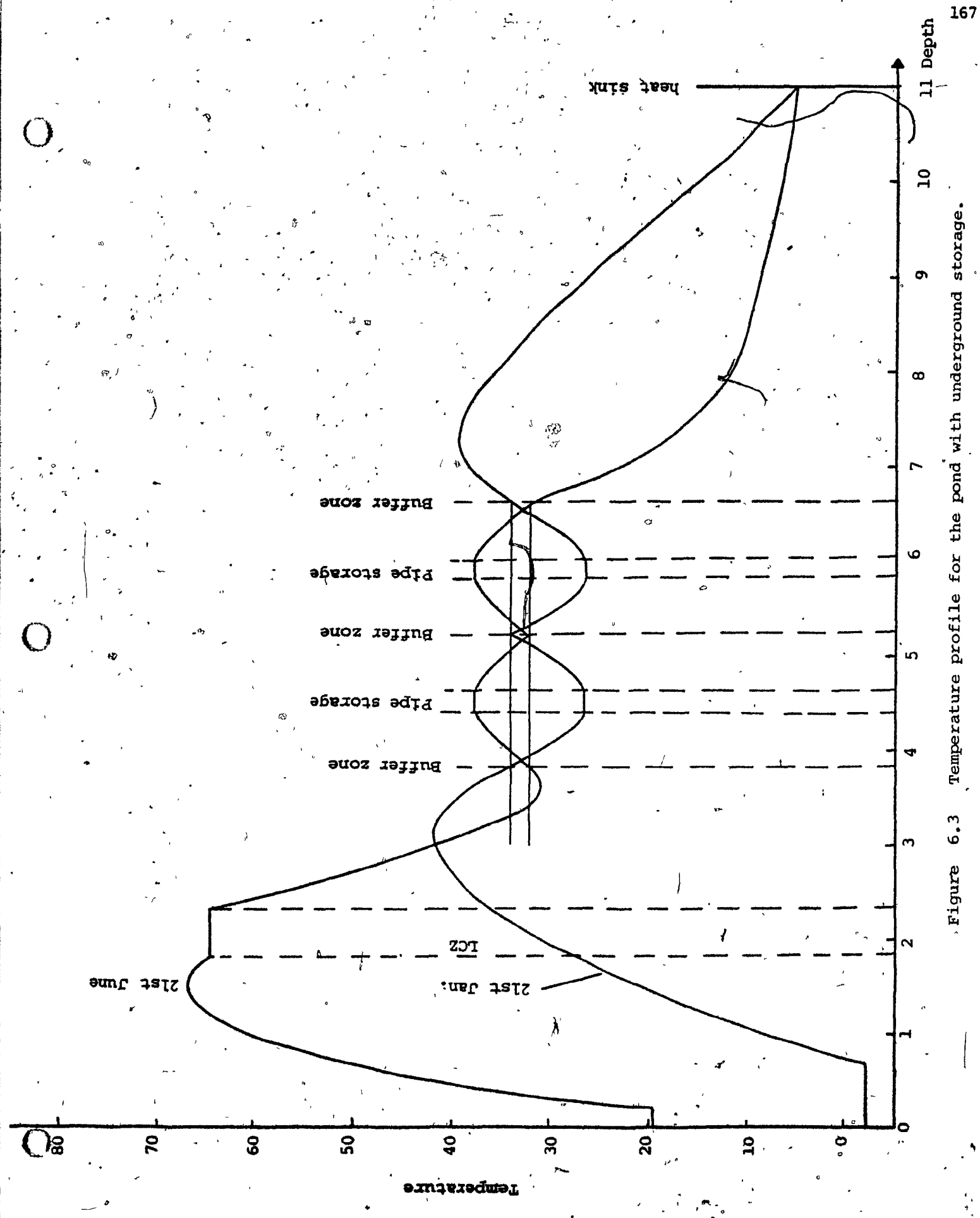
A solar pond power plant with underground storage is assumed which has an area of 3.54 km<sup>2</sup> and NCZ depth of 1.68 m (the same as those obtained in Section 3.6.2). The optimization described in previous sections of this chapter was carried out with the help of the GRG package and using the mathematical model which was developed earlier in the chapter.

The optimal heat extraction from the LCZ , U(t) , and the optimal heat injected or extracted from pipe networks, U, (t), are depicted in Figure 6.2 . It is assumed that the LCZ thickness is set at its minimum value achievable in practice (0.5 meters) . It can be seen from Figure 6.2 that the amount of heat injection and extraction from the pipe storage is small compared to the heat extrac-This can be explained by the fact that it is not tion from LCZ . possible to inject any heat once the LCZ temperature becomes equal or less than the internal pipe temperature. Also, since the LCZ is emptied into an evaporation pond during the winter time, its temperature variation is considerable because of its very small thermal inertia., Furthermore, some of the heat stored in the pipe storage network will be conducted away into the pond. The existence of the single step function (Figure 6.2) in early March can be explained by the fact that the pipe had been given some time to warm up after being cooled by a relatively large rate of heat extraction.



Pond temperature profiles for two instants of time are illustrated in Figure 6.3. It can be seen that the temperature difference between the pipe and the buffer zone is always of the order of 5 °C. The pipes are warmer than the buffer zone when they act as heat sources (June profile), and cooler when they act as heat sinks (January profile).

The data used for the SPPP with underground storage appears in Table 6.1. The energy cost of 20.86 ¢ / Kwh is slightly lower than that of an ordinary pond (20.97 ¢ / Kwh). Conclusions on the advisability of operating solar ponds in the reverse mode will be drawn in the next chapter.



Temperature profile for the pond with underground storage.

TABLE 6.1

POND PARAMETERS FOR REVERSE OPERATION

()

(\_)

Pond area (Km <sup>2</sup> )	3.5
UCZ depth (m)	0.2
LCZ depth (m)	0.5
NCZ depth (m)	1.68
Distance between pond	
Bottom and Buffer zone (m)	1.5
Distance between Buffer zone	
and heat sink (m)	4.3
Pipe spacing (m)	1.5
Pipe radius (m)	0.1
n , number of pipe layers	2 .
Total length of pipe (m)	4.7 x 10 <sup>6</sup>
	•
Cost of piping and trenches (\$)	22 × 10 <sup>6</sup>
•	,
Energy cost (¢ / Kwh)	20.86

#### CHAPTER VII

## CONCLUSIONS AND RECOMMENDATIONS

#### FOR FUTURE RESEARCH

# 7.1 The Significance of this Research

The principal objective of this research has been to develop a methodology for the simulation and optimization of electric power generation by solar ponds. The need for this kind of study was felt some two decades ago, and so far no published methodologies for achieving these objectives were available. The present study has, in addition to providing such a methodology, shown that the commonly held belief that solar pond power systems can only function at acceptable efficiencies under semi-tropical conditions is a fallacy. There are two reasons for this: first, the determining factor involved in power cycle efficiency is not only the highest temperature achievable by the pond, but the range of temperatures available to the heat engine (that is the temperature difference between source and sink) . Second, the optimum operating conditions and design of a solar pond power system in a semi-tropical climate are not necessarily the same as those of a northern climate pond. In fact this study shows that northern ponds can produce electric power with costs close to those estimated by the Israelis for semi-tropical conditions if proper modifications to the pond construction and operating conditions are made.

The floating pond power system proposed in this study explored the possibility of making the pond float on a layer of fresh water in natural bodies of water. It was shown that such a construction would greatly reduce salt costs in ponds equipped with deep storage layers. Such a procedure would permit the location of large solar ponds power systems close to densely built urban centers, where they could not otherwise be installed because of space limitations.

# 7.2 Conclusions

The following concluding remarks apply to Chapter II:

The analytical solution of the governing equations for three layer solar pond revealed the following:

- (1) The time table of heat extraction from LCZ plays an important role in the applicability of the pond to different end uses.
- (2) Ponds operating in the same range of temperatures are more efficient in semi-tropical conditions than those in northern climates (as demon-

strated in Section 4.4, lowering the operating temperature of a northern pond can however result in acceptable costs).

- (3) The yield of a solar pond could be increased if it were possible to vary the thickness of the NCZ as a function of the pond temperature and climate conditions. The pond efficiency can be maintained at the optimum value as it heats up by making the NCZ depth equal to the value characterized by the straight line tangent to the optimal efficiency curve at the given pond temperature.
- (4) The numerical solution of the governing equations by finite difference is in very good agreement with the analytical solution, and can be found in almost the same amount of computer time.
- (5) The assumption of constant sun declination angle, which has been used by many other researchers, does not affect the LCZ temperature considerably and is a slightly conservative assumption.
- (6) The ice coverage of the pond surface has a considerable effect on the LCZ temperature because of the lower solar radiation penetration through the ice.

The following concluding remarks apply to Chapter III :

(1) The method developed for power cycle analysis yields excellent

results (2% error on the average from the thermodynamic charts and / or tables for prediction of cycle efficiency) .

- The method is applicable to any fluid for which sufficient data is available. It can be used for selection of the most efficient fluid for a particular system.
- (2) The static optimization of a solar pond power plant revealed that using F-113 as the working fluid yields lower unit energy cost than using F-11.
- The optimum operating conditions of the SPPP are dependent upon the choice of working fluid.
- Considering the generation of power for the whole year, the energy cost of a SPPP located in a semi-tropical climate (e.g., Shiraz) is much lower than that for a SPPP in northern climate (e.g., Montreal). (As demonstrated in Section 5.4.5 operating a northern pond for part of the year only will result in acceptable costs).
- (3) The SPPP with F-113 as the working fluid can be expected to reach an efficiency of 64% of that of the ideal Carnot Cycle.

The following concluding remarks can be made for Chapter IV:

(1) The optimal amplitude of heat extraction is equal to the optimal average

value of heat extraction for a northern climate pond (when sinusoidal excitations are considered). This implies that it is not economical to have a deep storage layer to keep the system producing electric power for the entire year.

- An SPPP in semi-tropical conditions is capable of producing electric power for the entire year even for a solar pond with shallow LCZ because of the relatively lower seasonal variation of solar radiation.
- The optimal heat extraction rate will have a constant value for LCZ thicknesses greater than 3.5 meters for ponds located in semi-tropical climates. This does not necessarily mean that electric power can be generated at constant rate (because there are still variations in the source and sink temperatures).
- Although the excitations (solar radiation and ambient temperature) have been assumed with the same phase lags for the semi-tropical and northern climates, the phase lags of the optimal heat extraction and electric power generation will have different values for the two locations.
- (2) The optimization of an SPPP by discretizing the control variable and using mathematical programming confirmed that the optimal control (heat extraction) appears to be a sinusoid for the locations where all excitations can be well approximated by sinusoidal functions.

(3) The best operating strategy and construction for an SPPP in a northern climate would be to equip the pond with a shallow LCZ and produce power only during certain parts of the year.

The following conclusions can be drawn from Chapter V:

- (1) The floating pond power system can produce cheaper electric energy than an ordinary SPPP. Even if it still gives rise to higher energy costs than conventional means of electric power generation, the floating pond presents the following advantages:
- making the NCZ float on a layer of fresh water would eliminate a major fraction of the pond cost in the area where salt is expensive.
- (2) If technological improvements could be made in the manufacture of transparent membranes (i.e., increase their life time to more than ten years) an important reduction in electric energy costs from floating pond power plant would result.
- (3) Introduction of an ice storage pit as a cooling means for an SPPP, despite the added expenses caused by extra excavation and in- sulation costs, results in an energy cost 22% lower than that of a pond where the UCZ is used for cooling water in northern climatic conditions.

7

- (4) The solar pond can be used for the efficient generation of electric power in northern climates (latitude = 45°) if the pond's construction and operation are performed according to the following rules:
- Reduce the pond's thermal inertia so as to permit a rapid increase in temperature in the spring. This obviously also brings about a substantial reduction in the pond's construction costs.
- Use accumulated ice to reduce the temperature of the cooling medium of the SPPP during the warmer part of the year.
- Operate during the warmer part of the year only, and make use of the residual heat available in the winter for purposes other than electric power generation (Moshref, Crevier, (1982)).

 $\bigcap$ 

The following conclusions apply to Chapter VI:

The solar pond power system with underground storage can produce more power than a conventional SPPP. However, due to the additional costs of installing the pipe network, the electric energy cost would be only slightly lower than that of a conventional SPPP.

Because of the colder pond temperatures during the reverse operation, more of the heat stored underground would be lost to the

surface. During the charging period the bottom zone would be at a higher temperature than a conventional pond.

It therefore appears that reverse operation, although feasible, is not particularly advantageous. These conclusions should however be verified using a more exact model than ours. The further investigation of ponds with underground storage should include a complete two dimensional numerical study, as well as a consideration of the effect of convection in the ground, and of ground properties other than those assumed in this study.

### 7.3 Recommendation for Future Research

The following topics can be suggested for future research in connection with the present work:

The optimization methodology described in this research can be modified to be used for different applications such as combined water desalination and electric power generation, space heating, and industrial process heating. In particular, the dual purpose plant (desalination and electric power generation) can be of great importance to countries where a shortage of potable water exists. The works of other researchers such as Johnson et al. (1981); Tleimat and Howe, (1982) can be helpful for their thermodynamic analysis of the energy and mass balances of the system.

- electric conversion. The simulation and optimization of such a system would be required for the estimation of conversion efficiencies and costs. The study would require the exact modelling of the thermal and electrical behavior of the thermoelectric conversion unit and its proper integration into the pond model. Its compatibility with low temperature pond operation and heat rejection (pond UCZ or ice storage) should be verified.
- should also be studied. A direct contact heat exchanger coupled to a solar pond for the purpose of electric power generation was thermally analyzed by Sonn and Letan, (1981). In their analyses the pond was not modeled: the pond's geometry, operating temperature and efficiency were assumed to be known. Therefore a study is required to first simulate the complete system components and optimize its geometries and operating conditions.
- (4) The optimization presented in Chapter IV, which was carried out in the time domain, can be studied in the frequency domain. Since the excitations signals such as ambient temperature and solar radiation can be considered periodic then the optimal control input (heat extraction) may be computed faster in terms of Fourier series coefficients.

(3)

- trol for optimal heat extraction purposes is worth exploring. This requires, as a first step, the representation of the solar pond system as a sampled-data system. In a typical sampled-data system control inputs are held constant over some sampling interval. The representation of the system as a sampled-data system permits a simple on-line one-step optimization which does appear reasonable to implement with a microprocessor. This procedure may be integrated into an automated microprocessor-based system for operation and maintenance of salt gradient.
- (6) A two-dimensional thermal analysis of the solar pond with ground storage pipe network can be helpful in double checking the one-dimensional model developed here.
- (7) The possibility of using aquifer storage, in conjunction with an SPPP should also be considered.

#### REFERENCES

Akbarzadeh, A., Ahmadi, G., 1980: "Computer Simulation of the Performance of a Solar Pond in the Southern part of Iran". Solar Energy, Vol. 24, 1980, pp. 143-151.

Akbarzadeh, A., Ahmadi, G., 1981: "On the Development of the Salt Concentration Profile in a Solar Pond". Int. J. of Energy, Vol. 6.

Akbarzadeh, A., Macdonald, R.W.G., 1982: "Introduction of a Passive Method for Salt Replenishment in the Operation of Solar Ponds", Solar Energy, Vol. 29, No. 1, pp. 71-76.

Anderson, C.G., 1958: "Limnology of a Shallow Saline micromitic Lake".
Limnology and Oceanog., Vol. 3, pp. 259-269.

Anonymous, 1979: "Solar Pond Newsletter, Issue No. 1". October 1979. Editor: Tom Ochs, Desert Research Institute, Boulder City, Nevada.

Anonymous, 1980: "Solar Pond Newsletter, Issue No. 2". February 1980.

Anonymous, 1980a: "International Solar Pond Newsletter, Issue No. 3". May 1980.

Anonymous, 1980b: "SCE, Energy Commission May Develop Power from Solar Salt Ponds", Research and Development Newsletter of the Southern California Edison Co., Vol. 9, No. 1, first quarter 1980.

Anonymous, 1981: "California Energy Commission, Solar Salt Pond Generating Facility, A Feasibility Study for California", Consultant Report prepared by Ormat Turbines, Israel, Vol. 182.

ASHRAE, 1974: Handbook of Fundamental. Chapter 30, p. 570, McGraw-Hill, Inc.

ASHRAE, 1975: Equipment Handbook. Chapter 30, pp. 30.1 - 30.10, McGraw-Hill, Inc.

Assaf, G., 1976: "The Dead Sea: A Scheme for a Solar Lake". Solar Energy, Vol. 18, No. 4, pp. 293-299.

Assaf, G., Doron, B., Weinberger, Z., Vroebel, E., Hershman, H., Katz, A., sarig, S., 1981: "Large Size Solar Ponds for Electricity Production", Prof. of ISES, p. 1020.

Athans, M., Falb, P.L., 1966: Optimal Control: An Introduction to the Theory and its Applications. McGraw-Hill, Inc.

Atkinson, J.F., Harleman, D.R.F., 1983: "Wind Mixing in Solar Ponds", Presented at the ASES Meeting, Minneapolis, MN, June 1-3, 1983, pp. 393-398. (Also to appear in Solar Energy).

Bansal, P.K., Kaushik, N.D., 1981: "Salt Gradient Stabilized Solar Pond Collector", J. of Energy Conversion and Management, Vol. 21, pp. 81-95.

Bansal, P.K., Kaushik, N.D., 1981a: "Thermal Analysis of Constant Flow Partitioned Solar Pond", J. of Energy Conversion and Management, Vol. 21, pp. 141-156.

Bechtel Corporation, 1975: "Technical and Economic Assessment of the ...

Prospects for Electrical Power Generation by Use of Solar Ponds".

Report to the U.S. Energy Research and Development Administration,

Washington, D.C., August 1975, pp. 1.1 to 6.3.

Benson, D.K., Jayadev, T.S., 1981: "Thermoelectric Energy Conversion: Economical Electric Power from Low Grade Heat". Solar Energy Institute, Technical Report.

Berardi, P.G. et al., 1978: "Numerical Prediction of Temperature Field in Nonconvecting Solar Pond". 2. Internationales Sonnenforum, July 12, Munich, Germany. Deutsche Gesellschaft fuer Sonnenergie e.v.

Blancheton, 1979: "Analyse du fonctionnement d'un etang solaire par) modelisation a partir de donnees recueillies sur un etang experimental a Palavas". Doctoral Dissertation, Laboratoire d'Hydrologie Mathematique, Universite des Sciences et Techniques du Languedoc, Montpellier, France.

BNW, 1975: "The Non-Convecting Solar Pond, an overview of Technological status and Possible Pond Applications". Pacific Northwest Laboratory of the Battelle Memorial Institute, Report BNWL-1891, January 1975.

Boehm, R.F., Newell, T., 1980: "Key Questions in the Application of Salt-Stratified Solar Ponds". 14th Intersociety Energy Conversion Engineering Conference, Seattle, Washington, August 18-22, pp. 1438-1443.

Bohn, M.S., Benson, D.K., and Jayadev, T.S., 1980: "Thermoelectric Ocean Thermal Energy Conversion". J. of Solar Energy Engineering, Vol. 102, pp. 119-127.

Bronicki, L.Y., 1972: "The Grmat Rankine Power Unit". Proceedings of the 7th IECEC, pp. 327-334.

Bronicki, Y.L., Lev-Er, J., Porat, Y., 1980: "Large Solar Electric Power Plants Based on Solar Ponds", Proc. of the 11th World Energy Conference, Munich, West Germany, September 8-12, 1980, pp. 739-758.

Bronicki, Y.L., 1981: "A Solar Pond Power Plant", IEEE Spectrum, February 1981, pp. 56-59.

Bronicki, L.Y., 1982: "Twenty Years of Experience with Organic Rankine Cycle Turbines: Their Applicability and Use in Energy Conservation and Alternative Energy Systems". Proceedings of the 17th IECEC, pp. 1118-1121.

Bryant, H.C., Colbeck, I., 1977: "A Solar Pond for London?" Technical Note, Solar Energy, Vol. 19, pp. 321-322.

Bryant, B.S., Bowser, R.P., Wittenberg, L.J., 1979: "Construction and Initial Operation of the Miamisburg Salt-Gradient Solar Pond". International Solar Energy Congress, Atlanta, May 28 - June 1, 1979, pp. 1005-1009, Pergamon Press, New York, 1979.

Bryant, H.C., 1980: "Solar Pond Studies: Phase III. The University of New Mexico". Annual DOE Active Solar Heating and Cooling Contractors' Review Meeting, March 1980.

Bryson, A.E., and Ho, Y.C., 1972: Applied Optimal Control. Blaisdell Publishing Co., Waltham, Massachusetts.

Carslaw, M.S., Jaeger, J.C., 1959: Conduction of Heat in Solids. Oxford University Press, Second Edition.

Cha, Y.S., Sha, W.T., Hull, J.R., 1981: "Design, Construction and Initial Operation of the ANL Research Salt Gradient Solar Pond", Report No. ANL-81-55, Argonne National Laboratory.

Chepurniy, N., 1976: "Predictive Analyses for the Temperature Development and Performance of Solar Ponds". Doctoral Dissertation, McGill University, Montreal.

Chinery, G.T., Siegel, G.R., Irwin, W.C., 1983: "Gradient Zone Establishment and Maintenance at TVA's 4000 sq.m. (1-acre) Nonconvecting Salt Gradient Solar Pond", Presented at the ASES Meeting, Minneapolis, MN, June 1-3.

Coffay, B., 1980: "Commercialization Potential of Open Cycle OTEC Water Plant". Westinghouse Electric Company.

Crevier, D., 1979: "District Heating by Solar Ponds in Canada". Seminar at N.R.C. Research Center, Ottawa, March 23, 1979.

Crevier, D., 1980: "State of the Art Review of Solar Ponds". Solar Energy Project Report No. Pond-1, August 1980, National Research Council of Canada.

\*Crevier, D., 1981: "Theoretical Appraisal of Seven Solar Pond Concepts Adapted to Northern Climates", Final Report to N.R.C., Canada.

Crevier, D., Moshref, A., 1981a: "The Floating Solar Pond", Proc. of the American Section of ISES, pp. 801-805.

Crevier, D., 1981b: "Enhanced Ground Storage for Solar Ponds". Proc. of the American Section of ISES, pp. 796-800.

Crevier, D., 1982: Private Communication.

Crevier, D., 4982a: "An Experimental Solar Pond for Industrial Process Heat", Canadian Section of ISES, pp. 709-714.

Delnore, V.E., 1980: "Numerical Simulation of Thermohaline Convection in the upper ocean". J. of Fluid Mechanics, Vol. 96, part 4, pp. 803-826.

Dickinson, W.C., Clark, A.F., Day, J.A., Wouters, L.F., 1976: "The Shallow Solar Pond Energy Conversion System". Solar Energy, Vol. 18, No. 1, pp. 3-10.

Dickinson, W.C., Neifert, R.D., 1975: "Parametric Performance and Cost Analysis of the Proposed Sohio Solar Process Heat Facility", Lawrence Livermore Laboratory Report, VCRL-51783, April 1975.

Drumheller, H., et at., 1975: "Comparison of Solar Pond Concepts for Electrical Power Generation". Final Report to ERDA, Contract E(45-1)-1830, October 1975.

Edesess, M., Henderson, J., Jayadev, T.S., 1979: "A Simple Design Tool for Sizing Solar Ponds". Report No. SERI/RR-351-347, Solar Energy Research Institute, Golden, Colorado, 80401.

Elata, C., Levin, O., 1965: "Hydraulics of the Solar Pond". 11th Congress of the Int. Association Hydraulic Research, Leningrad.

Eliseev, et al., 1971: "Theoretical Investigation of the Thermal Regime of a Solar Pond". Geliotekhnika, Vol. 17, 1971, pp. 17-23.

Eliseev, V.N., et-al., 1973: "On Determining the Efficiency of a Salt Solar Pond". Geliotekhnika, Vol. 9, No.1, 1973.

Elwell, D.L., Short, T.H., Badger, P.C., 1977: "Stability Criteria for Solar (Thermal-Haline) Ponds". Proceedings of the International Solar Energy Society, American Section, Orlando, Florida, June 6-10, 1977.

French, R.L., Lin, E.I.H., 1981: "Salton Sea solar Pond Power Plant", Proc. Intersociety Energy Conversion Engineering Conference, Seattle, Washington, August 18-22, pp. 1716-1719.

French, R.L., Meitlis, I., 1980: "Salton Sea solar Fond Project", Proc. Intersociety Energy Conversion Engineering Conference, Seattle, Washington, August 18-22, pp. 1430-1431.

French, R.L., 1982: Private Communication, June 28, 1982.

French, R.L., 1982a: Private Communication, August 3, 1982.

Fynn, R.P., Badger, P.C., Short, T.H., Sciarini, M.J., 1980: "Monitor-ing Sodium Chloride Concentrations and Density Profiles in Solar Ponds by Electrical Conductivity and Temperature Measurements". Proceedings of the American Section of the International Solar Energy Society Meeting, Phoenix, Az., June 2-6, 1980, pp. 386-390.

Fynn, R.P., and Short, T.H., 1983: "Solar Ponds: A Basic Manual". The Ohio State University, Ohio Agricultural Research and Development Center, February 1983.

George, A., and Lin, J.W.H., 1981: 'Computer Solution of Large Sparse Positive Definite Systems. Prentice Hall, Inc.

Gill, P.E., Long, E.M.R., Murray, W., and Wright, M.H., 1978: "Elementary Linear Algebra and Multivariate Analysis for Optimization". NPL NACS Report No. 3178.

Gill, P.E., Murray, W., and Wright, M.H., 1981: Practical Optimization.

Academic Press.

Giulianelli, J.L., and Naghmush, A.M., 1982: "The Spectrophotometric Method of Determining Solar Energy Penetration Profiles for Solar Ponds". International Solar Pond Letters, Vol. 1, Nos. 1 and 2.

Harleman, D.R.F., 1983: Notes on Israel Dead Sea Visit, January 31, 1983". International Solar Pond Letters, Vol. 1, Nos. 3 and 4.

Hawlader, M.N.A., Brinkworth, B.J., 1981: "An Analysis of the Non-convecting Solar Pond", Solar Energy, Vol. 27, pp. 204-245.

Hildebrand, F.B., 1968: Finite-Difference Equations and Simulations. Prentice Hall.

Hillis, D., Sather, N., Panchal, C., Stevens, H., Hull, J., Thomas, A., 1983: "A Study of Small Scale Solar Pond/OTEC (SPOTEC) Power Systems", Presented at the ASES Meeting, Minneapolis, MN, June 1-3, 1983.

Hirschmann, J.R., 1970: "Salt Flats as Solar-Heat Collectors for Industrial Purposes (Review Article)", Solar Energy, Vol. 13, No. 1, 1970, pp. 83-97.

Holmes, B.J., 1979: "Energy Loss to the Soil Surrounding a Below-Grade Solar Energy Storage Pond". Doctoral Dissertation, Virginia Polytechnic Institute, Blacksburg, 126 pp. Available from: University Microfilms, Ann Arbor, Mich. Order No. 79241-11.

Hudec, P.P., Sonnefeld, P., 1974: "Hot Brines on Los Roques, Venezuela". Science, No. 185, p. 440.

Hull, J.R., 1978: "Effects of Radiation Absorption on Convective Instability in Salt Gradient Solar Ponds", Meeting of the American Section of the International Energy Society, Denver, Colorado, August 1978.

Hull, J.R., 1979: "Membrane Stratified Solar Ponds". International Solar Energy Society Meeting, May 1979, Atlanta, Ga. (Also in Solar Energy, Vol. 25, pp. 317-325, 1980).

Hull, J.R., 1979a: "Physics of the Solar Pond". Doctoral Dissertation, Iowa State University, 140 pp. Available from: University Microfilms, Ann Arbor, Mich. Order No. 79162-00.

Hull, J.R., 1980: "Computer Simulation of Solar Pond Thermal Behavior", Solar Energy, Vol. 25, pp. 33-40.

Hull, J.R., 1980a: "Wind Induced Instability in Salt Gradient Solar Ponds". Proc. of the American Sections of ISES Meeting, Phoenix, Az., June 2-6, 1980, pp. 371-375.

Hull, J.R., Cha, Y.S., Sha, W.T., Schertz, W.W., 1982: "Construction and First Years Operational Results of the ANL Research Salt Gradient Solar Pond", Annual Meeting, Proc. of the American Section of the ISES, Vol. 5, Part 1 of 3, pp. 197-202.

Hull, J.R., Liu, K.V., Cha, Y.S., Domanus, H.M., Sha, W.T., 1981: "Solar Pond Salt Gradient Instability Prediction by Means of a Thermo-Hydrodynamic Computer Code". Proc. of AS of ISES, pp. 812-816.

Hull, J.R., Liu, K.V., Cha, Y.S., Sha, W.T., Kamal. J., Nielsen, C.E., 1981a: "Dependence of Ground Heat Loss upon Solar Pond Size and Perimeter Insulation: Calculated and Experimental Results", Proc. ISES, Brighton, August 1981.

Hunder, P.P., and Sonnenfeld, P., 1974: "Hot Brines on Los Roques, Venezuela". Science, Vol. 185, pp. 440-442. Hyacinthe, J.L., 1976: "Lagunes Solaires a Stratification de Densite: Elements Physiques, Resultats Anterieurs, Projet d'Experimentation". COMPLES, Revue Internationale d'Heliotechnique, 2eme Semestre 1976.

Hyacinthe, J.L., 1977: "Etangs Solaires a Stratification de Densite:.

Premier Rapport Scientifique et Technique". Publication du Centre
National d'Exploitation des Oceans, 1977, No. 33, pp. 1-21.

IMSL, 1982: International Mathematical and Statistical Libraries Manual, Chapter D, Edition 9, June 1982. IMSL, Inc.

Jain, G.C., 1973: "Heating of a Solar Pond". ISES Congress on Solar Energy, Paris, France, July 1973.

Jayadev, T.S., Henderson, J., 1979: "Salt Concentration Gradient Solar Ponds - Modeling and Optimization". Proc. of 1979 ISES Conference, Atlanta, Ga., May 28, 1979, (also SFRI/TP-35-277, 1979).

Jayadev, T.S., and Henderson, J., 1980: "Salt Concentration Gradient Solar Ponds: Modeling and Optimization". Proc. of AS of ISES Meeting, pp. 1015-1019.

Johnson, D.H., Leboeuf, C.M., and Waddington, D., 1981: "A Solar Pond Driven Distillation and Power Production System". 16th IECEC, pp. 2221-2226.

Kalecsinsky, A.V., 1902: "Ungarische Warme und Heisse Kochsalzeen", Ann. D. Physik, Vol. 7, No. 4, pp. 408-416.

Kirkland, D.W., Bradbury, J.P., Dean, W.E., 1980: "The Heliothermic Lake - a Direct Method of Collecting and Storing Solar Energy", USGS Open-file Report 80-807.

Kooi, C.F., 1978: "The Circular Cylindrical Reflector: Application to a Shallow Solar Pond Electricity Generating System", Solar Energy, Vol. 20, pp. 69-73.

Kooi, C.F., 1979: "The Steady-State Salt Gradient Solar Pond". Solar Energy, Vol. 23, pp. 37-45.

Kooi, C.F., 1980: "Salt Gradient Fond with Reflective Bottom", Solar Energy Magazine.

Korn, G.A., and Korn, T.M., 1968: Mathematical Handbook for Scientists and Engineers. Second Edition, McGraw-Hill Book Company.

Kreith, F., 1976: Principle of Heat Transfer. Third Edition, 1976 Impression, Intext Educational Publisher, N.Y.

Kreith, J., Kreider, J., 1978: <u>Principles of Solar Engineering</u>.

Hemisphere Publishing Corporation, pp. 552-559.

Kuberg, D.W., 1981: "A Review of TVA's Non-convective Solar Pond Activities", Proc. of the Annual Meeting of AS/ISES, Philadelphia, PA, p. 777.

Kuhn, H.W., and Tucker, A.W., 1951: "Nonlinear Programming". Proceedings 2nd Berkeley Symposium on Mathematical Statistics and Probability, J. Neyman (Ed.), University of California Press.

Kuhn, H.W., 1976: "Nonlinear Programming: A Historical View", in Nonlinear Programming, R.W. Cottle and C.E. Lemke (Eds.).

Lasdon, L.S., Warn, A.D., Ratner, M.W., and Jain, A., 1975: "GRG System documentation". Technical Memorandum CIS-75-01, Cleveland State University.

Lasdon, L.S., and Warn, A.D., 1978: "Generalized Reduced Gradient Software for Linearly and Nonlinearly Constrained Problems", in <u>Design and Implementation of Optimization Software</u>, Ed. H. Greenberg, Sijthoff and Noordhoff, Netherlands.

Leboeuf, C., Edesess, M., Jayadev, T.S., 1980: "Generation Solar Ponds for District Heating and Electricity". 15th IECEC, Seattle, Washington, August 18-22, pp. 1453-1458.

Levi, M., 1979: "Experimental Study of a Low Temperature Rankine Cycle Engine", M.Eng. Thesis, Department of Mechanical Engineering, McGill University, September 1979.

Lin, E.I.H., 1982: "Regional Applicability and Potential of Salt-Gradient Solar Ponds in the United States", Vols. I and II, JPL Document No. 82-10 (5107-1), DOE/JPL-1060-50.

Lin, E.I.H., 1982a: "A Review of the Salt-Gradient Solar Pond Technology", JPL Document No. 81-116 (5107-3), DOE/SF-11552-1.

Lin, E.I.H., French, R.L., 1982b: "Solar Pond Regional Applicability Study: Summary of Results", Annual Meeting, Proc. of the American Section of the ISES, Vol. 5, Part 1 of 3, pp. 209-214.

Lin, E.I.H., 1982c: "A Saltless Solar Pond", Annual Meeting, Proc. of the American Section of the ISES, Vol. 5, Part 1 of 3, pp. 215-219.

Lin, E.I.H., 1983: "Outdoor Performance of a Honeycomb-Covered Solar Pond Model", Presented at the ASES Meeting, Minneapolis, MN, June 1-3, 1983, pp. 411-416.

Lin, E.I.H., Sha, W.T., Soo, S.L., 1979: "Stability Considerations and a Double-Diffusive Convection Model for Solar Ponds". Internal Report No. ANL-CT-79-34, April 1979, Argonne National Laboratory, Urbana, Ill.

Little, A.D., Inc., 1979: "Assessment of the Feasibility of Solar Ponds in the Region Served by the Tennessee Valley Authority", Study Funded by TVA under Contract No. TV-51797A (August 31, 1979).

Loewe, F., 1950: Notos, Vol. 2, p. 270. (Hungarian lakes).

Margen, P., 1978: "Central Plants for Annual Heat Storage". Solar Age, October 1978.

Marsh, H.E., et al., 1981: "Salt-Gradient Solar Ponds in the Salton Sea: Brine Optical Quality and Performance", 16th IECEC, pp. 1720-1725.

Margen, P., Roseen, R., 1979: "Solar Heat for Small District Heating Systems", The International Total Energy Congress, Copenhagen, Denmark, October 9-12, 1979.

Mehta, G.D., 1975: "Nonconvecting Solar Ponds". Technical Report ETG-4, Hydronautics, Incorporated.

Mehta, G.D., 1979: "Salt Stratified Solar Ponds". Presented at the United Nations "Unitar" Conference on Long Term Energy Resources, Montreal, Canada, November-December, 1979. CF7/XIII/5.

Meyer, K.A., 1981: "A One-Dimensional Model of the Dynamic Layer Behavior in a Salt Gradient Solar Pond", Proc. of AS/ISES.

Moshref, A., Crevier, D., 1982: "Electric Power Generation by Solar Ponds: Modelling and Optimization", Annual Meeting, Proc. of the American Section of the ISES, Vol. 5, Part I of 3, pp. 203-208.

Nadeau, M.J., 1973: "Solar Sea Energy Systems". Master's Thesis, Massachusetts Institute of Technology.

NASA, 1978: "United States Patent No. 4,091,800: Solar Pond". Granted to NASA by the United States Patent Office, May 30, 1978.

Newell, T., Pande, J., Boehm, R., 1980: "Development of Performance Information for Large Scale Solar Pond Applications". Proc. of the American Section of ISES Meeting, Phoenix, Az., June 2-6, 1980, pp. 376-380.

Nielsen, C.E., 1977: "Salt Gradient Solar Ponds for Low Temperature Heat". Invited paper presented at Annual Meeting, American Physical Society, Chicago, IL., February 1977.

Nielsen, C.E., 1978: "Salt Gradient Solar Pond Development". Paper presented at Solar Heating and Cooling Contractor's Meeting, U.S. Dept. of Energy, Washington, D.C., September 1978.

Nielsen, C.E., 1978a: "Equilibrium Thickness of the Stable Gradient Zone in Solar Ponds". Proc. Am. Sect. International Solar Energy Society, Vol. No. 1, Denver, 1978, pp. 932-935.

Nielsen, C.E., 1978b: "Conditions for Absolute Stability of Salt Gradient Solar Ponds". Paper No. 1203, Proceedings of the January 1978 Congress, International Solar Energy Society, New Delhi, India.

Nielsen, C.E., 1979: "Control of Gradient Zone Boundaries". Presented at the International Solar Energy Society Meeting, Atlanta, GA., May 1979.

Nielsen, C.E., 1980: "Nonconvective Salt Gradient Solar Ponds".

Solar Energy Technology Handbook, edited by W.C. Dickinson and P.N.

Cheremisinoff, published by Marcel Decker, Inc., New York, 1980.

Nielsen, C.E., 1980a: "Design and Initial Operation of a 400 square meter Solar Pond". Proceedings of the American Section of the International Solar Energy Society Meeting, Phoenix, Az., June 2-6, 1980, pp. 381-385.

Nielsen, C.E., Kamal, J., 1981: "Toward Understanding the Surface Zone in Salinity Gradient Ponds", Proc. ISES Congress, Brighton, England, pp. 179-184.

Nielsen, C.E., 1982: "Work in Progress at the Ohio State University", International Solar Pond Letters, Vol. 1, Nos. 1 and 2.

Nielsen, C.E., 1982a: "Salt Transport and Gradient Maintenance in Solar Ponds", Proc. of the American Section of ISES Meeting, Vol. 5, Part 1.of 3, pp. 179-184.

Ochs, T.L., Bradley, J.O., 1979: "Stability Criteria for Saturated Solar Ponds". Proceedings 14th Inter-Society Energy Conversion Engineering Conference, August 5-10, 1979, Boston, MA.

Office of Conservation and Solar Applications, R & D Branch, U.S. Government: "Solar Salt Gradient Pond Development in the U.S.A. and Israel (informal report)", January 1979.

Ophir, A., Nadav, N., 1982: "Solar Energy as a Source for Power and Desalinated Water", Desalination, Vol. 40, pp. 103-124.

Perry, R.H., and Chilton, C.H., 1973: Chemical Engineers Handbook. Section 3, 5th Edition, McGraw-Hill Book Company.

Por, F.D., 1970: "Solar Lake on the Shores of the Red Sea". Nature, Vol. 218, pp. 860-861.

Pradhan, A.V., and Larson, V.H., 1980: "Power Cycles Analyses by Generalized Thermodynamic Properties". 15th IECEC, pp. 680-685.

Rabl, A., Nielsen, C.E., 1975: "Solar Ponds for Space Heating", Solar Energy, Vol. 17, No. 1, pp. 1-12.

Rohsenow, W.M., and Hartnett, J.P., 1973: <u>Handbook of Heat Transfer</u>.

McGraw-Hill Book Company.

Rothmeyer, M.K., 1979: "Saturated Solar Ponds: Modified Equations and Results of a Laboratory Experiment". Master's Thesis, Department of Physics, The University of New Mexico, Albuquerque, New Mexico.

Sargent, S.L., 1979: "An Overview of Solar Pond Technology". International Process Heat Conference Proceedings, 1979.

Sargent, S.L., Neeper, D.L., 1980: "Overview of the DOE National and International Program for Salt Gradient Solar Ponds". Proceedings of the American Section of the International Solar Energy Society Meeting, Phoenix, Arizona, June 2-6, 1980, pp. 395-399.

Savage, S.B., 1975: "Solar Ponds - A Review". Technical Report No. 75-3 (F ML), Department of Civil Engineering and Applied Mechanics, McGill University, Montreal, Quebec, Canada, August 1975.

Scgock, A., 1965: <u>Industrial Heat Transfer</u>. Chapman and Hall, pp. 148-149.

Shaffer, L.H., 1978: "Viscosity Stabilized Solar Ponds: Phase I". Proceedings of the International Solar Energy Society Congress, January, 1978, New Delhi, India, pp. 16-21.

Shah, S.A.M., 1979: "Dynamic Modeling of Solar Pond-Greenhouse Heating System", M.Sc. Thesis, The Ohio State University.

Short, T.H., Roller, W.L., Keener, H.M.M., 1979: "State of the Art: Agricultural Applications of Solar Storage Systems". Solar Energy Storage Options Conference, March 19-20, 1979, San Antonio, Texas, Vol. 1, Part 1, p. 67.

Sodha, M.S., Kaushik, N.D., and Rao, S.K., 1981: "Thermal Analysis of Three Zone Solar Pond". Energy Research, Vol. 5, pp. 321-340.

Sonn, A., and Letan, R., 1982: "Thermal Analysis of a Solar Pond Power Plant Operated with a Direct Contact Boiler". J. of Solar Energy Engineering, Transactions of the ASME, Vol. 104, pp. 262-269.

Speyer, J.L., and Bryson, A.E., 1968: "Optimal Programming Problems with a Bounded State Space". AIAA Journal, Vol. 6, No. 8, pp. 1488-1491.

Stewart, G.W., 1973: Introduction to Matrix Computations. Academic Press.

Streeter, V.L., 1961: Handbook of Fluid Mechanics. McGraw-Hill Book Company, N.Y.

Styris, D.L., Zaworski, R.J., Harling, O.K., Leshuk, J., 1975: "The Nonconvecting Solar Fond Applied to Building and Process Heating", Final Report to ERDA, Contract No. AT (45-1)-1830, 1975.

Tabor, H., 1959: "Solar Collecto- Developments", Solar Energy, Vol. 3, No. 3, 1959, pp. 8-9.

Tabor, H., 1963: "Solar Ponds: Large Area Solar Collectors for Power Production". Solar Energy, Vol. 7, No. 4, pp. 189-194.

Tabor, H., 1966: "Solar Ponds". Science Journal, Vol. 66, June 1966.

Tabor, H., 1973: "Solar Energy as a Contribution to the Energy Crisis". NP-21255, 23 pp.

Tabor, H., 1975: "Status of Solar Pond Research", Paper prepared for First Israel Solar Energy Conference, Rehovot, June 1975.

Tabor, H., 1978: "Solar Ponds". Solar Energy: The Royal Society Discussion Meeting, November 15-16, 1978, London, England.

Tabor, H., 1979: "Solar Ponds (non-convecting)". Presented at the United Nations Unitar Conference on Long Term Energy Resources, Montreal, Canada, November-December 1979.

Tabor, H., 1980: "Non-convecting Solar Ponds", Phil. Trans. R. Soc. Lond., Vol. A 295, pp. 423-433.

Tabor, H., and Weinberger, Z., 1981: "Nonconvecting Solar Ponds", in Solar Energy Handbook, Chapter 10, pp. 1-29, McGraw-Hill Book Company, New York.

Tabor, H., 1982: "Review Article: Solar Ponds", Solar Energy, Vol. 27, No. 3, pp. 181-194.

Thomas, L.C., 1981: <u>Fundamental of Heat Transfer.</u> Prentice Hall, Englewood Cliff, N.J.

Torgerson, D., 1978: "Energy-Short Israel may Achieve First Commercial Solar Power Breakthrough". Los Angeles Times, December 4, 1978.

Touryan, K.J., 1979: "Research Studies in Solar Energy at the Solar Energy Research Institute", Seminar at Hydro-Quebec Institute of Research, May 4, 1979.

Turner, J.S., 1974: <u>Buoyancy Effects in Fluids</u>. Cambridge University Press, Chapter 8.

Tybout, R.A., 1967: "A Recursive Alternative to Weinberger's Model of the Solar Pond". Solar Energy, April-June, 1967, pp. 109-111.

Usmanov, et al., 1971: "Optical Characteristics of a Solar Reservoir", Gelioteknika, Vol. 7, No. 1, 1971, pp. 28-32.

Usmanov, et al., 1973: "Experimental Study of the Removal of Heat from a Solar Salt Water Pond", Geliotekhnika, Vol. 9, No. 6, 1973, pp. 23-26.

Velarde, M.G., Gonez-Abad, J.V., 1975: "From Solar to Electric Energy via Thermal Energy. II. The Solar Pool". Electron Fis. Appl., Vol. 18, No. 2, pp. 67-72.

Viskanta, R., Toor, J.S., 1978: "Absorption of Solar Radiation in Ponds". Solar Energy, Vol. 21, No. 1, pp. 17-25.

Weeks, D.D., Long, S.M., Emery, R.E., Bryant, H.C., 1981: "What Happens When a Solar Pond Boils", Article 7, Int. Solar Pond Newsletter No. 4, Solar Energy Group, Los Alamos National Laboratory, Los Alamos, NM.

Weinberger, H., 1964 № "The Physics of the Solar Pond". Solar Energy, Vol. 8, No. 2, 1964, pp. 45-46.

Wilkins, E., 1978: "Experiments with a Non-Convective Model of a Solar Pond". Solar Energy and Conservation Symposium-Workshop, Miami Beach, Florida, December 11-13, 1978.

Wilkins, E., Pinder, K., 1979: "Experiments with a Model Solar Pond". Sunworld, Vol. 3, No. 4.

Wilkins, E.S., El-Genk, M., El-Husseini, K., and Thakur, D., 1982: "An Evaluation of the Gel Pond Performance". Proc. of the Winter Meeting of the American Society of Mechanical Engineers, November 1982.

Williams, C.S.; Beckland, O.A., 1972: "Optics: A Short Course for Engineers and Scientists". Wiley-Interscience, New York.

Wilson, A.T., Wellman, H.W., 1962: "Lake Vanda: An Arctic Lake". Nature, No. 196, p. 1171.

Winsberg, S., 1980: "Solar Pond Power, the Israel-California Connection", Sunworld, Vol. 4, pp. 170-173.

Wittenberg, L.J., Harris, M.J., 1980: "The Miamisburg Salt-Gradient Solar Pond", DOE Non-convective Solar Pond Workshop, Desert Research Institute, University of Nevada System, p. 13-1.

Wright, J.D., 1982: "Selection of a Working Fluid for an Organic Rankine Cycle Coupled to a Salt-Gradient Solar Pond by Direct Contact Heat Exchange". J. of Solar Energy Engineering, Vol. 104, pp. 286-292.

Zangrando, F., Bryant, H.C., 1976: "Solar Ponds for Residential Heating", Final Report for State of New Mexico Energy Resources Board, Grant No. ERB-161, Technology Application Center, NASA, LSS-155/Suppl. 1, August 1976.

Zangrando, F., Bryant, H.C., 1977: "Operation and Maintenance of a Salt Gradient Solar Pond". Proceedings of the Helioscience Institute Conference, Palm Springs, California.

Zangrando, F., Bryant, H.C., 1978: "A Salt-Gradient Solar Pond", Solar Age, Vol. 3, No. 4, April 1978.

Zangrando, F., 1979: "Observation and Analysis of a Full-Scale Salt Gradient Solar Pond". Doctoral Dissertation, Department of Physics, University of New Mexico, Albuquerque, New Mexico, May 1979.

ľ

#### APPENDIX A

#### ABSORPTION OF SOLAR RADIATION IN A SOLAR POND

This appendix reviews some of the basic theory of radiation absorption in a salt-gradient solar pond. Even though radiation absorption is well established and many good treatises are available on the subject, the absorption of radiation in a solar pond is still an active research topic in the solar pond area (Viskanta and Toor, 1978, Marsh et al, 1981, Giulianelli and Naghmush, 1983). For the sake of completeness, the basic concepts required to define the source function, which is part of the solar pond model, will be presented here.

The absorption of radiation in a homogeneous and transparent medium can be described by Lambert's law, which states that, "a thickness dx of the homogeneous absorber reduces the intensity of the incident radiation of wavelength  $\lambda$ , by an amount dH $_{\lambda}$  proportional to both the intensity H $_{\lambda}$  and dx ", thus:

$$dH_{\lambda} = -\mu_{\lambda} H_{\lambda} dx$$

where  $\mu_{\lambda}$  is the proportionality factor called the spectral absorption coefficient. The above equation upon simple integration yields:

$$\int_{H_{\lambda}^{1}}^{H_{\lambda}^{t}} \frac{dH_{\lambda}}{H_{\lambda}} = \int_{0}^{x} -\mu_{\lambda} dx \quad \text{or} \quad H_{\lambda}^{t} = H_{\lambda}^{1} e^{-\mu_{\lambda}^{t} - x}$$

where superscripts i and t stand for incident and transmittent respectively. The spectral transmittance is defined by the ratio of transmitted radiation to that of incident:

$$\tau_{\lambda} = \frac{H_{\lambda}^{t}}{H_{\lambda}^{1}} = e^{-\mu_{\lambda}x}$$
 or  $\mu_{\lambda} = -\frac{1}{x} \operatorname{Ln} \tau_{\lambda}$ 

Usmanov, (1971) has presented spectral absorption coefficients for various uniform concentrations of Magnesium Chloride (Cl<sub>2</sub> Mg) solutions. But he has not given sufficient details for one to readily make use of these results for the case of a concentration varying with depth, as occurs in a solar pond. Weinberger, (1964) measured the fraction of radiation remaining as a function of the underwater pathlength for six samples of sea water coming from different parts of the world. Rabl and Nielsen, (1975) presented a simple way of expressing the intensity of the radiation at any depth in a solar pond. They found that the fraction of radiation remaining after a pathlength x can be well approximated (within 3%) as the summation of four bands (range of wavelength) each characterized by its own intensity and absorption coefficient as follows:

$$H(x, t) = \tau H_{s}(t) \sum_{n=1}^{4} \eta_{n} e$$
(A.1)

where H(x, t) is the radiation remaining after a pathlength x and  $H_{\alpha}(t)$  is the radiation intensity at pond surface, x = 0;

13

and n is a weighting coefficient.

Hull, (1980) has used a similar expression with forty spectral coefficients and results obtained by him are in close agreement with the above equation. The values of  $\mu_n$  and  $\eta_n$  suggested by Rabl and Nielsen, (1975) appear in Table A.1. Absorption coefficients derived by Crevier, (1980) from a set of measurements, made by Nielsen, (1980) in an experimental solar pond, are also presented in this table. The latter coefficients result in a more pronounced absorption of sunlight with depth, which induces smaller solar pond efficiencies. This more pessimistic set of coefficients will be used for the simulations described in the present work.

The efficiency of a solar pond is limited by some intrinsic physical properties. Firstly, there are reflection losses at the surface of the pond. Then, having penetrated the surface, the radiation is rapidly attenuated by approximately fifty per cent since half the solar radiating energy is in the infra-red, to which water is almost opaque (see Table A.1). This half is thus absorbed in the first few centimeters of the surface. Thus a very shallow pond only a few centimeters deep, yielding negligible temperature rise, could not collect at the bottom more than fifty per cent of the solar radiation.

ABSORPTION AND WEIGHTING COEFFICIENTS
FOR RADIATION PENETRATION EQUATION

N	μ <sub>n</sub> (m <sup>-1</sup> ) Rabl and Nielsen,(1975)	μ <sub>n</sub> (m <sup>-1</sup> ) Crevier,(1980)	ηn	Wavelength Range
1	0.032	0.545	0.237	0.2 - 0.6
2	0.45	0.547	0.193	0.6 - 0.75
3	3.0	0.637	0.167	0.75 - 0.9
4	35.0	35.0	0.179	0.9 - 1.2
Remaining 355.0  Sodha et al,(1981)		5.0	0.224	1.2 - Over

The computation of the amount of radiation reaching a given depth is affected by the latitude of the site, as well as the time of the day and year. To reach a unit depth, the radiation must travel along an oblique path a distance of sec r, where r is the angle of refraction, assuming a constant value for the index of refraction 'N. For direct (beam) radiation the angle of incidence is given closely by (Weinberger, 1964):

 $\cos i = \cos L \cdot \cos D \cdot \cos (2\pi t / 24) + \sin L \sin D$ 

where i is the incidence angle;

L is the latitude;

t is the time in hours from solar noon;

and . D is the declination of sun which is approximately:

$$\dot{D} = \dot{D}_0 \sin{(\frac{2\pi n}{365.25})}$$

where D<sub>0</sub> .= 23.45° is the sun declination at equinox;

n is the number of days measured from the spring equinox.

The angle of refraction, r, is given by Snell's law (Williams and Becklund, 1972):

sin i = N · sin r

Rabl and Nielsen. (1975) used a constant effective incidence angle corresponding to the position of the sum at 2.00 P.M. at equinox. They used an effective absorption coefficient  $\mu^*$  as follows:

$$\mu_n^* = \mu_n \cdot \sec r \tag{A.2}$$

This modification of the absorption coefficient should be applied to equation (A.1).

### APPENDIX B

#### OPTIMALITY CONDITIONS

reviews optimality conditions for the minimum of nonlonear functions subject to nonlinear constraints. Based on these conditions there are many numerical approaches for nonlinear optimization, but no general consensus as to the best. The optimality conditions which follow are often referred to as the Kuhn-Tucker conditions (see Kuhn-Tucker (1951), and Kuhn, (1976)).

# 3.1 Conditions for a Minimum with Nonlinear Equality Constraints

When all the constraints are equalities, the problem form

becomes :

minimize F(x

(B.1

subject to C(x) = (

where  $x^2$  is the  $n \times 1$  vector of variables and C is the  $t \times 1$  vector of equality constraints. A point  $x^*$  is a local minimum of problem (B.1) if:

(a) 
$$\hat{C}_{i}(x^{*}) = 0 \quad \forall i, i = 1, ... t (x^{*} is' feasible)$$
.

(b) 
$$F(x) \leq F(x)$$
 for all feasible x in some neighbourhood of x.

To verify whether a point  $x^*$  satisfies (b), it is necessary to characterize feasible perturbations from  $x^*$ , so that the behavior of F(x) along such directions may be analyzed. In order to determine whether feasible perturbations exist, it is necessary to impose conditions on constraint functions (Gill et al (1978)). These conditions are commonly termed constraint qualifications. The constraint qualification with respect to the constraints of the nonlinear equality problem (NEP) holds at  $\bar{x}$  if:

- (i) The functions  $\hat{C}_{i}(x)$  are twice-continuously differentiable.
- $(ii) \quad \widehat{C}(x) = 0$
- (iii) Any non-zero vector p satisfying :

$$\hat{\mathbf{A}}(\mathbf{x})^{\mathrm{T}} \mathbf{p} = \mathbf{0} \tag{B.2}$$

is tangent to a twice-differentiable arc emanating from x along which

all constraints are satisfied in some neighbourhood of  $\bar{x}$ . In the above, the matrix  $\hat{A}(x)^T$  is called the Jacobian matrix of the set of constraint functions, i.e.:

$$\hat{\mathbf{A}}(\mathbf{x})^{\mathrm{T}} = \frac{\hat{\mathbf{A}}(\mathbf{x})}{\hat{\mathbf{A}}^{\mathrm{T}}}$$

Satisfaction of the constraint qualification allows a specification of necessary conditions for a point to be a solution of the nonlinear equality problem. If F(x) and C(x) are continuously differentialle, and the constraint qualification holds at x, the following conditions are necessary for x to be a solution of (NEP):

$$(i) \quad \hat{C}(x) = 0.$$

(ii) If Z(x) denotes a matrix whose columns form a basis for the set of vectors orthogonal to the columns of A(x), then:

$$Z(x)^{T}g(x) = 0$$
 (B.3)

where 
$$g(x) = \frac{\partial F(x)}{\partial x}$$

or equivalently :

$$g(x') = \hat{A}(x') \lambda' \qquad (B.4)$$

where the vector  $\lambda^*$  is called the vector of Lagrange multipliers, and

represents the coefficients in the expansion of  $g(x^*)$  as a linear combination of the columns of  $A(x^*)$ . The condition (B.4) is equivalent to the statement that  $x^*$  is a stationary point with respect to x of the Lagrange function defined by:

The state of the s

$$L(x, \lambda) = F(x) - \lambda^{T} \hat{C}(x)$$

This characterization of  $x^{\frac{\pi}{2}}$  is quite significant in the design of algorithms to solve (NEP).

Second-order necessary conditions for a minimum of (NEP) in addition to the above conditions, (i) and (ii), are that F(x) and C(x) be twice - continuously differentiable and that the following condition hold:

- (iii)  $Z(x^*)^T$   $W(x^*, \lambda^*)$   $Z(x^*)$  must be positive semi-definite where  $W(x, \lambda)$  is the Hessian of the Lagrange function. Sufficient conditions for  $x^*$  to be a solution of (NEP) are:
- (i) F(x) and C(x) are twice continuously differentiable.
- (ii) C(x) = 0
- (iii)  $Z(x^*)^T g(x^*) = 0$ , or there exists a vector  $\lambda^*$  such that  $g(x^*) = A(x^*) \lambda^*$ .

- (iv) The matrix  $Z(x^*)^T W(x^*, \lambda^*) Z(x^*)$  is positive definite.
- B.2 Optimality Conditions for a Minimum with Nonlinear

  Inequality Constraints

The problem to be considered is that of minimizing F(x) subject to a set of m nonlinear inequality constraints:

minimize F(x)

subject to  $C_i(x) \ge 0$  i = 1, ..., m

To determine the conditions at a minimum, it is necessary to define the set of constraints that are active  $^{1}$  at a point. To characterize feasible perturbations with respect to active inequality constraints, it is necessary to impose as in (NEP) a constraint qualification. The constraint qualification with respect to the constraints of the non-linear inequality problem, (NTP), holds at  $\bar{\mathbf{x}}$  if:

- (i) The functions C(x) are twice continuously differentiable.
- (ii)  $C(\bar{x}) \ge 0$ . If t constraints are active at  $\bar{x}$ ,  $C(\bar{x}) = 0$  denotes the active constraint functions, and the Jacobian of the active constraint functions is denoted by  $\hat{A}(\bar{x})$ .

 $C_{i}(x) = 0$ 

A constraint is active at point x if:

(iii) Any non-zero vector p which satisfies :

$$\hat{\mathbf{A}}(\mathbf{\bar{x}})^{\mathrm{T}} \mathbf{p} > 0$$

is tangent to a twice - differentiable feasible arc emanating from  $\bar{x}$  and any non-zero vector p that satisfies:

$$\hat{\mathbf{A}}(\mathbf{\bar{x}})^{\mathrm{T}} \mathbf{p} = 0$$

is tangent to a twice - differentiable arc emanating from  $\bar{x}$  along which all constraints active at  $\bar{x}$  remain identically zero. As in the (NEP) if  $A(\bar{x})$  has a full column rank then, the constraint qualification holds.

The necessary conditions for  $x^{2}$  to be a minimum of (NIP) can be summarized as follows (Gill et al (1978)):

(1) 
$$C(x^*) \ge 0$$
 ,  $\hat{C}(x^*) = 0$ 

(ii) 
$$Z(x)^{T} g(x) = 0$$
 or,  $g(x) = \lambda(x)^{*} \lambda^{*}$ 

(iii) 
$$\lambda^* > 0$$

(iv)  $Z(x^*)^T$   $W(x^*, \lambda^*)$   $Z(x^*)$ , where  $W(x^*, \lambda^*) = G(x^*) - \sum_{i=1}^t \lambda_i^* G_i(x^*)$  be non-negative definite.  $W(x^*, \lambda^*)$  includes only the Hessians of the active constraints.

In the above, the satisfaction of the constraint qualification is assumed and F and C are considered twice - differentiable. The sufficient conditions in addition to the first three conditions above, require the following:

 $Z(x^*)^T$   $W(x^*, \lambda^*)$   $Z(x^*)$  be positive definite and if  $\lambda_1^* = 0$  then, for any vector p:

$$\hat{a}_{i}(x^{*})^{T} p > 0$$

and

#### APPENDIX C

### THERMAL ANALYSIS OF THE AUXILIARY POND

It is assumed that the LCZ has been extracted from the main pond and stored in an auxiliary pond a few weeks prior to reverse operation. The operation procedure of the auxiliary pond is as follows: at nights the concentrated brine would be exposed to the atmosphere, to take advantage of the very cold winter sky temperature, while during the day time it would be protected from solar radiation by floating a white foam (such as that used by fire fighters) on top of it. A mathematical model has then to be derived for both the night time and day time periods.

#### C.l Night Time Operation

The energy balance equation for the concentrated brine in the auxiliary pond can be given by :

heat deposited into heat loss to the heat loss to auxiliary pond from - atmosphere due - the atmosphere condenser of power to radiation due to conplant vection

heat gained due to bottom conduction

change of

(C.1)

internal energy

The heat losses to the atmosphere due to evaporation are neglected since they are small compared to other terms in equation (C.1).

The heat loss to the atmosphere due to radiation,  ${\tt q}_{\tt r}$  , (from Stefan-Boltzmann law) can be expressed as follows :

$$g = \sigma_{sb} A_{aux} (T_{aux}^4 - T_{sky}^4)$$
 (C.2)

where,  $\sigma_{\rm sb}$ , is the Stefan-Boltzmann constant, A is the surface area of the auxiliary pond, and T aux and T are auxiliary pond and sky temperatures respectively.

The forced convection losses due to wind action for wind velocity less than 5 m/sec. (Scgock (1965)) can be given by:

$$q_{fc} = h_{fc} A_{aux} (T_{aux} - T_{a})$$
 (C.3)

where  $h_{\mbox{\it fc}}$  , the heat transfer coefficient, is obtained from the following expression :

$$h_{fc} = 5.7 + 3.8 V_W$$
 (C.4)

where,  $V_{w}$ , is the wind velocity in m/sec.

The heat gained by the auxiliary pond due to ground conduction at the bottom, as in the steady state operation of the pond described in Chapter II, is assumed to be as follows:

$$q_{DC} = A_{aux} \frac{K_{q}}{\ell_{2}} (T_{aux} - T_{w})$$
 (C.5)

where,  $K_g$ , is the ground conductivity,  $\ell_2$  and  $T_W$  have their previous meanings.

Using equations (C.2) - (C.5), the relation in (C.1) can be expressed mathematically as follows:

$$q_{dep} - \sigma_{sb} A_{aux} (T_{aux}^4 - T_{sky}^4) - (5.7 + 3.8 V_W) A_{aux} (T_{aux} - T_a)$$

$$- \frac{K_g}{l_2} A_{aux} (T_{aux} - T_W) = (\rho C l A)_{aux} \frac{d T_{aux}}{dt}$$
 (C.6)

The analytical solution of equation (C.6) can easily be obtained if the radiation losses are approximated as follows:

$$q_{r} = (492)^{\frac{4}{3}} \sigma_{sb} a_{aux} \left[ \left( 1 + \frac{f_{aux}}{273.15} \right)^{4} - \left( 1 + \frac{T_{sky}}{273.15} \right)^{4} \right]$$

$$\sigma_{r} = \frac{4(492)^{4}}{273.15} \sigma_{sb} a_{aux} \left[ \left( T_{aux} - T_{sky} \right) \right]$$

$$(C.7)$$

In the above equation, the temperatures are expressed in degrees Celcius.

Substitution of equation (C.7) into (C.6) and re-arranging the terms yield:

$$\frac{d T_{aux}}{dt} = - (5.7 + 3.8 V_W + \frac{K_g}{\ell_2} + 8.58 \times 10^8 \sigma_{sb}) \frac{T_{aux}}{(\rho C \ell)_{aux}} + \frac{5.7 + 3.8 V_W}{(\rho C \ell)_{aux}} T_a + \frac{8.58 \times 10^8 \sigma_{sb}}{(\rho C \ell)_{aux}} T_{sky} + \frac{K_g}{\ell_2 (\rho C \ell)_{aux}} T_W + \frac{1}{(\rho C \ell A)_{aux}} q_{dep}$$
(C.8)

### C.2 Day Time Operation

The white foam is assumed to reflect all the solar radiation.

The energy balance can be given by the following:

$$q_{dep} = \frac{K_{g}}{l_{2}} A_{aux} (T_{aux} - T_{w}) - U_{oh} A_{aux} (T_{aux} - T_{a})$$

$$= (\rho ClA)_{aux} \frac{d T_{aux}}{dt}$$
(C.9)

where U is the overall heat transfer coefficient which takes into account the conduction through foam layers and free convection, therefore :

$$\frac{1}{U_{\text{oh}}} = \frac{\ell_{\text{f}}}{K_{\text{f}}} + \frac{1}{h_{\text{fr}}}$$
 (C.10)

where  $l_f$  and  $k_f$  are the thickness and thermal conductivity of the foam, and  $h_{fr}$  is the free convection heat transfer coefficient.

Equations (C.6) and (C.9) can be integrated alternatively for the night and day time operation for the period of reversed operation.

## C.3 Temperature Response of the Auxiliary Pond

Prediction of the auxiliary pond's temperature was achieved by a numerical method using an IMSL subroutine based on the Runge-Kutta method. The temperature response as well as the data used for its calculation appear in Figure C.1 (the zero of the time axis corresponds to the middle of October). The increase of the auxiliary pond temperature during day time operation was in the order of a fraction of a degree and it is not represented in Figure C.1. It can be seen that the temperature of the auxiliary pond drops to - 10 °C in about three weeks. The ambient temperature has a minimum of - 9.5 °C and that of the auxiliary pond has a minimum of - 13 °C which occurs about a week later

